TRANSPORT AND REACTION OF HEAVY METALS
IN ALASKAN FJORD-ESTUARIES

David C. Burrell

Prepared for the U.S. Department of Energy,
Office of Health and Environmental Research
Contract No. EY-76-C-06-2229 TA #1

UNIVERSITY of ALASKA INSTITUTE of MARINE SCIENCE

SEMPER PROFUNDIUS PENETRARE

June 1979
RLO-2229-T1-50

V. Alexander
Acting Director

DISCLAIMER

RLO-2229-T1-50

TRANSPORT AND REACTION OF HEAVY METALS IN ALASKAN FJORD-ESTUARIES

ANNUAL REPORT

July 1, 1978 - June 30, 1979

David C. Burrell
Institute of Marine Science
University of Alaska
Fairbanks, Alaska 99701

Prepared for the U.S. Department of Energy,
Office of Health and Environmental Research
Contract No. EY-76-C-06-2229 TA #1

June 1979

V. Alexander
Acting Director

TABLE OF CONTENTS

LIST OF FIGURES

LIST OF TABLES

SECTION I

WORK IN PROGRESS

Work in Progress

In the 1977-78 Annual Report to DOE a preliminary analysis of the seasonal hydrography and nutrient chemistry of Yakutat Bay was given. This estuary is a complex multi-silled fjord of topical interest because of projected impact due to off-shore oil exploration. The entrance sill is shallow, and flushing of the outermost basins at least appears to be complete by late spring-early summer. In April of this year we managed to secure one further day of shiptime and the opportunity was taken to complete a detailed hydrographic survey (see attached Cruise Report #273). These data have not yet been fully analysed and will be included in a future report.

Three cruises have been made to Boca de Quadra (Fig. 1) inlet; October and December 1978 and April 1979. A mass of environmental baseline data has been collected on the hydrography and water circulation and on the nutrient and suspended sediment chemistry. One preliminary report has been issued, but much of the data are as yet undigested and will remain so until we have year-round coverage. DOE contract interest in this fjord is with the character and transport of the suspended sediment, complementing similar work being done much further north in Resurrection Bay. Some examples of work currently underway on particulates in Boca de Quadra are given below.

We have previously published an initial compilation of hydrographic water column chemistry for the period 1972-75 for Resurrection Bay (Fig. 2). During the current contract period, an analysis of nutrient fluxes across the sediment-basin interface and oxygen supply and consumption at depth within the basin over the same period has been completed (see extended abstract in Section II).

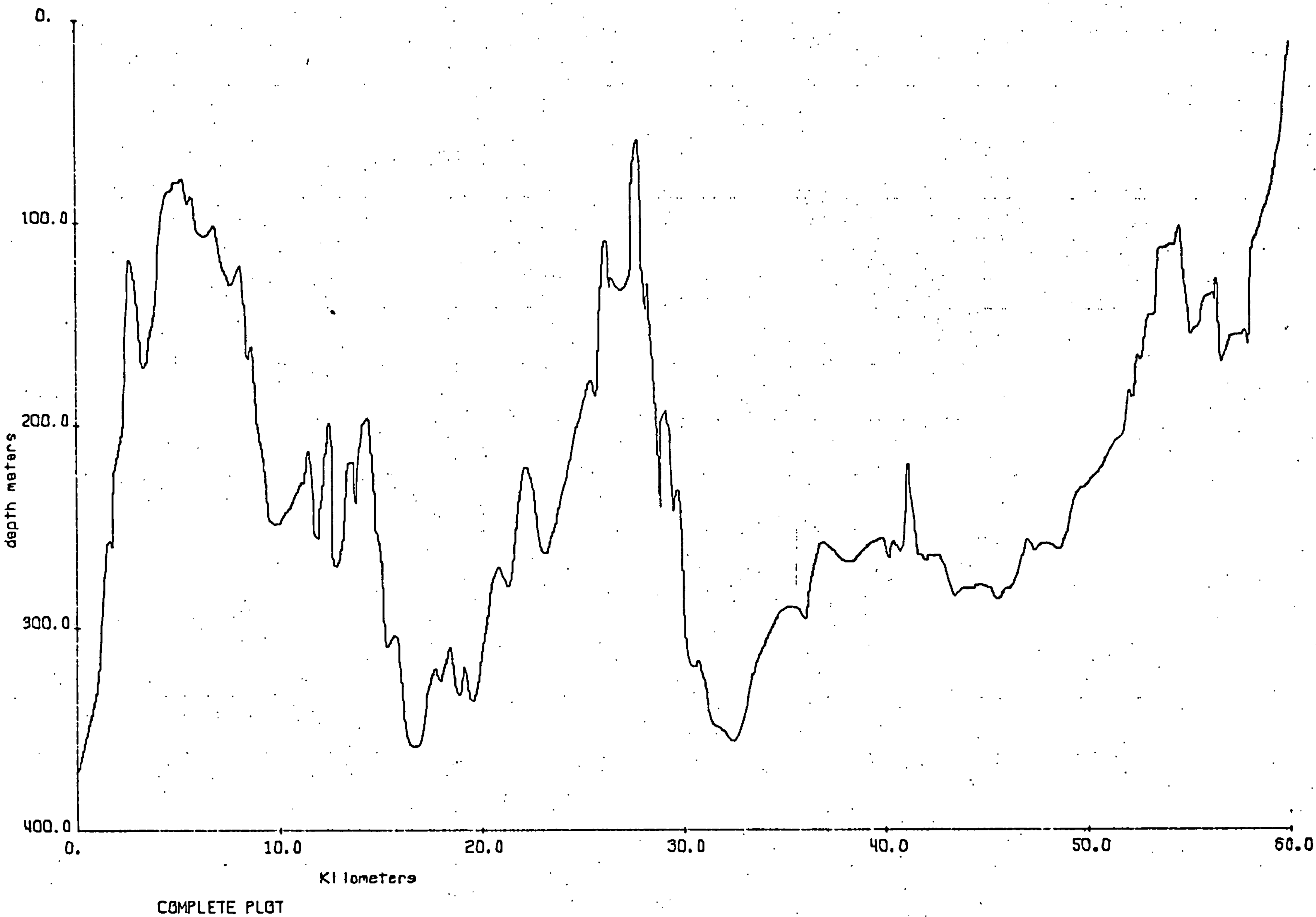

Figure 1. Boca de Quadra Inlet. Recent bathmetry showing basin structure.

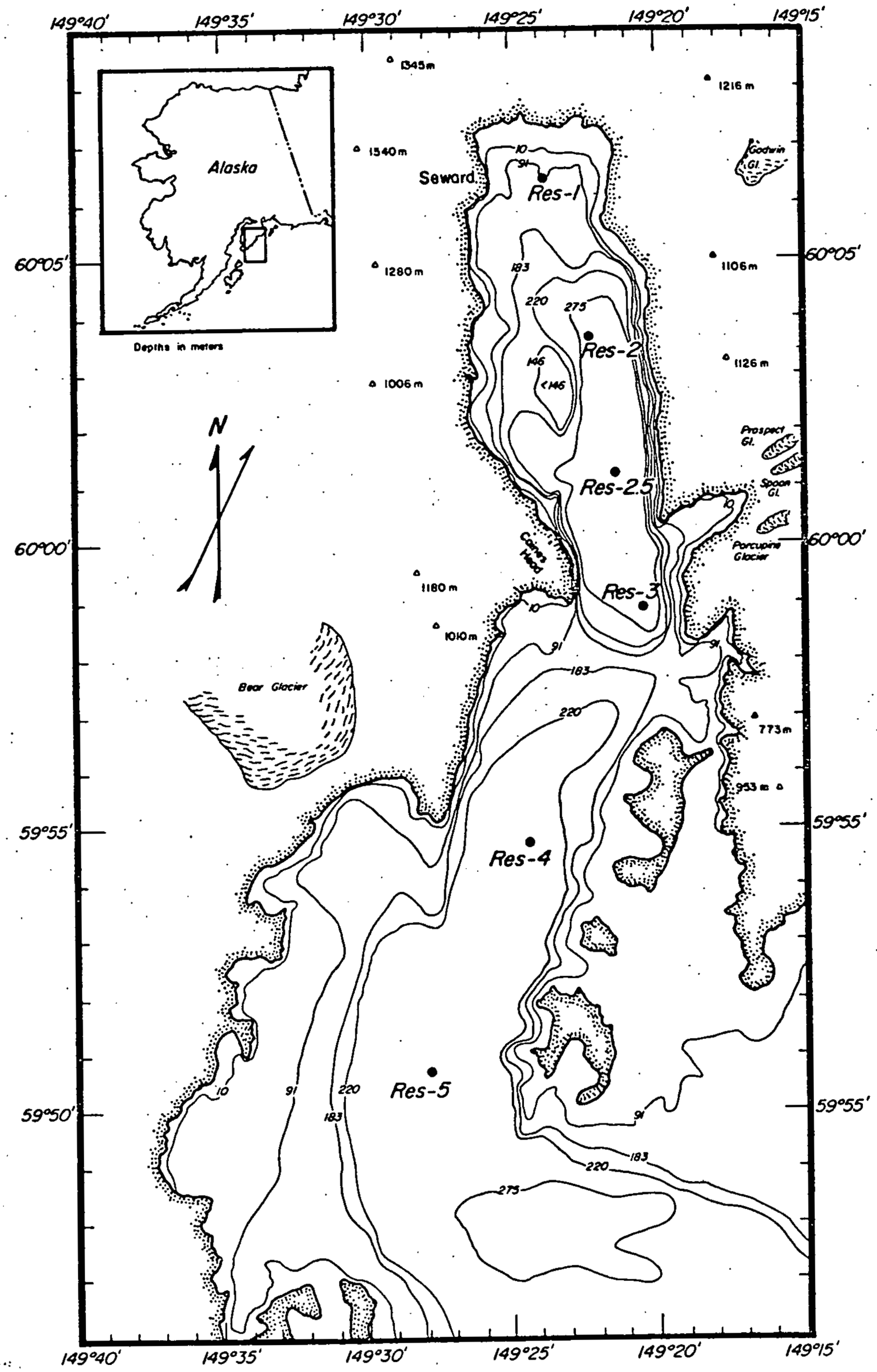

Figure 2. Resurrection Bay. Stations RES 2.5 and RES 4 are standard stations without and outside the single sill.

Resurrection Bay (Fig. 2) is an example of a single-silled Alaskan fjord having sill depth below the zone of minimum annual density variation (see Muench and Heggie reprint in Section II); i.e., major replacement of deep basin waters occurs during the oceanographic summer at the time of relaxation of the winter coastal convergence. Figure 3 illustrates the T-S character of the column inside and outside the sill (Stations 2.5 and 4 respectively; Figure 2) during September-October: the stippled area shows that the inner basin water corresponds to water at sill height outside the barrier. The corresponding late winter (April of 1973-1975) patterns are shown in Figure 4. At this time of year--i.e., towards the end of the period of relative advective isolation--the inner basin waters are well stratified.

Examination of the seasonal density (salinity) distributions within this fjord over a number of years, has shown that the local rate of change below sill depth within the basin may be approximated by two transport terms: vertical advection across the sill and vertical turbulent mixing. Thus for salt:

$$\frac{1}{\Delta t} \sum_{\text{bottom}}^{\text{sill}} \Delta S_z \, dz = w_z \, (S_I - S_E) - K_z \frac{\Delta S}{\Delta z} \quad \text{(sill)}$$

Here S_I and S_E are the salinity of the influx and efflux waters respectively and the other terms are as conventionally defined. We have further determined seasonal values for the vertical eddy coefficient at sill height by assuming that, during the winter months, the advective term is negligible. For the period September-October of 1973, transports through the inner basin have been estimated using this budget equation to be $2.5\text{-}5.0 \times 10^8 \ m^3 d^{-1}$; direct current meter observations over the same period give $4.1 \times 10^8 \ m^3 d^{-1}$.

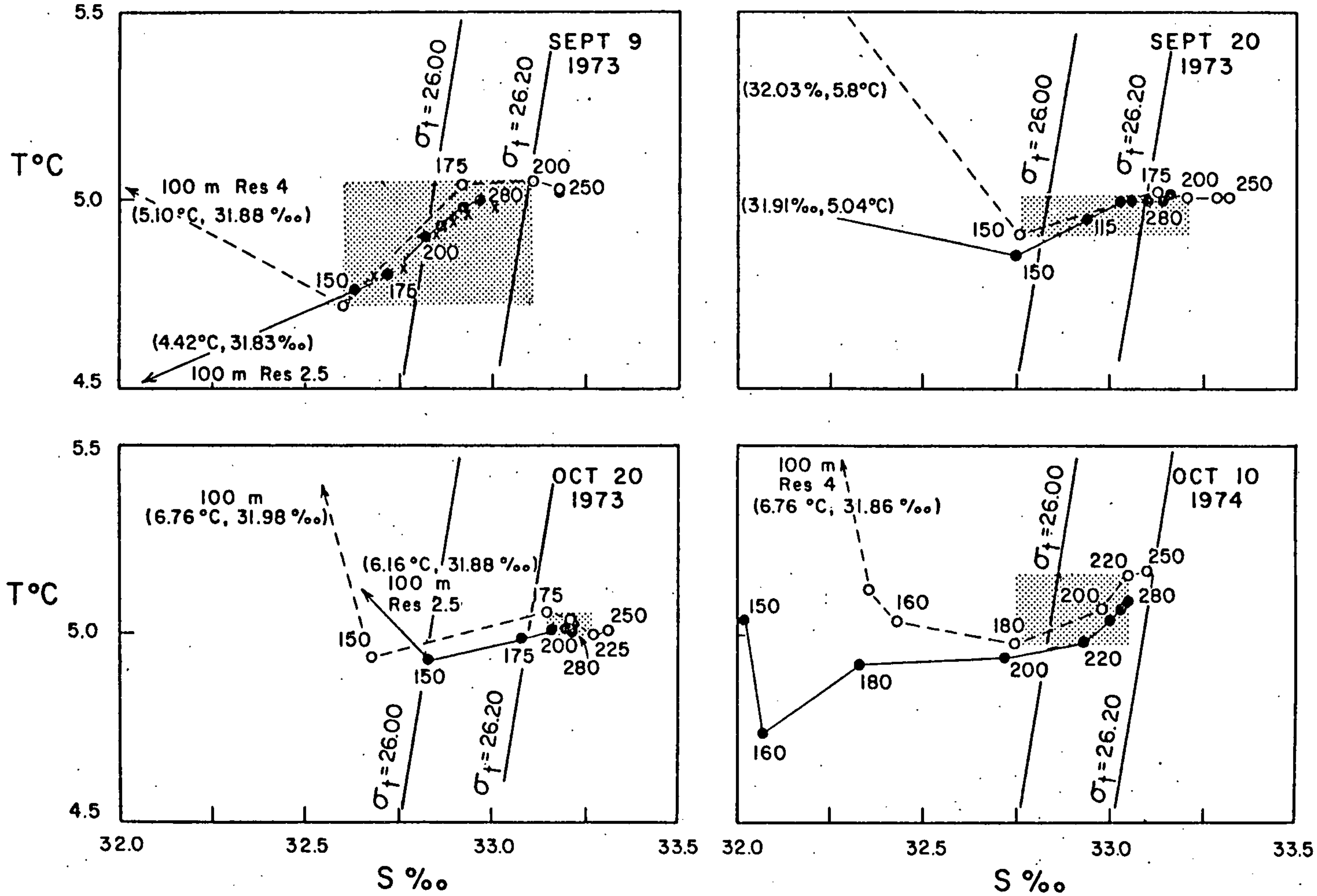

Figure 3. T-S distributions at Stations RES 2.5 and 4 September-October (stippled area encloses sill depth region).

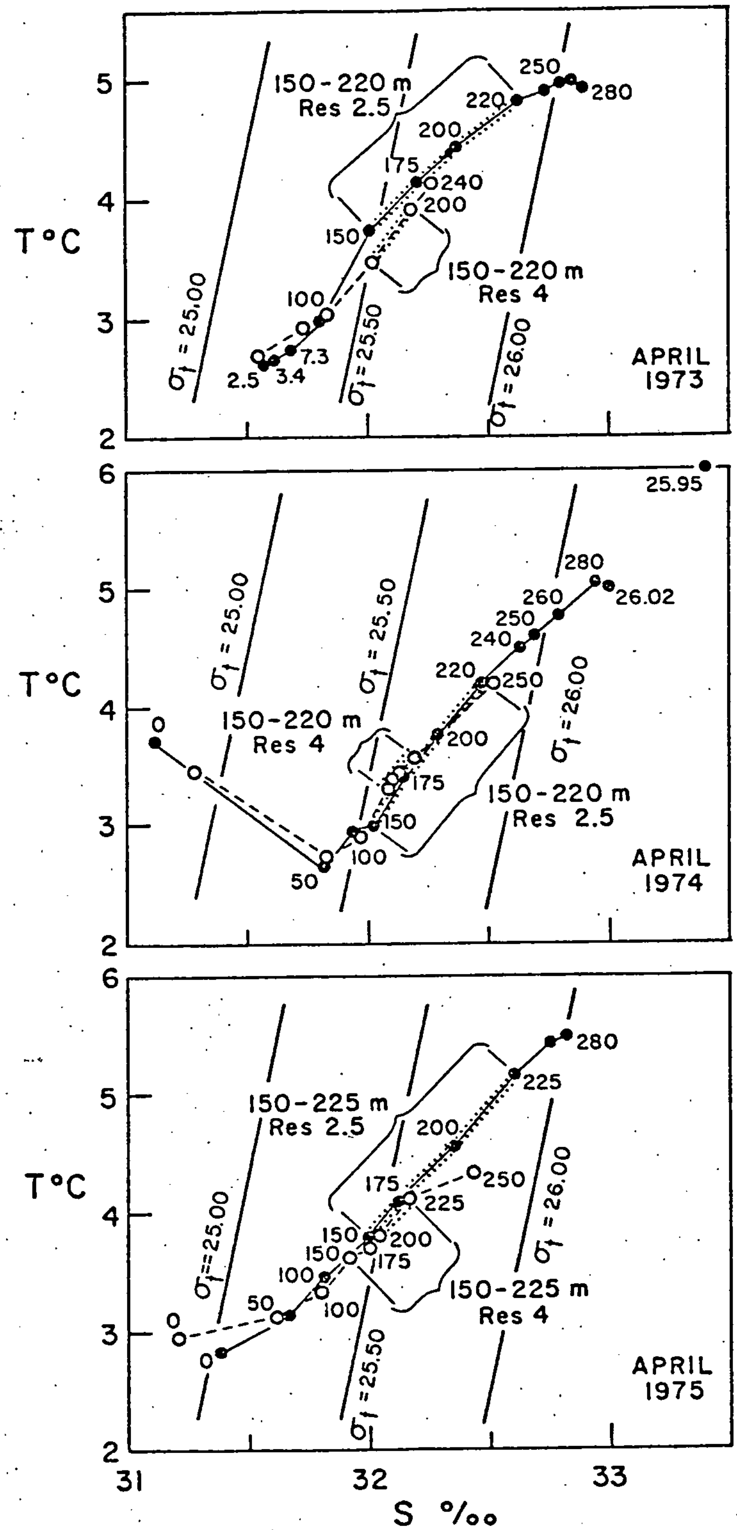

Figure 4. T-S distribution at Stations RES 2.5 and 4 towards the end of the oceanographic winter period (April 1973-75).

These volumes were sufficient to replace the inner basin over a 35-day period 2-3 times over. Figure 5 summarizes these data for the period 1973-1975.

The simplified distribution equation used here would clearly be unacceptable if our objectives were to define precise transports. There are clear indications of some advective inflow and horizontal transport within the basin and one of this coming year's objectives would be to analyze in detail density data obtained on previous current meter deployments within the basin. However, our principal objectives are chemical, not physical, and considering the range of errors associated with describing non-conservative behaviors, simplification of the advection-diffusion equation is not considered to be limiting.

The distribution and behavior of oxygen within the fjord-estuary basin is of fundamental importance and is perhaps the easiest to handle of the non-conservative parameters. Net primary productivity inside and outside the sill was estimated to be 285 and 230 gC m^{-2} respectively in 1974-1975. However, the distributions of oxygen at depth were quite different. Inside the sill, bottom concentrations of around 7 ml ℓ^{-1} at the time of renewal were decreased to >1.0 ml ℓ^{-1} by March-April. In fact, the integrated oxygen content of the basin remained approximately constant over this period and a strong gradient, positive away from the sediment, developed and intensified over this period. Over the winter period, the oxygen distribution may be approximately by:

$$\frac{1}{\Delta t} \sum_{\text{bottom}}^{\text{sill}} \Delta\, O_z dZ = -\, K_z \frac{\Delta O}{\Delta Z}\,(\text{sill}) + C + S$$

where C and S are column consumption and loss to the sediment terms respectively. We can estimate a mean value for (C + S) over the period 1973-1975

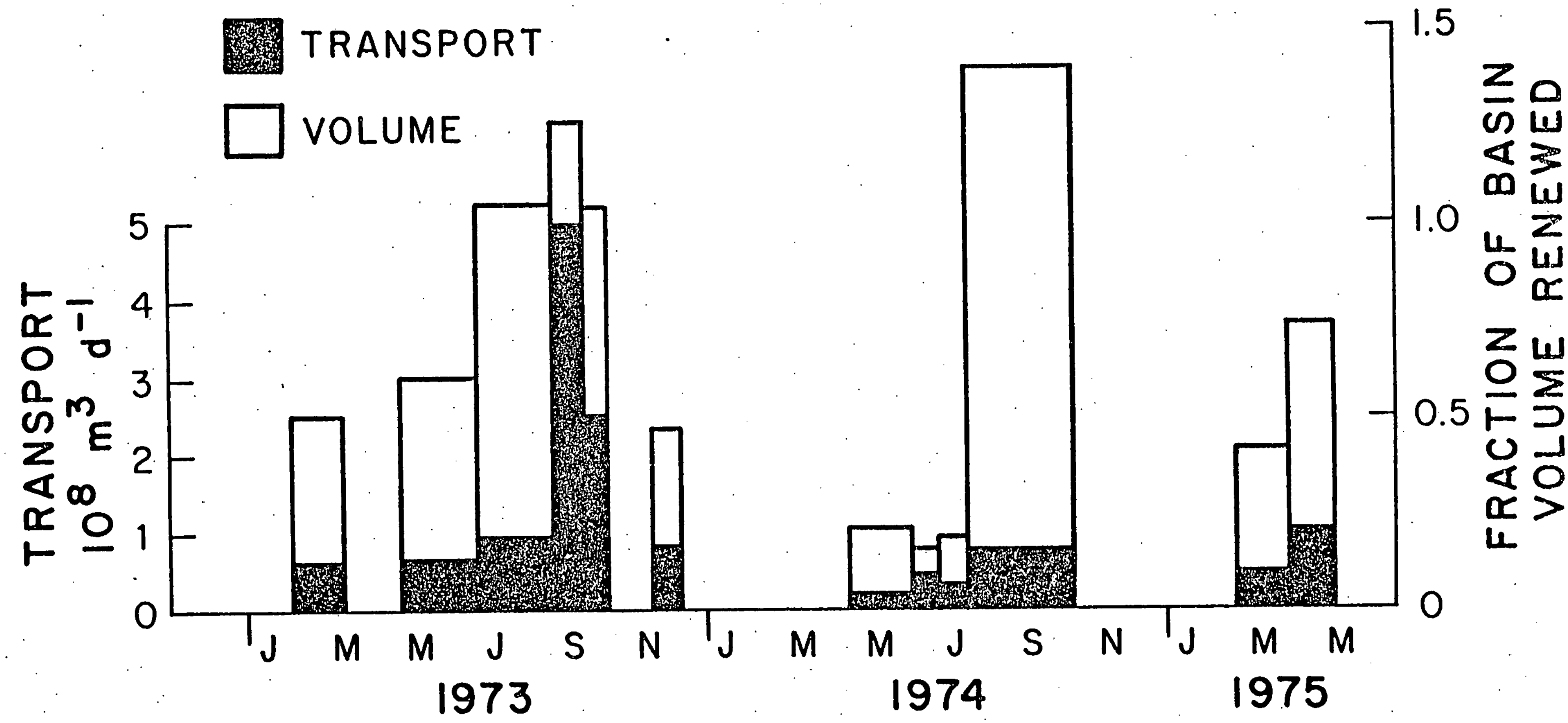

Figure 5. Seasonal variations in transports and volumes displaced during flushing of inner basin.

of 37 ml O_2 cm^{-2} yr^{-1}; i.e., a volumetric consumption rate within the basin below the sill of around 3.7 ml ℓ^{-1} yr^{-1}. This consumption accounts for approximately 30 percent of the maximum primary productivity measured in the summer.

There is one other interesting feature about the oxygen distribution in this fjord. Bottom basin concentrations fall to $\sim$ 1 ml ℓ^{-1} by March-April as noted. But, thereafter, until the next renewal cycle, contents remain at about steady state, or even increase slightly. It appears that diffusional transport to the deep basin is more than able to supply that required by the computed consumption; in fact, we estimate a spring-early summer flux to the bottom of 50-70 ml O_2 cm^{-2} yr^{-1}. This means that if a year passed when no late summer-fall replacement of the deep basin water occurred (this has never been observed) the bottom waters would not become anoxic.

As noted in the introduction, the thrust of this program is towards benthic fluxes and reactions likely to be impacted by industrial activity associated with energy exploitation. In last year's report, we briefly discussed the cycling of copper across the benthic boundary and within the basin water. (A reprint of this work will be included in a subsequent report to DOE.) Over the past years, we have looked at the transport of nutrients across the basin sediment interface (Heggie and Burrell, 1979; extended abstract in Section II). This work has indicated an interesting nitrification reaction in the surface sediments: oxidation of ammonia to give "excess" nitrate. The latter "excess" is computed at approximately 10 μ mole NO_3-N ℓ^{-1}. The ammonia concentration difference across the benthic boundary is in excess of two orders of magnitude (flux computed in the order of 17 μ mole cm^{-2} yr^{-1}) but the bottom water concentrations at no time exceed 1 μ mole ℓ^{-1}. Pore water concentrations of nitrate and nitrite indicate complete consumption at depths less than approximately 6 cm in the Resurrection Bay sediments. Thus, assuming that oxygen concentrations at the sediment surface approximate those in the bottom water, we may estimate a flux into the sediment of some 0.5 ml O_2 cm^{-2} yr^{-1}: this is equivalent to only about 1 percent of the annual net productivity in this locality (see previous discussion).

Due to restraints on ship-time, we were unfortunately unable to continue the previous seasonal coverage in this fjord until November 1977. Since then, we have obtained data on some nine cruises which are currently being processed. This more recent batch of data includes particulate organic carbon profiles which will enable us to refine the preliminary oxygen consumption model. One interesting feature in this respect is that in the interim between the earlier and latest batch of observations there has been a significant reduction of anthropogenic carbon (fish processing waste) added to the basin. There are early indications of reduced oxygen consumption through the winter, but detailed consumptions have not yet been made.

Because of the physical form of fjords in general, and the local shelf circulation patterns in particular, the estuarine surface mixing and chemical reaction zone is here directly coupled with a zone of physically confined ocean water: i.e. the simplifying geometry of an ocean basin directly coupled with the chemically reactive estuary. These are ideal conditions for studying benthic reactions and transport. There is today a great deal of work being done around the world on the flux of chemical species out of the sediments. However, experiments of the type which confine a sample of bottom water in free exchange with the sediment can only yield information on part of the cycle. The net transport of all species is to the sediment.

In the case of highly reactive species--such as the heavy metals--which have very short residence times, primary and secondary transport to the interface is of equal if not greater importance. Further, we believe that our fjord basins are a particularly advantageous environment for these studies since the system can be approximately simplified to a vertical diffusion model at certain times of the year as previously noted. In last year's Report, a copper distribution model was described. During the present contract period, we have given primary attention to a detailed sediment-water column model of manganese cycling. The initial publication on this work is reproduced in the accompanying Annual Report so that only brief details are included here.

One general profile for soluble (basin) manganese from Yakutat Bay was shown in the 1977-1978 DOE Annual Report. Figure 6 shows data for both particulate (IV) and soluble (II) manganese obtained towards the close of the oceanographic winter in Resurrection Bay (basin isolation period, March 1979), and Figure 7 gives the corresponding interstitial water distribution of the reduced form of the metal: our model assumes constant diffusion coefficients (K_z and D) to the sediment-water interface, and also steady state conditions so that manganese transported out of the sediment equals that oxidized within the basin column and re-sedimented. The basin "soluble" equation used is:

$$\frac{dc}{dt} = \frac{\delta}{\delta z} (K_z \frac{\delta c}{\delta z}) - kC$$

i.e. we incorporate an apparent first order oxidation rate constant (k). The particulate distribution is then:

$$\frac{dP}{dt} = - W \frac{\delta p}{\delta z} + kC$$

This model yielded a k value in both sediment and water of the order of

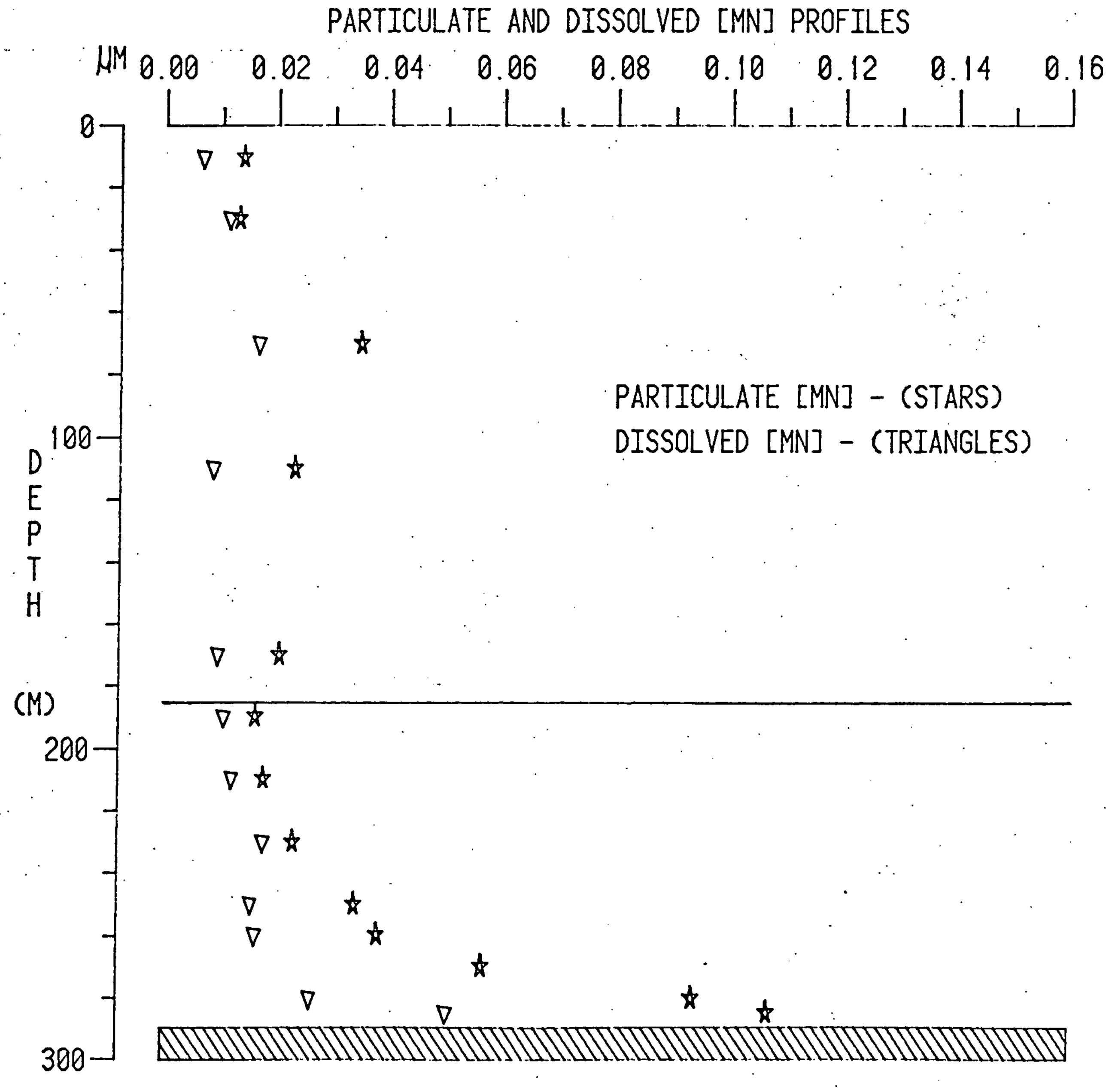

Figure 6. Distribution of manganese at RES 2.5 in March (1979).

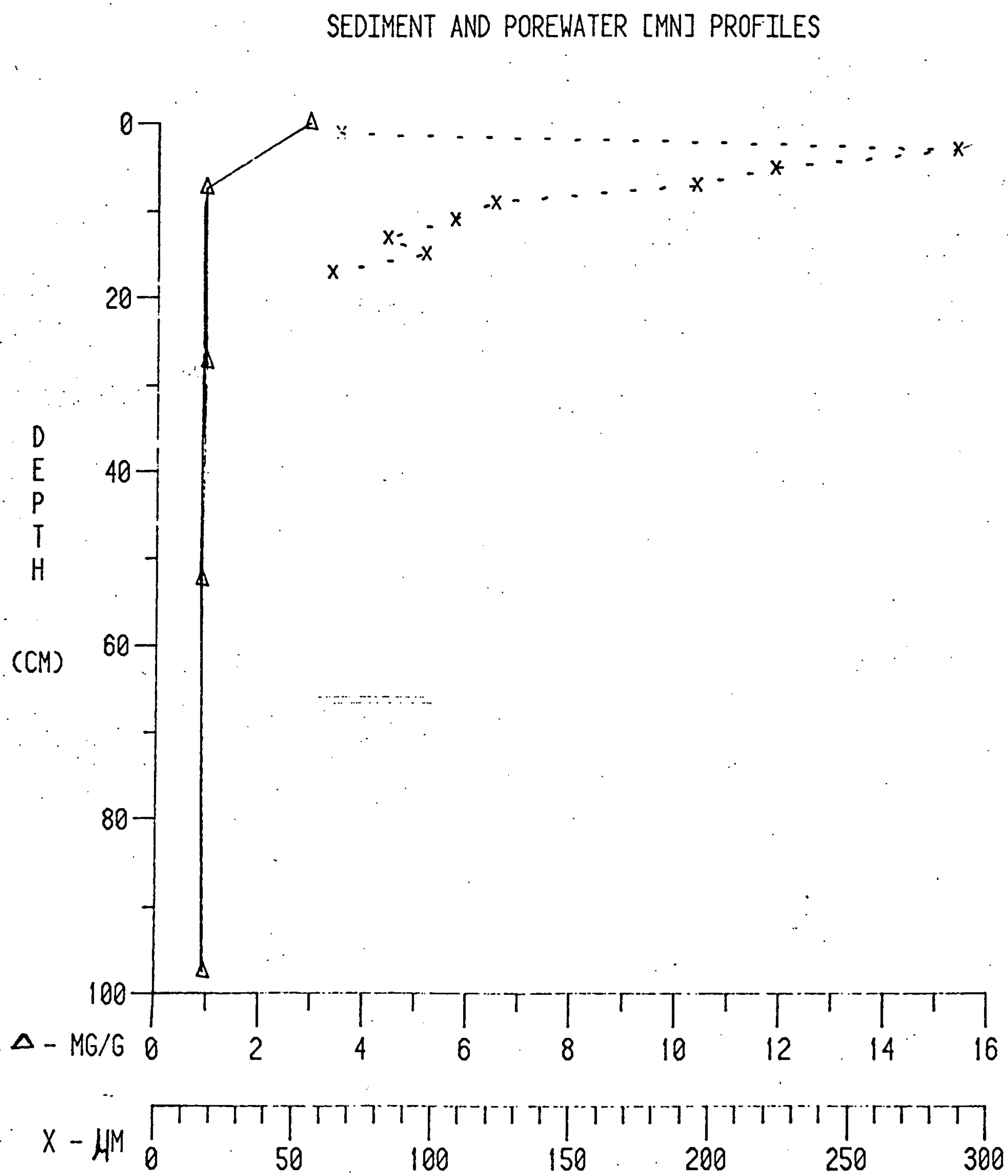

Figure 7. Interstitial water manganese at RES 2.5 in March

1×10^{-6} sec^{-1}, and a mean residence time for Mn(II) in the column of 8.4 days.

We have very recently obtained initial values for the distribution of particulate manganese at the head of Boca de Quadra. Figure 8 illustrates the Mn/Al ratio vertical profile at Station BQ-3. The pattern is clearly different to that obtained for Resurrection Bay: detailed analysis will have to wait for the hydrography and circulation background.

In the above model it was assumed that oxidized manganese sorbed onto settling particles. The settling velocity compiled in this case was 1×10^{-3} cm sec^{-1}; this corresponds to a mean particle size of around 20 μm diameter and emphasizes the need to know considerably more about the composition, reaction and flux of the particulates in the fjord basin. This topic was to have been the major objective of this year's work, but largely because of some equipment malfuction and late arrival of other items, only a start has been made and we are proposing continued effort during the coming year.

Figures 9 and 10 show preliminary values for the vertical seasonal distribution of total particulate load (PL) and particulate organic carbon (POC) at Station RES 2.5 (Figure 2). Corresponding particulate aluminum (PAL) has also been obtained for this fjord and for Yakutat Bay (see last year's report), and one initial objective has been an attempt to derive an aluminosilicate-biogenic distribution model for these estuarine basins.

Six particulate sediment profiles, from Yakutat Bay (*Acona* cruises 240 and 246) and from Resurrection Bay (*Acona* cruises 254, 260 and 262) have been run through a reiterative linear bivariate least squares curve fitting program which forced the intercept to less than 10% (i.e., the approximate precision of the data) of the mean particulate load for each

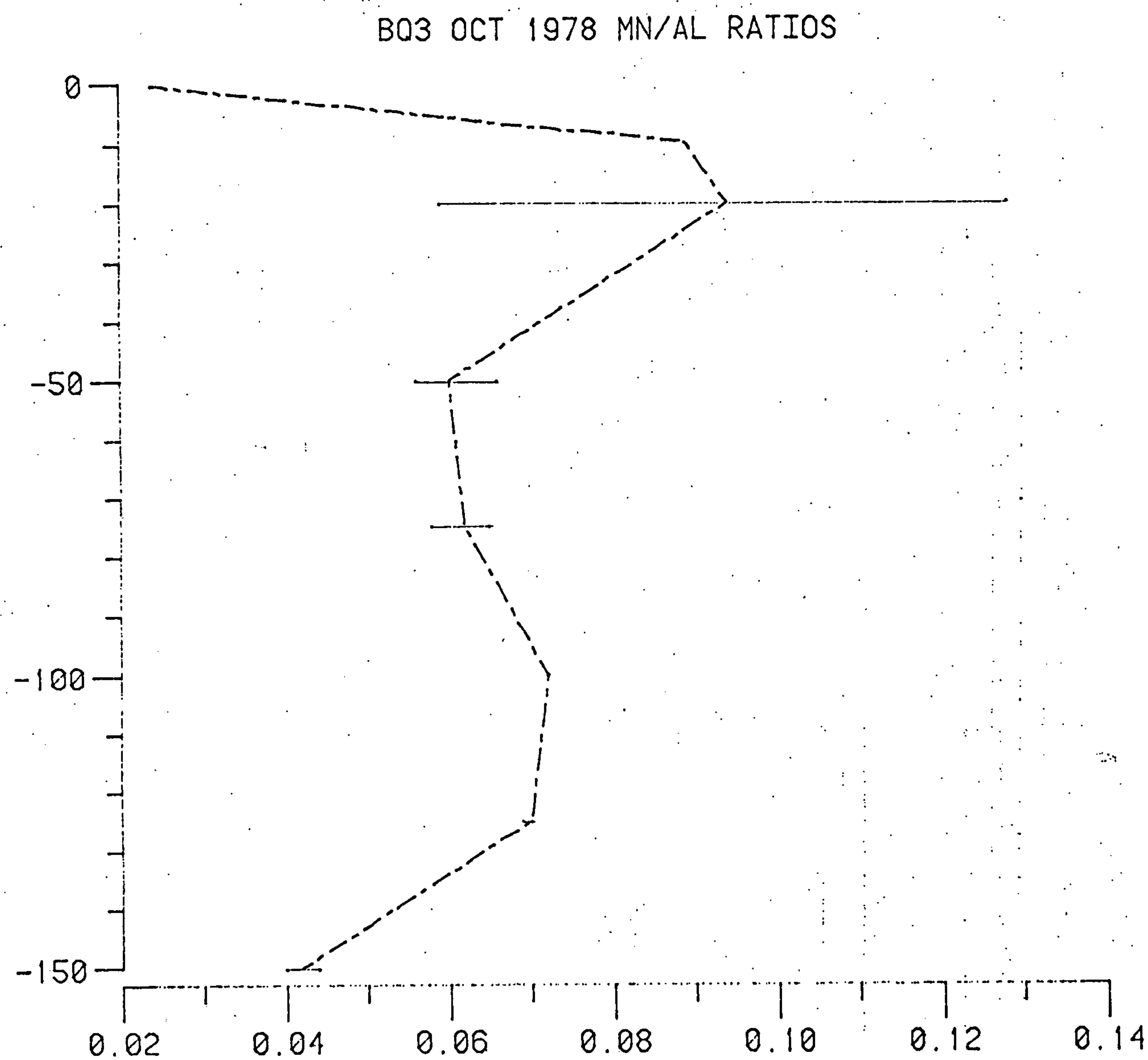

Figure 8. Mn/Al ratios at Boca de Quadra Station BQ-3.

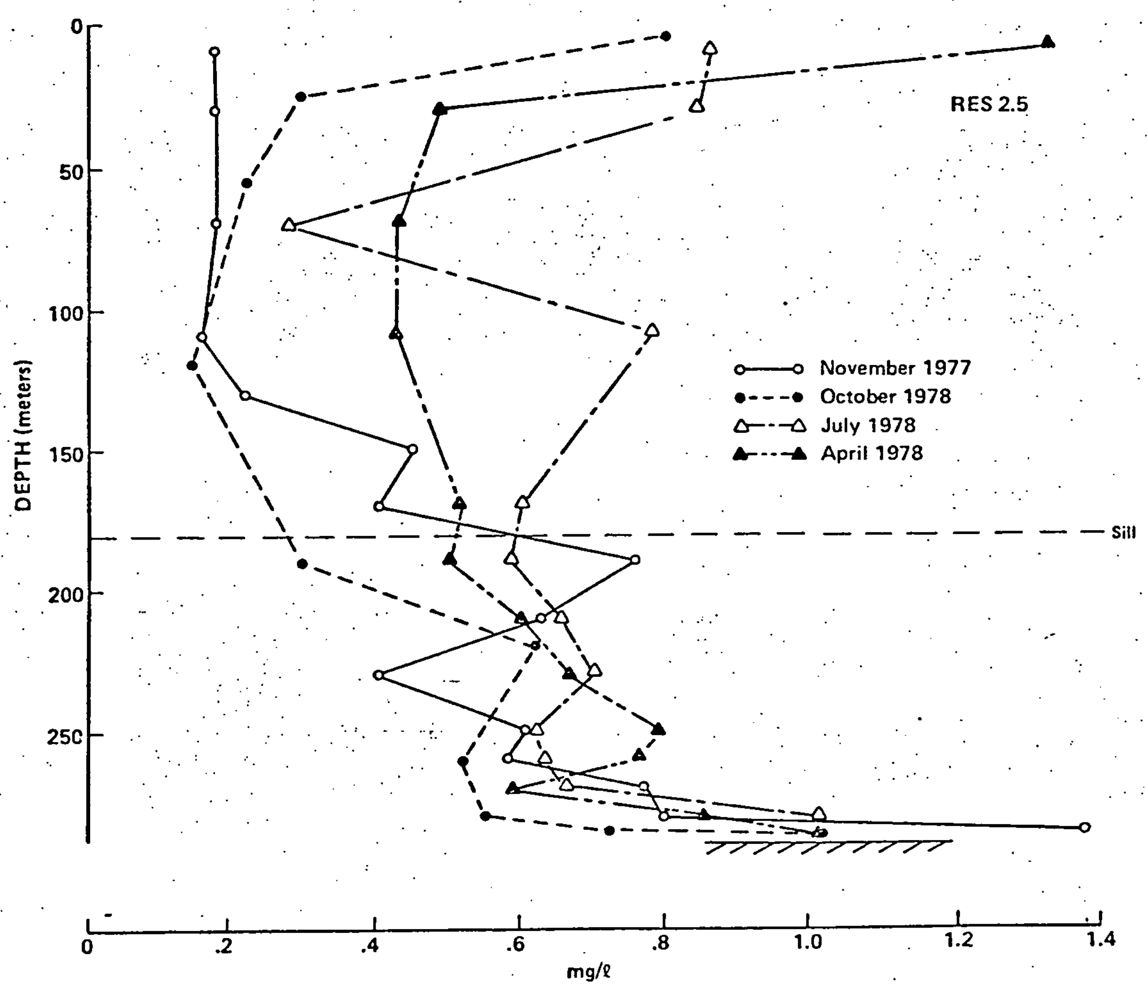

Figure 9. Seasonal vertical distribution of total particulate load at RES 2.5.

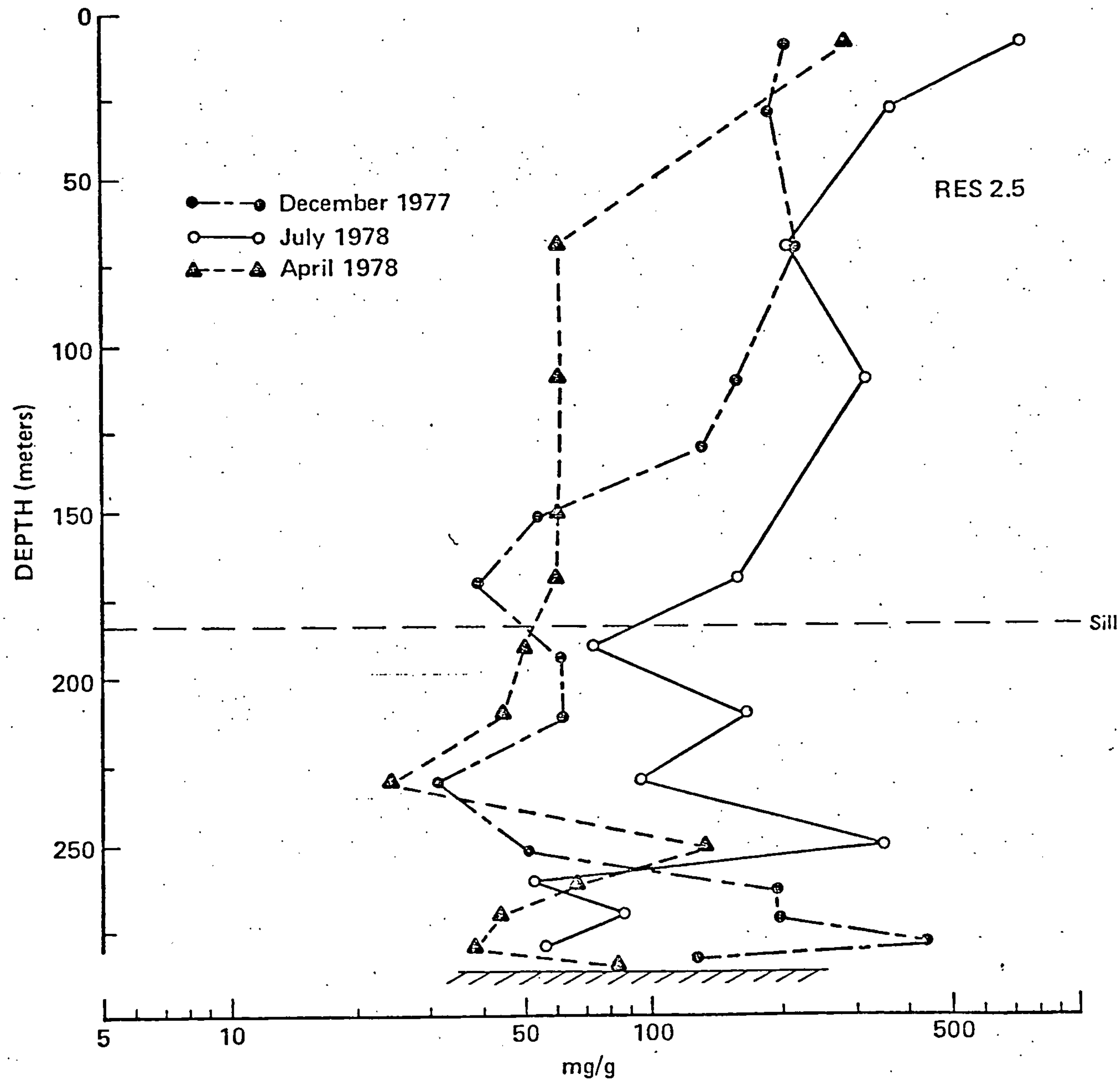

Figure 10. Seasonal vertical distribution of particulate organic carbon at RES 2.5.

profile. The fitted curve was thus of the form:

$$PL = A + (B \times PAL) + (C \times POC)$$

and values generated for the constants A, B, and C are given in Table I. This computed fractionation procedure assumes that the percent carbon content of the biogenic material and the percent Al content of the aluminosilicates remains constant with depth: it also assumes that the bulk of the inorganic material contains aluminum. Considering the precision and accuracy of the separate analyses and the resulting uncertainties caused by forcing the linear fit, these assumptions are probably acceptable for an initial model. Given these assumptions, the constant A should be zero: in the non-ideal case it represents a summation of the analytical error and violation of the assumptions.

The constants B and C are reciprocals of the average fraction of aluminum content of the inorganic and of the fraction of carbon content of the biogenic material respectively. All XRD studies of the clay fraction of the coastal sediments in the vicinity of Resurrection Bay show a preponderance of chlorite and illite. However, the low range obtained for B (∿ 5) would be consistent with low aluminum minerals. We are currently carrying

TABLE I

MODEL COMPUTATION OF PARTICULATE SEDIMENT COMPOSITION

Cruise No.	Station Name	Constants (see text) A	B	C	R
240	Yak-7	20.85	12.61	2.41	0.999
246	Yak-7	-10.95	14.08	2.02	0.994
246	Yak-9	15.82	12.83	2.24	0.999
254	RES-2.5	0.21	10.91	2.08	0.999
260	RES-2.5	- 2.00	10.80	2.15	0.995
262	RES-2.5	38.14	10.79	1.97	0.984

out direct microscopic examination of the particulate material in Resurrection Bay. Meanwhile it seems possible that the discrete sampling misses a substantial fraction of sedimenting material. Direct sediment trap experiments will help clarify this problem, but at the present time, sedimentation rates determined *via* the interstitial sulfate reduction method have given values an order of magnitude greater than could be supported by the indicated particulate flux based on discrete load measurements and assumed mean size. The range determined for the constant C fits, to a remarkable degree, the values expected for a predominantly diatomaceous bloom.

There has been some recent criticism concerning possible error in determining suspended sediment loads where sub-samples are drawn from the sampling bottle after various unsystematic delays. This potential problem has been of concern to us also. Where some delay is unavoidable the Niskin bottles are inverted several times (without agitation) prior to draining the sample. We attempt, however, to always drain immediately on collection. Replicate 1-liter subsamples have been filtered on separate cruises with the following results:

TABLE II

SUSPENDED LOAD SAMPLING TESTS

Cruise	Station	Depth (m)	Delay (min)	Mean load (mg)	Standard deviation
272	RES 2.5	20	∿ 2	0.35	0.08
276	RES 2.5	30	∿ 2	0.32	0.05
276	RES 4	20	∿15	0.42	0.15

It is clear that where even only a relatively small delay between sampling and analysis is allowed significant error results. Various other sampling bottles have been considered but it is intended to continue using Go-Flo Niskin but to use various sizes so that the entire volume can be filterd.

As described in last year's proposal, we have constructed two sediment traps of the type designed by PMEL (Lawrence *et al.*, unpublished data). Two separate deployments have been made in Boca de Quadra. The first trap was set in October (1978) and retrieved in December: at that time it was discovered that the timing mechanism had flooded and prevented closure. Although this voided quantitative data some material was retained for chemical analysis. This same trap was redeployed with a new timer unit in December for retrieval in April (1979) but the entire unit was lost because of severe corrosion of the attachment bolts. A second unit was set in Resurrection Bay on a current meter mooring in March of this year. When this instrument was recovered in May it was found that the trap had prematurely closed. It appears that similiar problems have been encountered by PMEL in Alaskan waters: a success rate of 15 out of 22 deployed. Because this project does not have the resources for more than a few instruments, and in view of the long time intervals involved before problems are discovered, it appears that a simpler design is required as discussed in the work proposed for 1979-80.

In the course of the last year a laser particle counting instrument manufactured by Spectrex Corporation has been evaluated for sizing marine suspensions. This potentially elegant technique has been unsatisfactory for the following reasons:

i. Inability to calibrate with external standards.

Standard solutions in optical quality quartz bottles are provided for calibration of the particle counter. Three of these standard solutions

(0, 205, 635 particles/counts per ml) are used progressively to set the threshold settings on the particle counter; however, for the two separate high count bottles, agreement between the stated figure (637, 635) and the instrument has never been achieved (the manufacturers admit their inability to do the same).

The manufacturers further imply that the original counting of the standard solutions was simply performed on a similar instrument; i.e., there is no independent external check on the counting accuracy. This process of "internal" calibration becomes more doubtful when one calibrates the particle sizing attachment, a multichannel analyzer with digital display and paper printout.

Standard settings (threshold, gain) are adjusted until the particle count readings on both instruments agree to within 5% for particles greater than 3 μ. The standard settings, however, have originally been determined to provide size intervals of 5 μ in 16 different channels so that any change in the gain setting alters this size interval. The manufacturer cannot provide information as to size intervals obtained for different settings of the gain knob thus introducing considerable uncertainty into the size distribution data (e.g., is the interval 4 μ or 6 μ or 7 μ).

ii. No significant difference detected between different seawater samples, apparently primarily due to lack of sensitivity and high count rates.

Although the lack of "absolute" calibration was suspected initially, it was hoped that relative size distributions could be used to distinguish different particle populations in different seawater samples. Analysis of the size distribution data has shown that the variation between samples is similar to the variation between duplicates; this is true for samples collected in two different localities over three seasons. Furthermore, when seawater samples were "spiked" with concentrations of standard size microspheres greatly in excess of expected natural populations, there was little or no difference in the resulting profiles and plots. It would thus appear that this light scattering technique is not sensitive enough to detect the differences expected in seawater particulate populations.

For the particle counter the manufacturer recommends that should counts exceed the display (999) the sample should be diluted in order to avoid multiple counting of the same particle. The average seawater sample usually exceeds the display 3 or 4 times, introducing another counting error.

Masking of particles by those closest to the laser source, while a problem in low density problem becomes a major constraint in normal seawater samples.

The above factors combined with the improbability of there being a representative particle population in the beam for the 20 seconds of the count renders the counting procedure somewhat doubtful. Dilution of the sample is not desirable since it drastically alters the particle populations (not a linear response), voids the obvious benefits of unmanipulated samples and dramatically increases the amount of time spent counting the samples.

iii. Inordinate processing time to obtain usable data.

To obtain usable data (even if of doubtful quality) an inordinately large amount of time is consumed in the initial counting, filtering of samples and counting of the filtrate to determine background, subtraction of both profiles, computer manipulation to plot different frequency curves and the final interpretation.

The data obtained, assuming validity, is not readily comparable to that of other researchers all of whom use Coulter Counter techniques which measure volume (independent of shape) rather than area (dependent on shape) measure by the Spectrex machine.

iv. Delicacy of the instrument for use at sea.

The instrument has proved to be delicate for shipboard use, malfunction 3 out of 5 times.

The Spectrex laser particle counter is, therefore, unsuitable for our purpose and its use will be discontinued in the future.

The DOE partially sponsored work performed by the Principal Investigator in Taiwan for a short period in 1977 on a designated U.S.-R.O.C. Cooperative Pollution Program. For various reasons most of this work was concerned with heavy metal pollution in river water rather than the oceans. It was determined that urban-industrial run-off resulted in very high down-stream soluble content of Fe, Mn and Zn which indirect evidence suggested was present as organic complexes. In our report we have also given preliminary evidence for removal of these metals to the sediment in the estuarine zone. (See separate report and abstract in this Report.)

The analytical techniques used in the above work were insufficiently sensitive to detect the presence of minor organo-metallic complexation in the marine environment. None would be expected however; even where, as in this case, the freshwater influx was highly contaminated. On the other hand, concentrations of suitable organic ligands may be high enough in (coastal) marine sediment interstitial water to allow this, and thus it is hoped to pursue this topic in the coming years as noted in the Proposal: data on the speciations of heavy metals in pore waters will help assess the role of the estuarine sediments as a source or sink (or both) for these minor constituents. Sediment cores have been collected, sectioned and squeezed from two stations in Resurrection Bay, one in Boca de Quadra and five in the vicinity of Dutch Harbor. These samples thus represent three natural environments: respectively, glacial run-off with low organic content and restricted planktonic activity; a "low latitude" non-glacial fjord; a shallow lagoonal basin subject to organic loading both from natural processes and industrial (fish waste) dumping. As noted elsewhere, the relatively low organic loading (and high near-bottom oxidation) produces an environment where the redox horizon is below about 5 cm and no free sulfide occurs in the interstitial water. Interstitial nutrient concentrations at the head of Boca de Quadra inlet indicates that denitrification has depleted nitrate below about 2 cm (nitrate and nitrite maxima of 7.4 and 1.0 μg at respectively occurs within the top 2 cm segment). The water column within Dutch Harbor appears to naturally go anoxic in late summer-fall and the sediment redox boundary is always close to the interface.

SECTION II

WORK COMPLETED

Benthic Flux and Near Bottom Reactions of Heavy Metals in Fjords

David C. Burrell

BENTHIC FLUX AND NEAR BOTTOM REACTIONS

OF HEAVY METALS IN FJORDS

Abstract of current work for DOE workshop: "Processes determining the input, behavior and fate of radionuclides and trace elements in continental shelf environments". 7-9 March 1979.

David C. Burrell

Institute of Marine Science
Universiy of Alaska
Fairbanks, Alaska 99701

Sub-arctic fjords are very favorable environments for studying estuarine transport and reaction of various chemicals, and particularly the heavy metals. Influx of fresh water and particulates and biological activity, is strongly seasonal; massive inorganic sediment (primarily fine-grained primary alumino-silicates) input predominating over part of the year. Man-produced contamination is presently negligible but is likely to increase substantially in the near future because of energy development. Most importantly, because of both the physical form of the fjords and the local shelf circulation patterns, the surface mixing and chemical reaction zone is directly coupled with a zone of physically confined marine water: the simplifying geometry of an ocean basin in direct contact with an estuary. These are ideal conditions for looking at transport to, from and within the sediments, and at benthic chemical reactions.

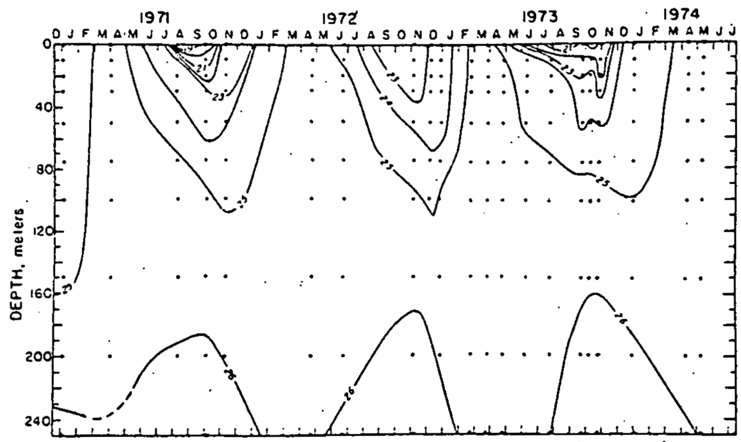

Fig. 1. Density time series at a Gulf of Alaska shelf station off Resurrection Bay.

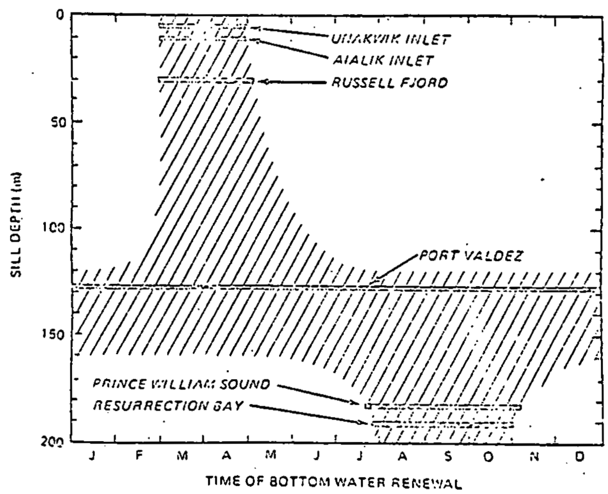

Fig. 2. Seasonal replacement of basin waters within various Alaskan fjords.

Gulf circulation in the winter causes intense downwelling along the Alaskan coast; relaxation of this system promotes upwelling in the summer (Royer, 1975). Waters of systematically varying densities are thus available at the heads of the coastal fjords through the year (Fig. 1). Periods of flushing of the fjord basins are related to the depth of the containing sill and the zone of minimum density change (Fig. 2; Muench and Heggie, 1978). Because of this, no Alaskan fjord studied to date has been observed to go anoxic. Moreover, largely because of low organic input (and high seasonal sedimentation rates) the sediment redox boundary is atypically depressed: 5-10 cm in the estuaries studies to date. What little evidence is presently available also suggests far less surface bioturbation than in more temperature localities.

Fig. 3. Vertical profiles of soluble copper (asterisks: totals) at same station within basin of

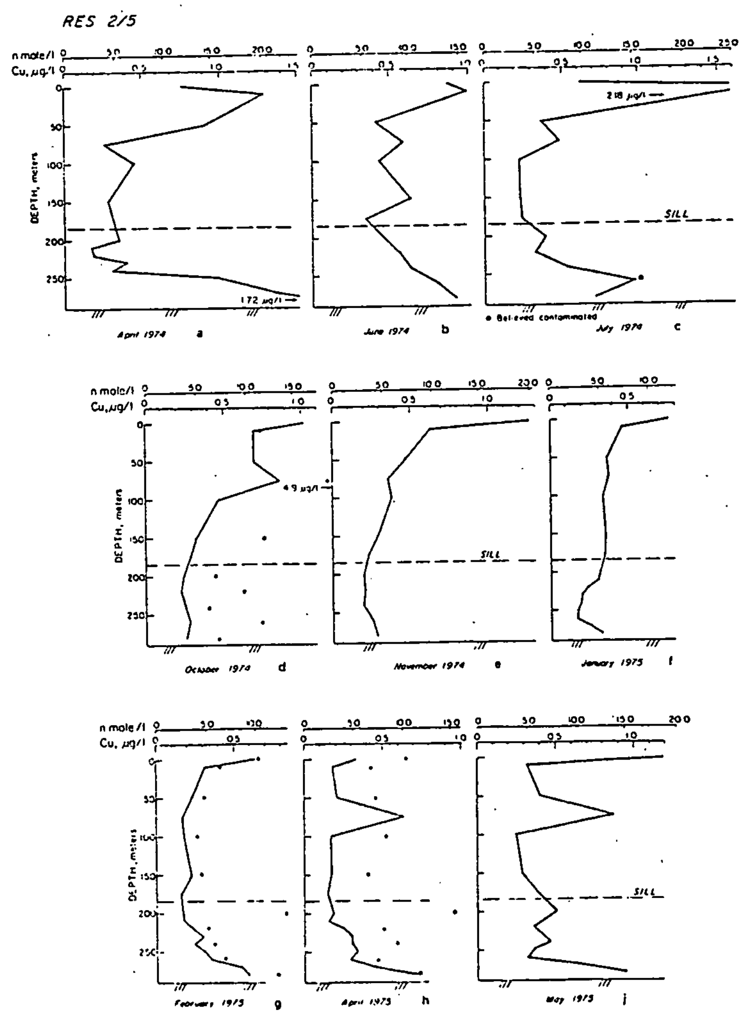

Fig. 4. Composite interstitial water profile of copper at same station as Fig. 3. (Heggie and Burrell, 1979).

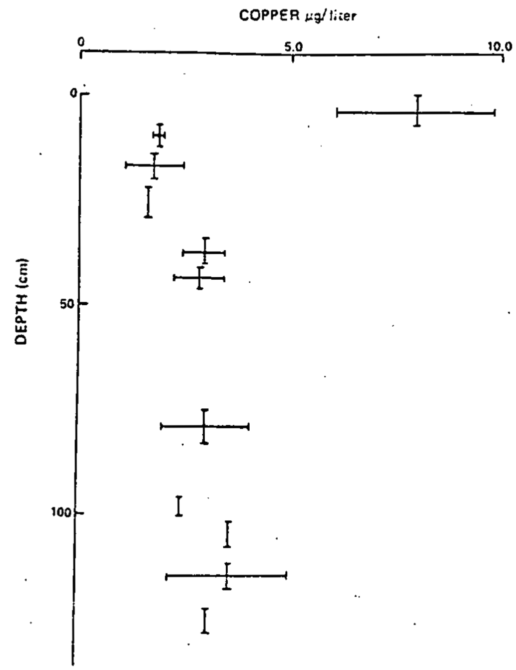

The mobilization and flux of copper at this sediment surface has been described (Heggie and Burrell, 1979). Positive gradients in the column to the interface develop during the oceanographic winter period (Fig. 3). This is the time when the basin is largely advectively isolated and, as a simplification, subject to vertical diffusive transport only. For computed eddy mixing coefficients in the range 3-5 cm^2/sec at sill height, copper appears to be mobilized at a net mean rate of around 0.5 µg Cu/ℓ/yr from a surface sedimemt reservoir constantly replenished by sedimentary particulate copper. Approximately 20% of the copper removed from the basin in this fashion is thus recycled in solution. A much smaller fraction diffuses from the surface sediment down to a reaction and removal zone beneath the redox discontinuity (Fig. 4).

Fig. 5. Distribution of salinity within Yakutat Bay in July (1977). Stations YAK-7 and 9 and localities of the profiles of Figs. 6 and 7.

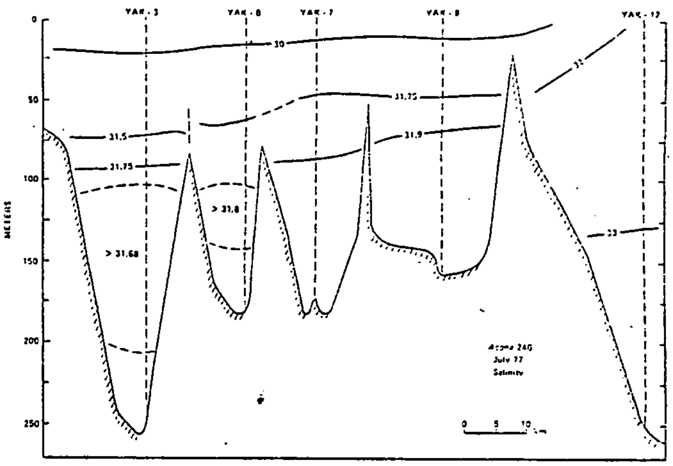

Yakutat Bay is a multi-basin fjord with a shallow entrance sill (and the projected site for major oil production staging and transfers). Replacement of water within the two outermost basins appears to be complete by late spring: Figure 5 illustrates the July salinity distribution. A substantial flux of soluble manganese across the benthic boundary (Fig. 6) maintains pronounced gradients within these basins to sill height through the "advectively stagnant" summer period (Fig. 7).

Fig. 6. Interstitial water manganese at Stations YAK-7 and 9 (mg/kg).

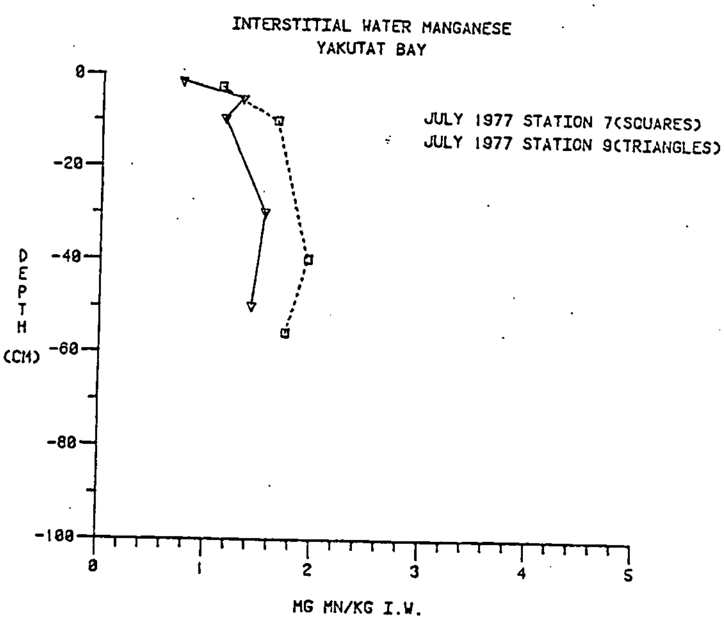

Fig. 7. Soluble (<0.4 μm) manganese profiles within outermost Yakutat Bay basins in July, 1977 (μg/kg).

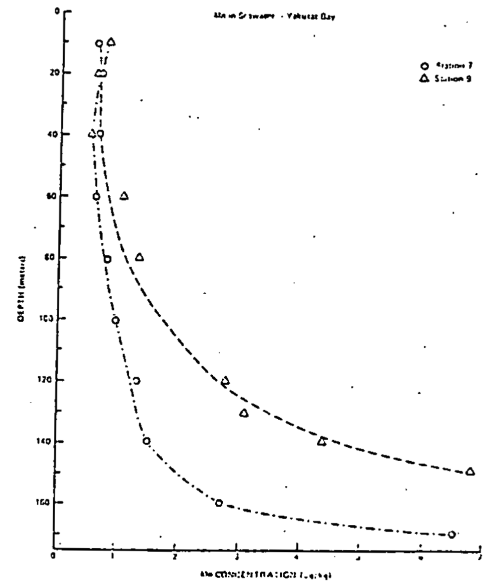

This behavior of manganese has been studied in more detail at the same locality (deep basin of Resurrection Bay, S. Central Alaska) as the copper project cited above. Figure 8 illustrates the late oceanographic winter bottom water soluble gradient: although the redox discontinuity is here at approximately 8 cm, there is an impressive flux of reduced manganese out of the sediments. Figure 9, although a coarsely spaced profile, indicates the distribution of this metal in the surface sediments at this time of year. It is also interesting to note that a significant fraction of the solid phase manganese in this oxic zone is apparently associated with biogenic sediment whereas iron, for example, is not.

Fig. 8. Soluble manganese in Resurrection Bay near end of oceanographic winter period (April 1978; μg/kg <0.4 μm). Same locality as Figs. 3 and 4.

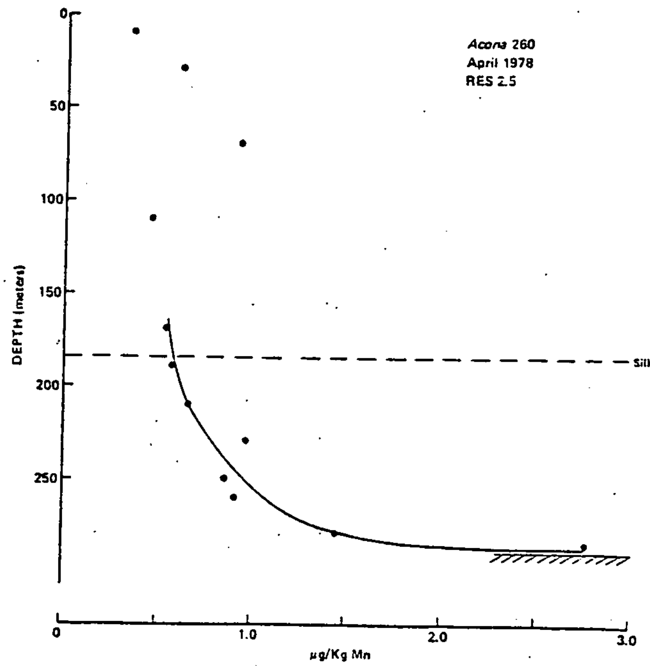

Fig. 9. Soluble interstitial and total particulate manganese within surface sediment of Resurrection Bay in March-April.

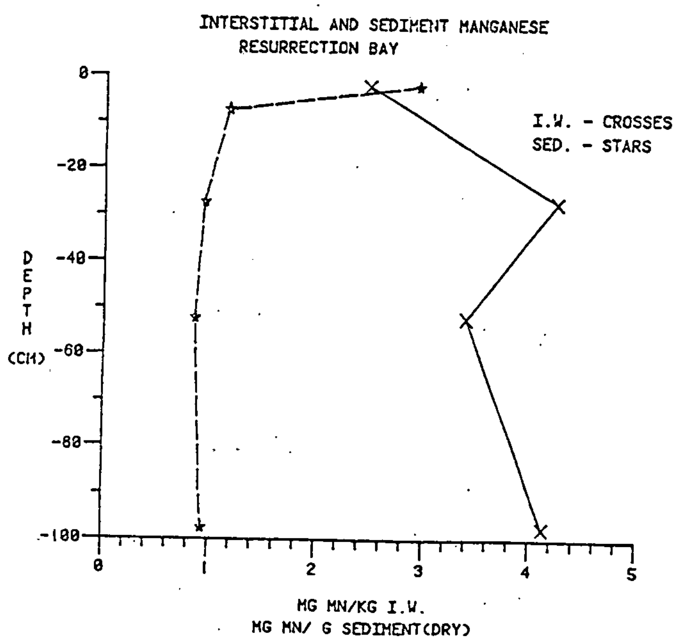

At this season (as with summer Yakatat Bay conditions) the distribution of soluble manganese within the basin may be closely modeled using vertical turbulent diffusion and oxidation removal terms only. Following oxidation within the water column, solid phase manganese is resedimented. Figures 10 and 11 again illustrate late winter conditions: the organic particulate fraction in the basin is small at this time. This benthic closed system cycling of the manganese is best observed in the absence of significant advective flows (Fig. 12).

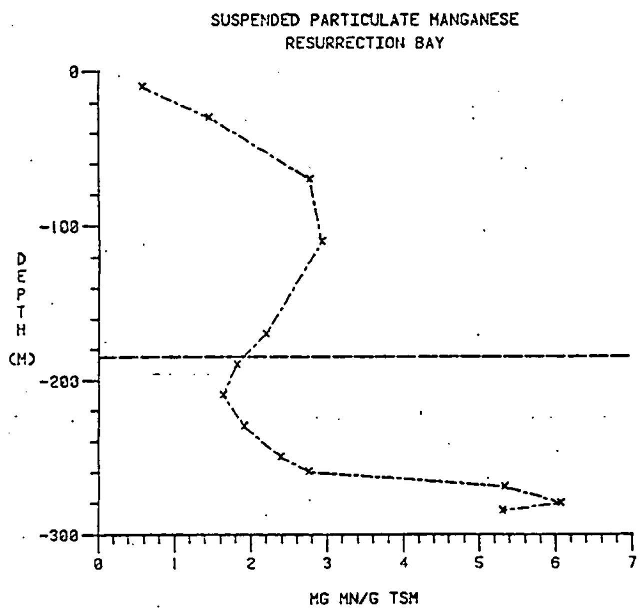

Fig. 10. Particulate manganese (mg Mn/g > 0.4 μm) at Station RES 2.5. Horizontal line marks sill height.

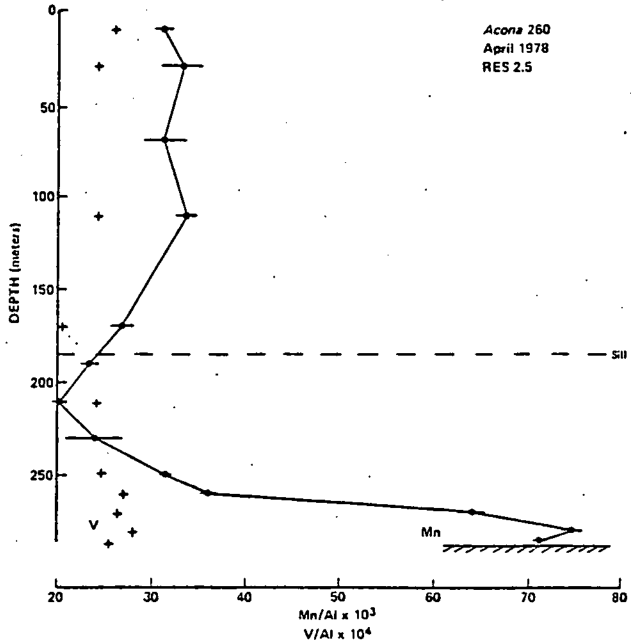

Fig. 11. Particulate Mn/AL rates ($x 10^2$; $V/AL x 10^4$) within water column at RES 2.5, same profile as Fig. 10.

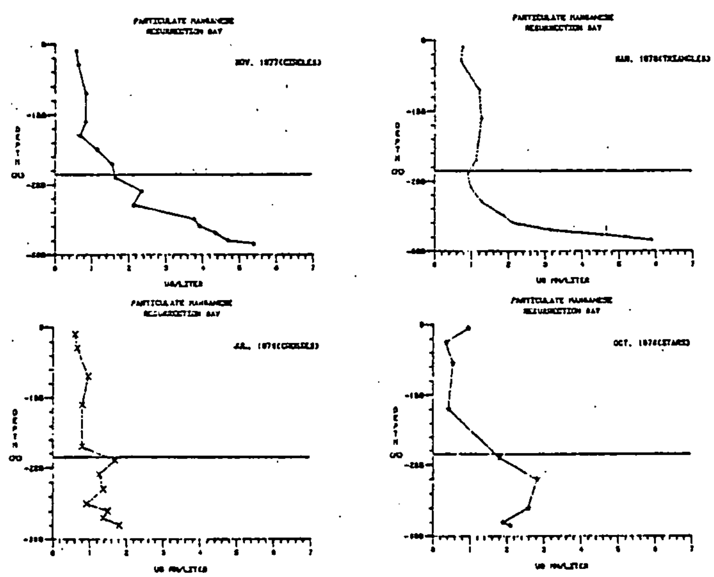

Fig. 12. Seasonal particulate manganese profiles at RES 2.5 (µg/ℓ).

Work on a mass balance model is in progress. Current research is emphasizing the seasonal distribution, flux, and character of the particulates and their role in transporting heavy metals in these estuaries.

References:

Heggie, D. T. and D. C. Burrell. 1979. Depth distributions of copper in the water column and interstitial water of an Alaskan fjord. *In* K. A. Fanning and F. T. Manheim (eds), *The Dynamic Environment of the Ocean Floor*, D. C. Heath, Lexington, in press.

Muench, R. D. and D. T. Heggie. 1978. Deep water exchange in Alaskan subarctic fjords. pp. 239-267 *In* B. Kjerfue (ed.), *Estuarine Transport Processes*. Univ. S. Caroline Press, Columbia, S. Carolina.

Royer, T. C. 1975. Seasonal variations of waters in the northern Gulf of Alaska. *Deep-Sea Res.* 22:403-416.

Deep Water Exchange in Alaskan Subarctic Fjords

R. D. Muench and D. T. Heggie

Deep Water Exchange in Alaskan Subarctic Fjords

Robin D. Muench *
David T. Heggie
Institute of Marine Science, University of Alaska, Fairbanks, AK 99701

Oceanographic conditions in deep waters of six different subarctic Alaskan fjords are discussed and related to circulation and mixing processes. The fjords are divided upon the basis of entrance sill depth into shallow, intermediate, and deep-silled fjords depending upon whether the sill depth is less than, equal to, or greater than a level where there is minimum annual density variation in source waters from the Gulf of Alaska. Deep water renewal in shallow-silled fjords occurs principally during winter, while that in deep-silled fjords occurs during late summer; in intermediate-silled fjords it occurs on a year-round basis. Renewal of deep waters is dependent upon both the annual variation of density in the source waters and upon vertical mixing decreasing the density of the deep water between renewal periods. Inflow of source water at sill depth may be due in part to local winds and tidal currents and occurs despite restricted silled fjord entrances. In deep-silled fjords, inflow appears to be strongly influenced by longshore winds in the Gulf of Alaska as these raise or lower isopycnal surfaces. The frequencies of renewal are adequate to prevent the anoxic conditions observed farther south from occurring in these systems. Estimated values for oxygen utilization in the deep waters and for vertical eddy mixing coefficients agree with previously determined values, supporting the hypothesis for periodic deep water renewals between which distributions are controlled primarily by vertical mixing.

Introduction

(a) Background

Fjords are estuarine systems having steep sides, relatively great bottom depths and, frequently, access to marine source waters limited by an entrance sill (Pritchard, 1967). By definition they are areas where terrestrial runoff and marine source waters mix. They are generally, but not necessarily, stratified in salinity, hence also in density. Maximum vertical stratification occurs during periods when the freshwater influx is high, as during spring

*Now at NOAA, ERL, PMEL, Seattle, Washington 98105.

snow melt or fall rainy seasons. Minimum stratification occurs during periods of minimal freshwater input, especially in midwinter when low air temperatures preclude melting and most precipitation occurs as snow. In some cases, cessation of freshwater input coupled with strong surface cooling may lead to thermohaline convection and subsequent vertical homogeneity in the water column.

Dynamically, fjords can be characterized as having an entrainment-driven estuarine flow confined to a surface layer which is shallow relative to the basin depth. Observational and theoretical treatments addressing this have been provided by McAlister *et al.* (1959), Hansen and Rattray (1966), Rattray (1967) and Winter (1973) This entrainment flow is driven by the pressure gradient consequent to freshwater input at the head of the basin, and therefore is a gravitational convective mode of circulation. In the presence of surface winds blowing down- or up-inlet, augmentation or attenuation of the seaward surface flow may occur, which in extreme cases leads to flow reversal. Volume continuity dictates that the subsurface flow adjust accordingly, and winds contrary to a seaward surface flow may lead to subsurface flow reversals (Pickard and Rodgers, 1959; Winter, 1973).

Freshwater input into fjords, responsible for the near-surface entrainment flow, varies considerably both with season and geographical location. Little quantitative information is available concerning freshwater input into southcentral Alaskan fjords (fig. 1). Stream gauging has been infrequent; one of the few available records was presented for several streams entering Port Valdez (Carlson *et al.*, 1969). This record shows a unimodal annual runoff distribution with a peak due to early spring-summer snow melting. Some unpublished USGS data are also available for the river which enters the head of Resurrection Bay. These show a unimodal pattern but the runoff peak is delayed until August-September. A second runoff peak due to autumn precipitation has been observed farther south in southeast Alaskan fjords, but is not present in southcentral Alaska where most autumn precipitation occurs as snow and

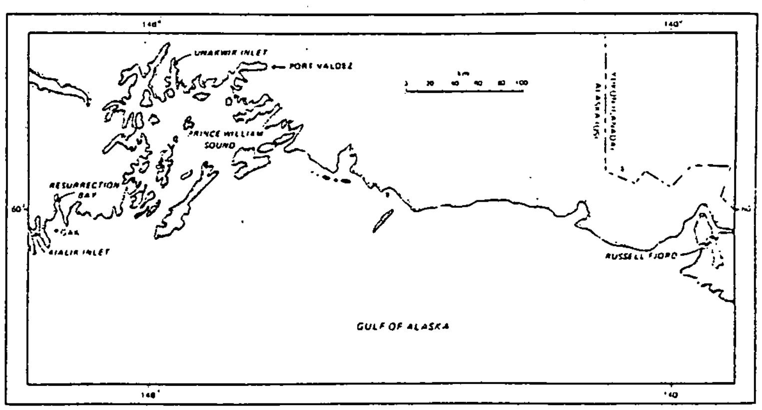

Figure 1. Geographical locations of the Alaskan fjords discussed in this paper, showing location of the time series oceanographic station in the Gulf of Alaska (GAK).

is therefore stored until the following spring. The storage of precipitation as glacier ice and in snowfields is an uncertain factor. Budget studies of these features have been inadequate to quantify such parameters as the timing and rate of release of meltwater (W. D. Harrison, University of Alaska, personal communication).

The southcentral Alaskan climate is severe. Fjords there are affected by mesoscale weather disturbances during the winter centered over the Gulf of Alaska and due to intensification of the Aleutian atmospheric low. They are also subject to katabatic drainage winds when cold, dense air masses from the continental interior drain seaward through the topographical depressions occupied by the fjords. At such times, air temperatures can drop well below -20°C and wind speeds may exceed 42 m s^{-1} (personal observation). Regional climate conditions have been summarized by Searby (1969).

Pickard (1967) has summarized the physical oceanographic aspects of some major southeastern Alaskan fjords. Farther north, however, the relative importance of driving forces for the circulation varies as freshwater input patterns change and the climate becomes more severe. During the winter, with cessation of freshwater input, these subarctic fjords would be expected to behave like embayments rather than as estuarine systems, and the dynamics would deviate accordingly. Rather than a convective circulation mode driven by freshwater input, we might expect to find appreciable circulation driven by winds, thermohaline convection, differential diffusion or combinations of these. Density differences between marine source water and water inside the fjord would be critical in the absence of a strong freshwater-induced seaward pressure gradient.

Despite the common presence of extremely shallow sills coupled with great basin depths, no subarctic Alaskan fjord has been found to contain anoxic waters (table 1). The intriguing problem, immediately raised, is how deep water exchange in these systems can be so effective despite the shallow sills, where we define deep water for our purposes as water within the fjord below sill depth. Apparently, an effective water renewal mechanism is present here which is not necessarily operative in more temperate regions where such silled systems may become anoxic. While the data for many of these fjords are seasonally incomplete, dissolved oxygen data are sufficient to indicate that none of the systems investigated have approached anoxic conditions except for Resurrection Bay, and this only near the sediment-water interface. It is of interest, then, to investigate possible mechanisms for this deep-water renewal.

Table 1. Sill and basin depths for selected Alaskan subarctic fjords, indicating minimum observed near-bottom dissolved oxygen concentrations. Locations of these systems are shown on fig. 1

Name of Fjord	Sill depth (m)	Basin depth (m)	O_2 min (ml/l)	Obs.depth (m)	Obs. month-year
Unakwik Inlet	4	270	5.89	245	7-66
Aialik Inlet	10	200	4.74	184	9-73
Russell Fjord	30	290	6.05	283	4-73
Port Valdez	125	230	5.64	228	8-71
Prince William Sound	180	750	4.71	732	5-73
Resurrection Bay	185	290	<1.00	280	3-76

Within the context of deep-water circulation, fjords may be conceptually viewed as falling upon a spectrum. At one end of this spectrum are those fjords in which deep-water renewal occurs continually throughout the year. At the other end lie those systems in which deep water is renewed only once every several years, possibly leading to anoxic conditions. The renewals are driven by processes which include gravitational convection, surface winds, subsurface water density differences and combinations of these. Other mechanisms, such as vertical thermohaline convection, may play a significant role in isolated cases. Southcentral Alaskan fjords appear to undergo deep-water renewal at least annually and, in some cases, continually. They span a relatively broad portion of the spectrum of fjord types. This paper addresses itself to a qualitative understanding of the mechanisms involved in deep-water circulation within a selected subset of these fjords (fig. 1).

(b) The Marine Source Waters

Water in a basin behind a sill may only be renewed if at some time the water outside the sill at or above sill depth has a greater density than water in the basin. It is known that the density of marine source water can exert a significant control over renewal of fjord deep waters (Saelen, 1967). This section examines the nature of, and variations in, marine source waters available to southcentral Alaskan subarctic fjords. In line with oceanographic convention, we will treat density as the dimensionless quantity σ_t.

Temporal variations in the characteristics of ocean waters may generally be classified as random (e.g., storm-induced and long-term changes) or periodic (tidal or seasonal changes). Available hydrographic data from the Gulf of Alaska are sufficient to delineate the time-mean and seasonal signals for temperature, salinity and hence density (Royer, 1975). During the winter months October-May a wind-driven coastal convergence leads to a downwelling condition in the northern Gulf of Alaska shelf region. The concurrent cooling and cessation of freshwater input act to increase the density of near-surface waters above summer levels when the water is warmer and less saline. However, below about 150 m, the coastal convergence has forced denser water off the shelf; water below that depth is therefore less dense than at other times of the year (fig. 2). Conversely, during summer, a weak wind-driven coastal divergence leads to upwelling which causes denser water to appear below about 150 m on the shelf. The combined effects of melt-water addition and insolation lead however to minimum densities in the waters above 150 m during the summer. The annual variations in density for Gulf of Alaska waters above and below 150 m are therefore about 180° out of phase, and it follows that there is a level of minimum annual density variation at about 150 m depth.

The depth dependence of annual density variation in the Gulf of Alaska has interesting implications for the deep circulation in adjacent silled fjords. A fjord with a sill shallower than 150 m will have maximum density marine source water at and above sill

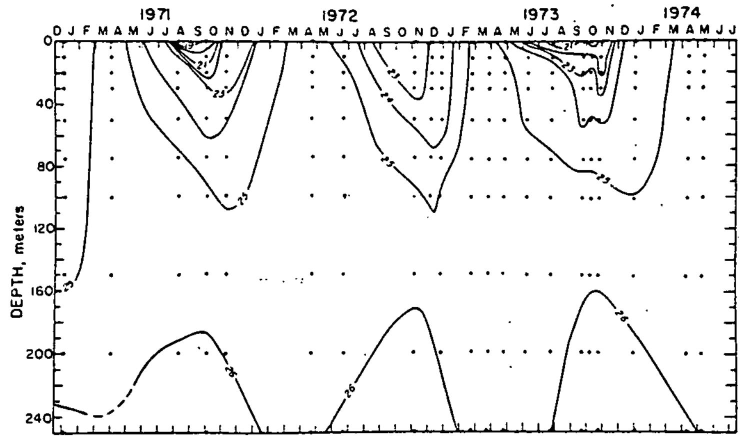

Figure 2. Density (σ_t) time series from an oceanographic station just off Resurrection Bay in the Gulf of Alaska (location indicated as GAK on fig. 1).

depth during winter. If the sill depth is greater than 150 m, maximum density marine source water will occur at sill depth during the summer. A fjord having a sill depth of 150 m would likely feel little variation in source water density at sill depth. It therefore appears that sill depth exerts control over both time of inflow and density of the marine source waters available to a fjord system. This hypothesis is examined below.

Deep-Water Motions

The fjords to be discussed may be divided on the basis of sill depth into three categories which in turn are relevant to deep water motions within the fjords. The categories are shallow, intermediate, and deep-silled fjords, depending upon whether the sill depth is less than, equal to, or greater than the depth at which minimum annual density variation occurs in the Gulf of Alaska source water.

(a) Shallow-silled Fjords

Three of the fjords discussed here may be considered as having entrance sills shallow relative to their interior basin depths (table 1); Unakwik Inlet, Aialik Inlet and Russell Fjord.

Unakwik Inlet, the shallowest silled of the systems considered, is located on northern Prince William Sound (fig. 1) and has the tide-water Meares Glacier at its head (fig. 3). Freshwater input into the system is uncertain, though it likely follows the pattern qualitatively discussed above. Peripheral streams are small and it is possible that appreciable freshwater might enter in the form of a subglacial stream at the head of the inlet. During winter, much of the upper inlet is covered with slush ice mixed with an occasional growler (small iceberg).

Oceanographic data obtained from upper Unakwik Inlet include longitudinal sets of stations occupied during the summers of 1966 and 1969 (fig. 3). The dissolved oxygen concentrations, representative values of which were obtained during July 1966 (fig. 4), are of

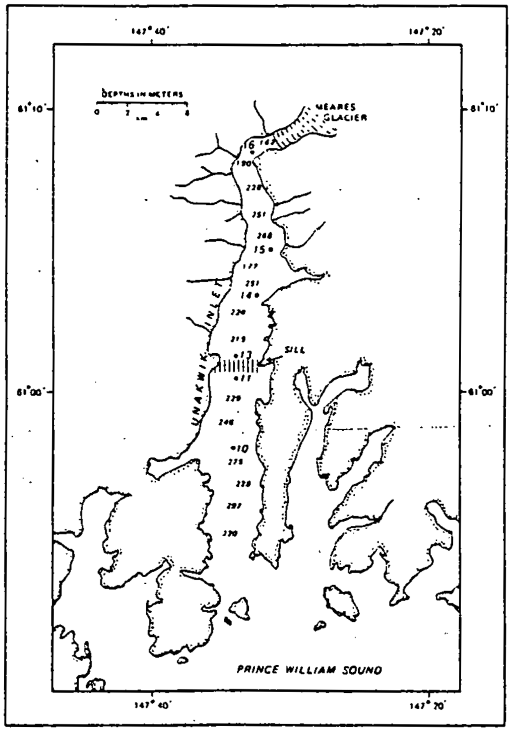

Figure 3. Geographical features of Unakwik Inlet, showing locations of oceanographic stations (larger numbers) and bottom soundings (from NOS Chart No. 16700).

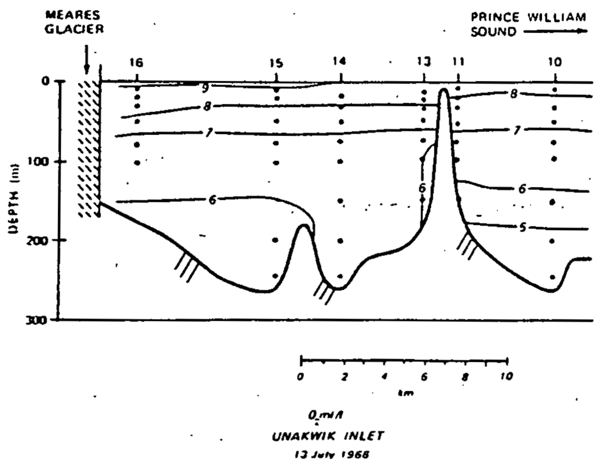

Figure 4. Longitudinal section showing dissolved oxygen distribution in Unakwik Inlet during summer 1966.

particular interest. Minimum dissolved oxygen concentrations slightly below 6 ml l^{-1} occurred deep in the basin. Concentrations were more nearly uniform than in the upper layers, showing a variation of only about 0.2 ml l^{-1} between 100 m depth and the bottom. Similar observations during August 1969 (not shown) indicated the same structure and minimum deep dissolved oxygen concentrations of about 6.1 ml l^{-1}.

These relatively high dissolved oxygen concentrations suggest either that consumption deep in Unakwik Inlet is extremely low, far below the estimates of 4 to 6 ml l^{-1} yr^{-1} for lower latitude fjords (Barnes and Collias, 1958; Coote, 1964) and of about 4 ml l^{-1} yr^{-1} in Resurrection Bay (Heggie, in preparation), or that regular renewal of deep water must be occurring. Since no *à priori* reason exists for oxygen consumption to be excessively low, the case in favor of regular deep-water renewal will be discussed.

Regional oceanographic and climatic conditions suggest two possible mechanisms for deep-water renewal; horizontal advective replacement and vertical convective mixing. The density of water in Prince William Sound, which provides marine source water for Unakwik Inlet, undergoes an annual cycle similar to that in the Gulf of Alaska (fig. 5). Density (σ_t) and temperature-salinity relations between Prince William Sound surface and Unakwik Inlet deep water are shown on fig. 6. The surface-5 m layer, that having access to the Inlet over the sill, attained a maximum density ($\sigma_t \sim 25.6$) during March 1972. Unakwik Inlet bottom water had a density ($\sigma_t \sim 25.5$) which was lower than the Prince William Sound surface water at that time, and therefore the latter was capable, during winter, of sinking and replacing the existing fjord bottom water. Deep water densities during summers of 1966 and 1969 were somewhat lower, as was the Prince William Sound surface density during March 1973. These are likely normal year to year variations. An adequate mechanism for advecting surface water into the Inlet is present in the form of 6 to 8 m tides. Up-inlet winds may also force surface water northward over the sill, although such occurrences have not been documented.

This replacement mechanism depends on vertical mixing decreasing the density of the deep water between periods of replacement, sufficiently that the following winter's surface water is denser than the deep water. While the deep vertical temperature and salinity gradients were too small and the temporal coverage too poor for accurate computations, estimates based on the available data suggest that vertical eddy coefficients on the order of 1 cm^2 s^{-1}, not unreasonable for such systems, would lead to a sufficient annual decrease in deep water density for renewal to occur as suggested. A similar mechanism for deep-water renewal has previously been proposed in Endicott Arm, a silled southeastern Alaskan fjord (Nebert, 1972).

In addition to the advective mechanism suggested above, intense surface cooling coupled with cessation of freshwater input might lead to vertical thermohaline convection in Unakwik Inlet during the winter. If extended to the bottom, this would create a vertically homogeneous water column and transport oxygen downward. The observed vertical near-homogeneity of the water column below 100 m in Unakwik Inlet suggests that vertical convection might have occurred. Advective replacement of deep water occurs generally by interleafing. However, there was no evidence of such interleafing on the vertical profiles but it could have been erased by vertical mixing. Vertical

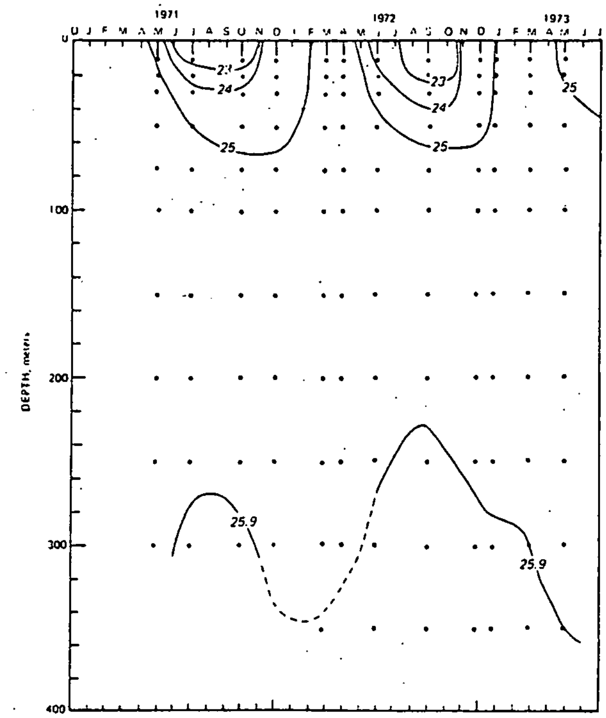

Figure 5. Density (σ_t) time series from an oceanographic station in eastern central Prince William Sound (location indicated as station 13 on fig. 18).

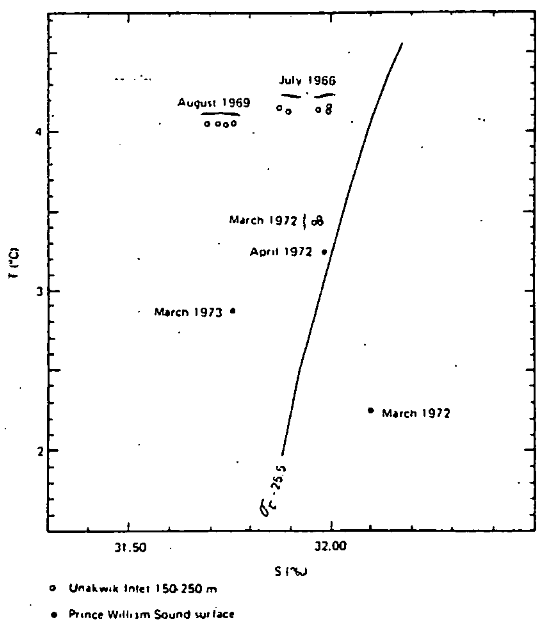

Figure 6. Temperature-salinity relations between summer (July-August) and winter (March-April) deep water in Unakwik Inlet and winter surface water from Prince William Sound.

traces of temperature and salinity throughout the water column obtained during March 1972 revealed a vertical density (σ_t) variation of 0.07 from surface to bottom in upper Unakwik Inlet. This was not, however, as vertically near-homogeneous as was Port Valdez during the same period. Additional information is required to determine whether or not vertical thermohaline convection contributes substantially to bottom water renewal in Unakwik Inlet.

Aialik Inlet is located on the northern Gulf of Alaska just west of Resurrection Bay (fig. 1). It has a sill depth of about 10 m and, like Unakwik Inlet, a tidewater glacier at its head (fig. 7). No major streams and few minor ones enter this system although a subglacial stream might add appreciable freshwater to the system. Weather conditions are undocumented but probably severe, though winter temperatures are likely tempered by proximity to the Gulf of Alaska.

Oceanographic data from Aialik Inlet are limited to a single station which was occupied inside the sill on three occasions; August 1970, May 1973 and September 1973 (fig. 8). The two 1973 stations were occupied in sequence during the same season and provide a time series which, though limited, is informative if viewed within the context of the foregoing.

Marine source water for Aialik Inlet comes from the Gulf of Alaska. The annual variation of density in the Gulf (fig. 2) is such that maximum density water is available at and above the 10 m

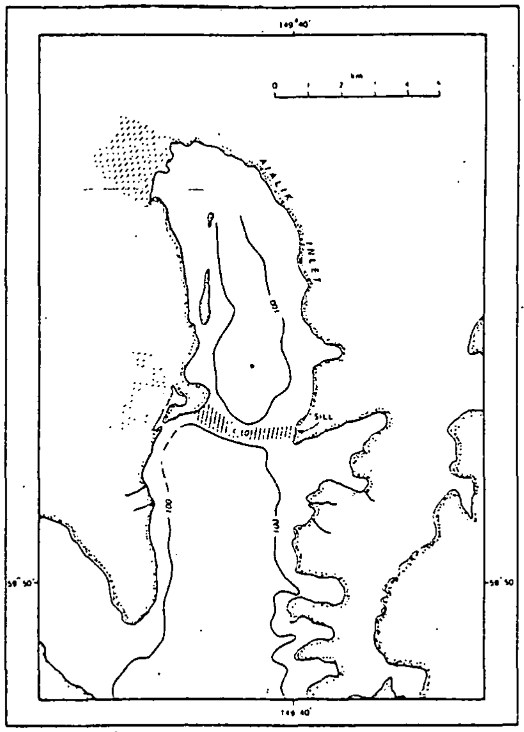

Figure 7. Geographical features of Aialik Inlet, showing location of the oceanographic station inside the sill. Depths are in meters (from C. & G.S. Chart No. 8529).

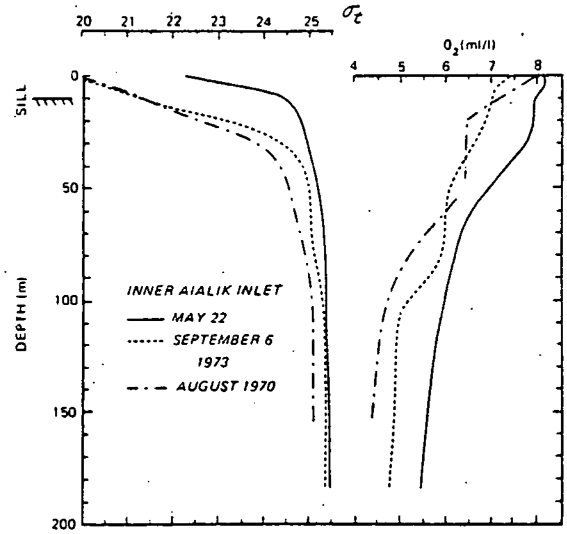

Figure 8. Vertical profiles of density (σ_t) and dissolved oxygen concentration in Aialik Inlet at three different times (station located on fig. 7).

sill during March-April. This water attains densities above σ_t = 25.5, and is therefore denser during winter than Aialik Inlet deep water during summer. It is hypothesized that a deep water replacement mechanism similar to that for Unakwik Inlet occurs in Aialik Inlet, so that the principal renewal of the deep water would occur during March-April. The May 1973 oxygen and σ_t profiles represent conditions directly following renewal. Changes in these profiles near the bottom following May must result from consumption and vertical diffusion. During the May-September period, σ_t decreased by about 0.1 and dissolved oxygen decreased by about 0.8 ml l^{-1}. The variation in σ_t was of the proper order to be due to vertical diffusion. The decrease in dissolved oxygen concentration extrapolated over a one-year period yields a consumption rate of about 3 ml l^{-1} yr^{-1}, allowing for the relatively small effects of vertical diffusion. This rate is similar to values (4 to 6 ml l^{-1} yr^{-1}) cited previously from some other fjords.

The 1970 data indicate that both dissolved oxygen concentration and density were lower then than in 1973, though the vertical structure was similar, and demonstrate that appreciable year-to-year variations can occur. These variations suggest that possibly a year might pass without deep-water renewal occurring. Flow of abnormally dense water into the fjord during a given year, followed by a year of abnormally low density surface water in the Gulf of Alaska, might create a situation where source water density is too low for deep-water replacement to occur. Such occurrences have, however, not been documented.

Russell Fjord is the third shallow-silled Alaskan subarctic fjord about which oceanographic information is available (fig. 9). This documents oceanographic conditions in the fjord during early spring-autumn 1973 and has been analyzed and reported by Reeburgh

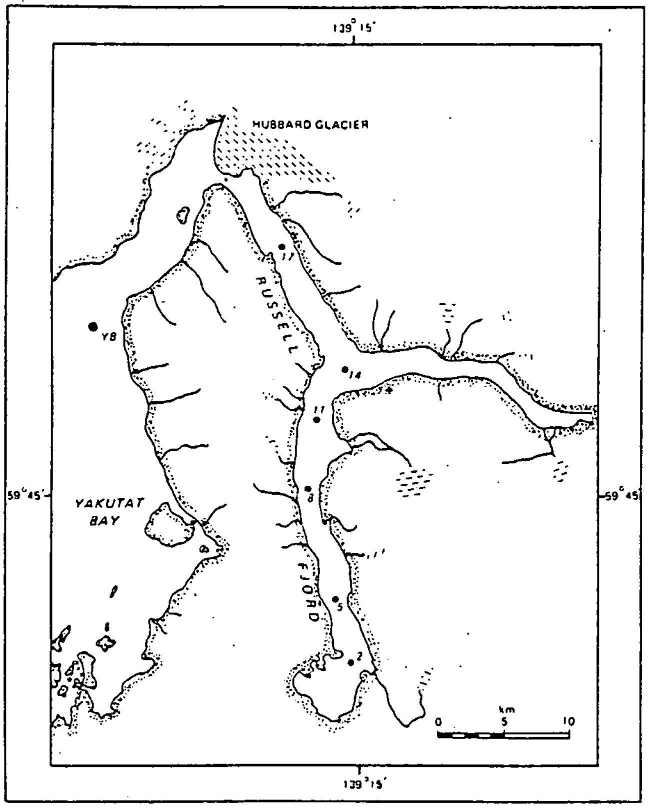

Figure 9. Geographical features of Russell Fjord, showing locations of oceanographic stations.

et al. (1976). Russell Fjord was singled out for study because it is being closed off from marine influence at its mouth by the advanc- Hubbard Glacier. In the summer of 1973 the entrance channel was only 300 to 400 m wide and about 30 m deep, severely restricting interchange between the fjord and marine waters in Yakutat Bay. Oceanographic data obtained from the fjord during May, June-July, and September 1973 revealed, however, that the system was well flushed and that deep water replacement was occurring during the course of the study.

The Gulf of Alaska provides source water for Russell Fjord. Implicit in justifying the use of data off Resurrection Bay (fig.2) to characterize source water for Russell Fjord is the assumption that water properties tend to remain constant along streamlines in the Alaska Current. Recent research in the Gulf of Alaska has substantiated that this is a valid assumption, and that temperature-salinity characteristics off Resurrection Bay are in fact closely similar to those off Yakutat Bay (T. C. Royer, University of Alaska, personal communication). Some temperature and salinity alterations may occur during passage of the water through the relatively broad, shallow reaches of Yakutat Bay, but it is unlikely that the annual pattern of density variation would be significantly altered; the same processes affecting density in the Gulf of Alaska hold for Yakutat Bay, and maximum surface water densities would still occur during March-April.

The oceanographic information from Russell Fjord indicated that marine water was continually added to the system during the April-September 1973 period. Reeburgh *et al.* (1976) utilized the concept of "NO" ($9NO_3^- + O_2$) (Broecker, 1974a) as a tracer to examine these renewals. The Gulf of Alaska source water was at its maximum density in the annual cycle during April and sufficient to sink nearly to the bottom of the fjord (fig. 10). The source water was of a lesser density by June-July and rather than sinking to the bottom it interleaved with the ambient water at 150 to 200 m. By September the density of the source water had decreased still further and was interleaving at about 50 m.

Deep temperature-salinity values from Russell Fjord substantiate the above picture (fig. 11). Assuming that renewal of the bottom water had occurred just prior to acquisition of the April data, the increase in temperature and decrease in salinity and density at 250 m during the period April-September can be accounted for by vertical mixing using an eddy coefficient of about 4 cm^2 s^{-1}. At the 200 and 150 m depths, however, advective inflow during June-July created a different situation. At 200 m, temperature and salinity changes of only about 0.1°C and 0.1 °/₀₀ occurred. While the salinity decrease was of the proper order to be due to vertical diffusion, the temperature difference was too small considering the gradients which were present and, in fact, there was virtually no

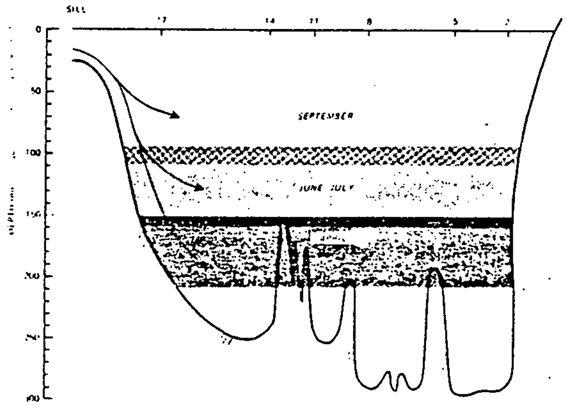

Figure 10. Conceptualization showing dependence of depth at which source waters interleaf in Russell Fjord upon time of year.

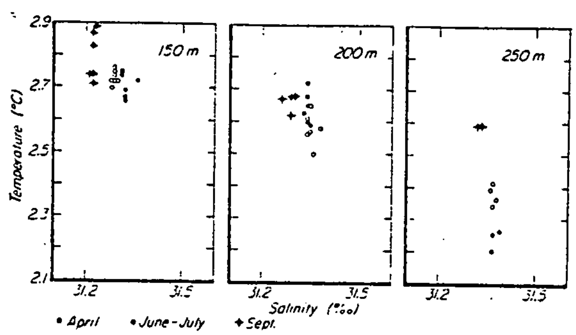

Figure 11. Variations in temperature-salinity characteristics of Russell Fjord deep waters during spring-summer 1973.

temperature change between June-July and September. At 150 m also, the variations could only have been due to advection.

Deep-water renewal in shallow-silled southcentral Alaskan fjords can be summarized, using the above three cases as examples: 1. Renewal of bottom water occurs during March-April when the density of marine source water is maximum at the surface; 2. Interleafing of marine source water occurs at progressively shallower depths within the fjords as the season progresses and source water density decreases; 3. Vertical thermohaline convection may, in certain cases, contribute to renewal of the deep waters; 4. During intervals between annual advective water renewal, distributions of temperature and salinity are controlled by vertical turbulent diffusion. Vertical diffusivities computed from the available data fall in the range between about 1-5 $cm^2\ s^{-1}$. The dissolved oxygen concentration between renewals is controlled by vertical mixing and biological consumption. Consumption is approximately 3 to 4 $ml\ l^{-1}\ yr^{-1}$, and this rate, coupled with the frequency of deep-water renewals, is insufficient to lead to anoxic conditions in any of the fjords studied. It appears, then, that regular flushing of deep waters within these fjords can occur regardless of the sill depth or other constriction at the mouth.

(b) Intermediate-silled Fjords

Port Valdez is the only Alaskan fjord falling in this category which has been sufficiently studied to yield meaningful results. It was the subject of a one-year intensive oceanographic survey which included two short-term sets of current measurements near the entrance sill.

Port Valdez is located on the northeastern extremity of Prince William Sound (fig. 1) and is characterized by a climate and marine source waters similar to those described above for Unakwik Inlet. The 125 m sill is however considerably deeper than the Unakwik sill, and the fjord itself is of larger dimensions (fig. 12). Winter ice

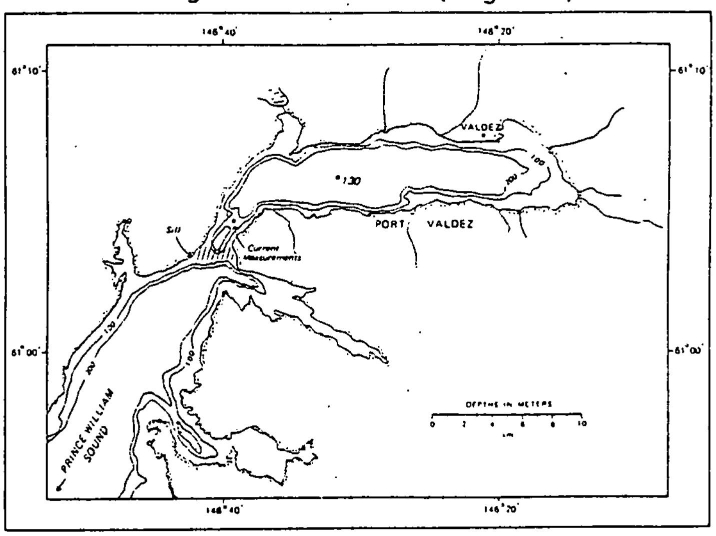

Figure 12. Geographical features of Port Valdez, showing location at which currents were measured.

has been observed to form in the fjord only near its head and during periods of exceptionally calm, cold weather. Wind action quickly breaks up and dissipates any ice so formed. Port Valdez can therefore be classified as an ice-free body of water.

Freshwater input into Port Valdez occurs via numerous streams around its periphery, but even during maximum runoff the freshwater input is less than 5% of the tidal prism. No longitudinal salinity gradient, averaged laterally across the Port and vertically over varying depths, was observed in Port Valdez either in the surface or in deeper layers (Muench and Nebert, 1973). This suggests that the freshwater-induced pressure gradient and consequent estuarine flow was negligible (fig. 13). During the winter months, freshwater input dropped to virtually zero (Carlson *et al.*, 1969).

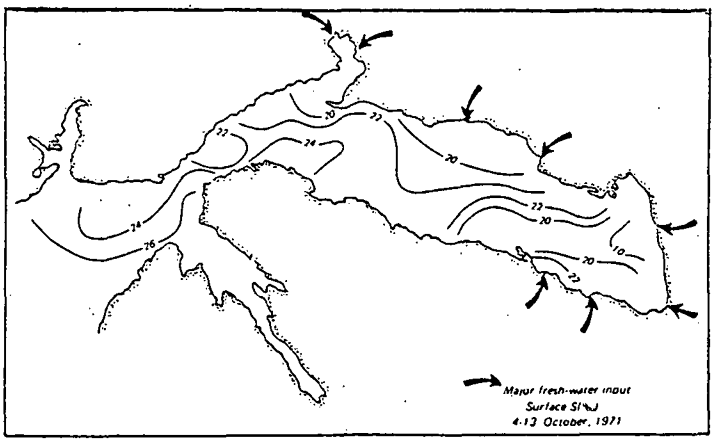

Figure 13. Surface salinity distribution in Port Valdez during autumn 1971, indicating locations of fresh water input (after Muench and Nebert, 1973).

Despite the apparent lack of an entrainment flow, hydrographic and current measurements indicated that flow was occurring through the entrance of Port Valdez and that deep water was being renewed. A time series of temperature, salinity and derived density data was obtained in Port Valdez (fig. 12) from May 1971 to April 1972 (figs. 14 and 15), and data from other locations throughout the Port indicated that these were representative. From August to December, a continual increase of temperature and concurrent salinity (hence density) decrease occurred below the 125 m sill depth. During December to March the vertical density structure became near-homogeneous although some fine structure remained in the near-bottom temperature and salinity traces. There was a slight increase ($\sim$0.2 ‰) in the deep salinity during this period which could only have resulted from inflow and admixture of more saline water (fig. 15). The near-homogeneity exhibited by the vertical density profile (fig. 14) suggests that thermohaline convection was appreciable and had probably acted in conjunction with advective renewal of the deeper water to create the observed conditions. Such vertical uniformity was not, however, observed during the following winter (1972-1973).

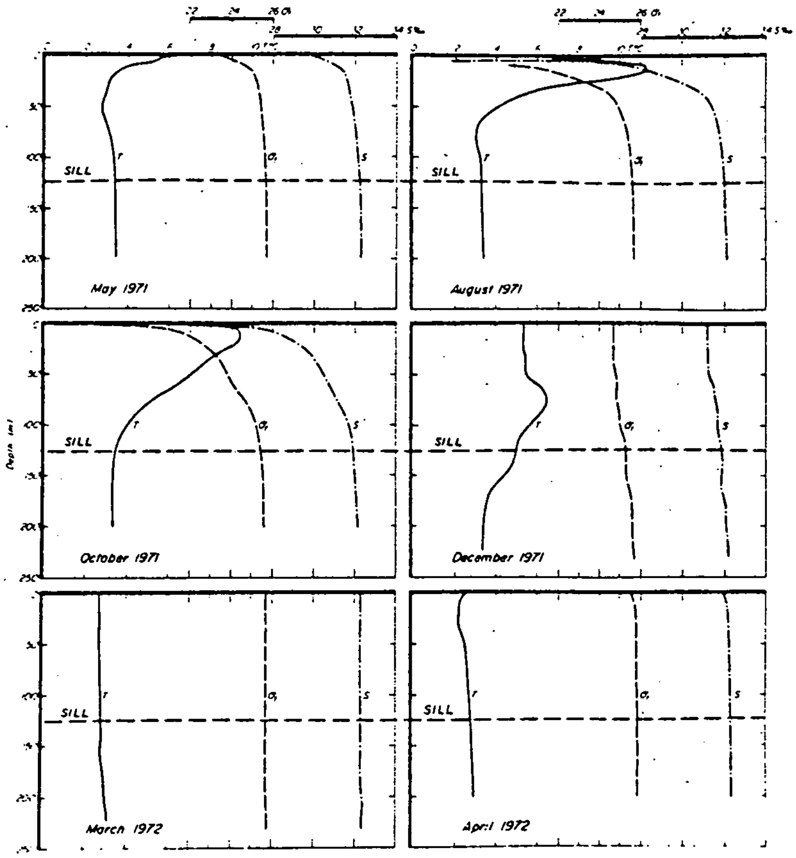

Figure 14. Variation in vertical temperature, salinity and σ_t (density) structure in Port Valdez from May 1971 to April 1972 (after Muench and Nebert, 1973). Curves are obtained from continuous vertical STD profiles.

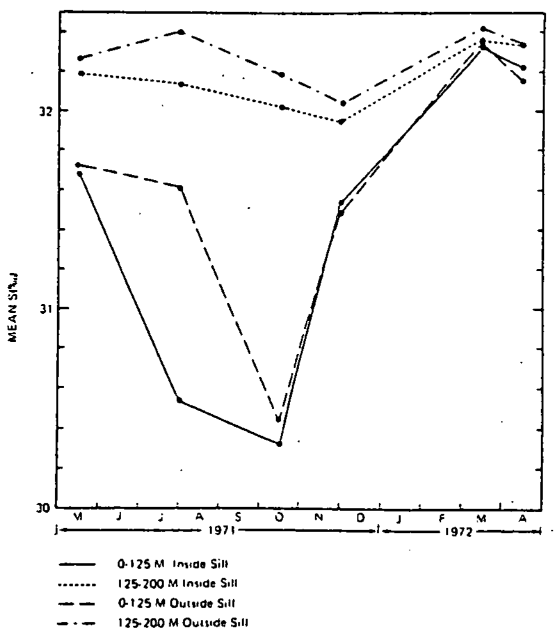

Figure 15. Mean salinities for surface (0-125 m) and deep (125-250 m) waters inside Port Valdez and outside the sill during 1971-1972.

This may have been because 1971 was a particularly harsh winter, leading to abnormally severe vertical convection and cooling, but the records in time are inadequate to define what might be "average" in terms of water column parameters.

Two five-day sets of current measurements were obtained from the entrance to Port Valdez (fig. 12); one during December 1971 and the other during March 1972 (figs. 16 and 17). These measurements were filtered, broken into harmonic constituents and a limited analysis carried out by Mungall (1973). Several points are apparent: 1). The mean currents varied markedly in speed and direction. These variations could have been due in part to surface winds, but wind observations were inadequate to test for correlation. 2). A surface outflow was occurring during both December and March. In the absence of freshwater input, this was a likely response of the surface water to northeasterly winds, which prevailed throughout the measurement periods. 3). The weak 8-m deep inflow in December had cross-channel components and coincided with a high temperature core (fig. 14). This warm layer was apparently being advected into Port Valdez. There was a deep outflow during 4-5 and 7-8 December, leading to a three-layered flow system (two flow reversals with depth). The 6-7 December bottom flow was inward but weak (< 3 cm/sec). 4). A deep inflow occurred during March, substantiating the supposition that an inflow of deep water was occurring over that period. This inflow may partially have been a continuity-imposed response to a wind-driven surface outflow, and partially driven by the occurrence of greater density water outside the sill. Appreciable horizontal circulation was therefore able to occur in and out of Port Valdez despite apparent lack of estuarine flow in the near-surface layers.

The Port Valdez entrance sill falls in the depth interval through which density variations in Prince William Sound, the source water, are near-minimum for the water column (fig. 5). In the absence of a well-defined pattern of density maxima and minima at sill depth, renewal of the deep water could occur more frequently than annually. Small perturbations in the sill depth density of source water at different times of year might be sufficient to cause inflow and displacement of the deep water in Port Valdez. The salinity time series for Port Valdez (fig. 15), which approximates density, below sill depth closely follows that in Prince William Sound and suggests that inflow may occur on a quasi-continuous basis. Additional evidence is present in the form of near-bottom dissolved oxygen concentrations in Port Valdez (table 2). If renewal of the bottom water occurred on an annual basis, oxygen values would be maximum at the time of renewal and would undergo a monotonic decrease in time until the following year's renewal. This pattern was not evident in Port Valdez; dissolved oxygen concentrations varied irregularly in time.

We conclude, based on the Port Valdez observations, that deep-water renewal in intermediate-silled fjords can occur quasi-continuously throughout the year because of the lack of a well defined

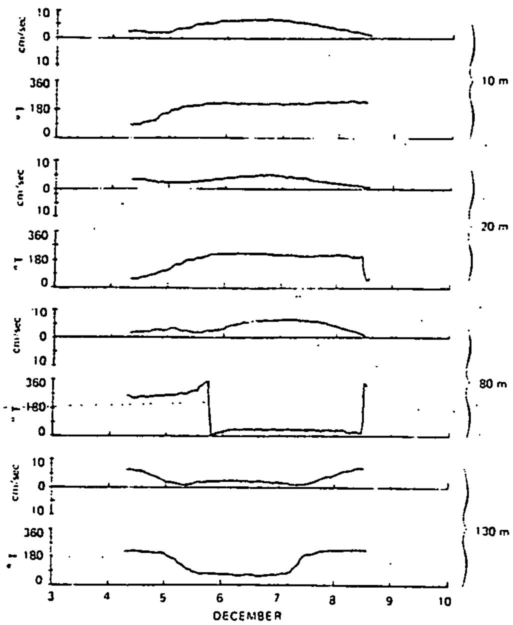

Figure 16. Current speed and direction measured in the entrance to Port Valdez during December 1971 at the location indicated on fig. 12.

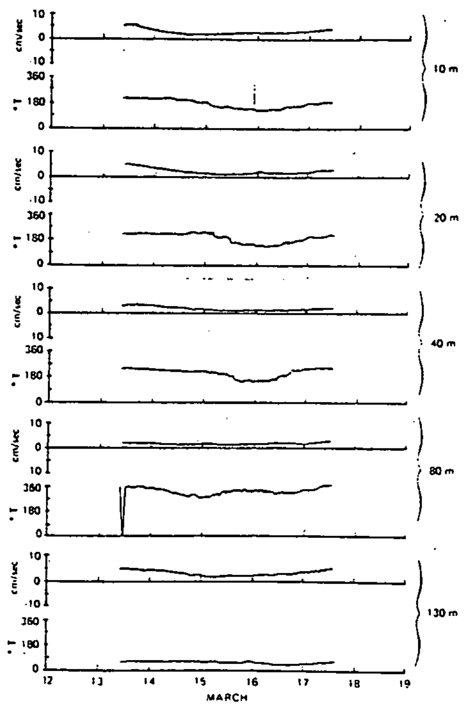

Figure 17. Current speed and direction measured in the entrance to Port Valdez during March 1972 at the location indicated on fig. 12.

Table 2. Mean dissolved oxygen concentrations (ml l^{-1}) one meter above the bottom of Port Valdez

1971			1972	
4 August	9 October	8 December	19 March	24 April
5.86	6.02	5.81	6.59	6.26

annual density variation in the source water at sill depth. Either shorter than annual period source water density variations at sill depth or strong surface winds may lead to an inflow of deep water over the sill.

(c) Deep-silled Fjords

Deep-silled fjords are those in which the sill depth lies below the depth of minimum annual density variation in the Gulf of Alaska, i.e. about 150 m; Prince William Sound and Resurrection Bay (fig. 1) fall into this category.

Prince William Sound is a geographically complex system consisting of a central basin and outward radiating subsidiary fjords including Port Valdez and Unakwik Inlet (fig. 18). Hinchinbrook Entrance, the major passage for communication with the Gulf of Alaska, is deeper than 200 m; the actual limiting sill depth of about 180 m is due to a topographic rise seaward of this passage. Interchange between the Gulf of Alaska and Prince William Sound is limited in other channels by shallower bottoms (∿100 m or less) and narrow, tortuous configurations. Freshwater input is distributed around the periphery of the Sound and there are no major river inputs. A seaward salinity gradient has never been observed, and the surface salinity distribution is complex (Muench and Schmidt, 1975).

Because of its great lateral extent relative to the other systems under consideration, Prince William Sound probably contains an appreciable horizontal circulation unrelated to its status as a fjord. Muench and Schmidt (1975) have hypothesized, based upon

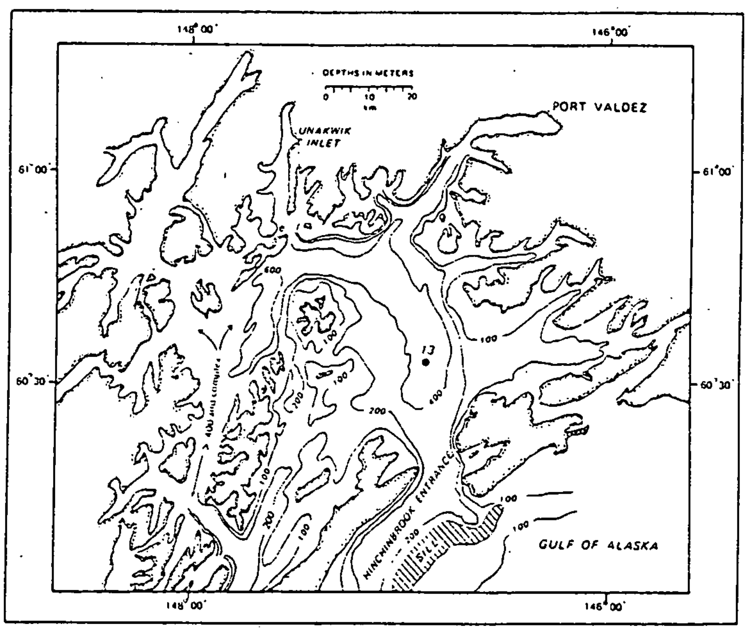

Figure 18. Geographical features of the Prince William Sound region, showing location of the oceanographic station used to construct the time series given in Fig. 5.

temperature and salinity data, the existence of a cyclonic circulation in the eastern central portion of the Sound. Local winds or tides might drive such a circulation. The offshore presence of the intense, westerly Alaska Current might create longshore sea level slopes capable of driving a circulation in the Sound similar to that suggested by Csanady (1974) for the Gulf of Maine. The presence of numerous islands separating Prince William Sound from the Gulf of Alaska would probably lessen this effect. No direct measurements of the circulation are however available to test these hypotheses.

Admitting ignorance as to the horizontal circulation, it is nevertheless possible to speculate upon renewal of the deep waters. The σ_t time series in the central eastern portion of the Sound (fig. 5) reveals a structure similar to that in the Gulf of Alaska (fig. 2). There are, however, some obvious differences. Vertical stratification during the summer is less between 100 and 250 m in Prince William Sound than in the Gulf of Alaska. Maximum observed deep densities are less ($\sigma_t \sim 25.9$) in Prince William Sound than in the Gulf of Alaska ($\sigma_t > 26$). Finally, maximum densities deep in Prince William Sound appeared to lead those in the Gulf of Alaska by about two months in 1972. The data were insufficient to detect such a lead time in 1971. The reason for this lead time of maximum density deep water in the Sound over presence of such water in the Gulf at sill depth is problematic. This was only evident during 1972, and it is possible that some irregularity in the Gulf of Alaska circulation occurred which might have affected the validity of our assumption that oceanographic data off Resurrection Bay were representative all along the coast. The region of the Gulf off Hinchinbrook Entrance is, in fact, dominated by an extremely complex circulation regime which includes a semi-permanent eddy and interaction with fresh water input from the Copper River to the east (T. C. Royer, University of Alaska, personal communication).

The similarities between density variations in the Gulf and in Prince William Sound do, however, suggest that deep-water renewal is occurring during late summer when the density of Gulf water at the 180 m sill is maximum. This sill only allows inflow of water with $\sigma_t \sim 25.9$ or less, which accounts for waters deep in Prince William Sound being of lower density than water at the same depth outside. The deepest water in the Sound can attain a maximum density only as great as the maximum density of the source water at sill depth. The slightly greater density of water at 180 m in the Gulf during 1972 than 1971 was reflected in the deep water density of the Sound. The density decrease between renewal periods is due to upward diffusion of salt and downward diffusion of heat, as in the shallower silled systems.

The decreased vertical density stratification in the Sound relative to the Gulf may be explained by the isolation of the Sound. Stratification in the Gulf is maintained by lateral advection. Water of maximum density which enters the Sound sinks to well below sill depth, leaving a relatively small range of densities to occupy the volume between sill depth and the bottom of the Sound. Thus a range of densities (25 < σ_t > 26) extends vertically from 100 to 200 m ir the Gulf, but from less than 100 to about 300 m in Prince William Sound.

Other oceanographic data from the Sound, specifically dissolve oxygen, were too incomplete to contribute substantially to clarification of deep water exchange processes. Available oxygen data indicated, however, that there were horizontal variations within th Sound. This is not surprising considering the probability of a lateral circulation.

Resurrection Bay opens directly onto the Gulf of Alaska (fig. 1), and is divided into two basins; the inner 290-m deep basin is separated from a shallower, 250-m outer basin by a 185-m sill (fig. 19). Some 60 km offshore in the Gulf of Alaska the bottom shoals to about 175 m, but this feature is not believed to effectively decrease the sill depth to less than 185 m because of its relatively great offshore distance.

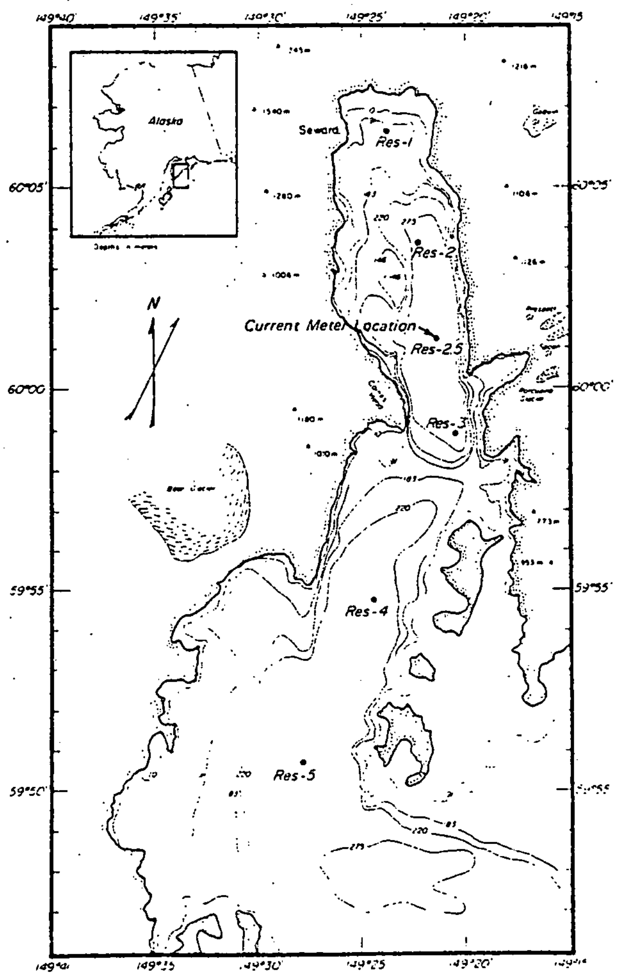

Figure 19. Geographical features of Resurrection Bay showing station locations, depth contours (m) and position of current meter array.

Freshwater input into Resurrection Bay occurs via numerous peripheral streams, but principally via Resurrection River at the head of the fjord. U.S.G.S. stream flow records from 1965 to 1968 indicated maximum freshwater input during June-September. Input varied from winter minima as low as $\sim 10\ m^3\ s^{-1}$ up to as high as $\sim 500\ m^3\ s^{-1}$ during September. The mean summer input ($\sim 110\ m^3\ s^{-1}$) amounts to only about 1% of the tidal prism.

Seasonal weather patterns in Resurrection Bay are governed primarily by the atmospheric conditions over the Gulf of Alaska. Dominant winter easterlies over the Gulf are directed by the steep mountains bordering the fjord into an axial direction, leading to predominantly northerly winter winds. Conversely, relatively weak westerlies over the Gulf during summer lead to variable, but primarily southerly, winds within Resurrection Bay. While air temperatures can be low during winter (below -20°C), significant ice formation has not been observed in Resurrection Bay.

Like Prince William Sound, maximum densities occur throughout the fjord below about 150 m during late summer and fall. Fig. 20 indicates the presence of maximum salinities (> 33 ppt) which correspond to maximum densities ($\sigma_t > 26$) below about 150 m during summer-fall. This is a consequence of the relatively dense water ($\sigma_t > 26$) on the shelf in the Gulf of Alaska during that period (fig. 2). In contrast to summer conditions, minimum deep water densities were observed during mid to late winter (February-April). Densities inside the sill, however, remained consistently higher than those outside. For example, minimum σ_t values at 250 m inside the sill varied during the three-year study period between 25.88 and 25.98 during February-April, while outside the sill σ_t values at the corresponding times were as low as 25.56 and 25.64. Significantly greater variabilities in temperatures and salinities of waters below 150 m were evident outside the sill, compared to variations behind the sill (fig. 20). The ranges of salinities and temperatures observed were 33.22 ppt to 32.61 ppt and 5.67°C to 4.57°C inside the sill, whereas they were 33.32 ppt to 32.06 ppt and 5.98°C to 4.15°C outside the sill. These greater variabilities outside the sill can be explained in terms of vertical migrations of isopycnal surfaces in the adjacent Gulf of Alaska. Easterly winds over the Gulf lead to a coastal convergence and a depression of the isopycnals, conversely, westerly winds lead to a coastal divergence and an elevation of the isopycnals. Cessation of the winds results in relaxations of the downwelling or upwelling conditions and a consequent raising or lowering, respectively, of the isopycnal surfaces. The vertical migration of isopycnals is probably dependent upon the relative setup of water at the coastline which, in turn, depends on the wind speed, direction and duration. While oceanographic documentation is not available from the region off Hinchinbrook Entrance, the same mechanisms operative off Resurrection Bay would be expected to affect the source waters for Prince William Sound.

The salinity (hence density) of the deep water inside the sill decreases during winter (fig. 21). Since source water flowing inward above the sill is of insufficient density during winter (fig. 21) to replace deep water below the sill, the observed changes in temperature and salinity and the density decrease must result from vertical mixing of heat and salt. Temperature and salinity observations from Resurrection Bay were used to compute coefficients of vertical eddy mixing assuming one-dimensional vertical mixing, neglecting horizontal transfer and assuming no heat or salt transport across the sediment-water interface. As energy for turbulent mixing is probably derived from tidal and mean currents above the sill, this leads to the assumption that the eddy coefficient varied with depth from just below sill depth (200 m) down to zero at the bottom. The value at 200 m was obtained from heat and salt budgets applied to the volume below that depth. Obtained values varied from 1.0 to 8.0 $cm^2\ s^{-1}$, fall within the range given by Craig (1969) 0.1 to 10 $cm^2\ s^{-1}$, and are consistent with values listed by Sholkovitz and Gieskes (1971) of 4 to 6 $cm^2\ s^{-1}$ at the sill depth of another deep-silled system, the Santa Barbara basin.

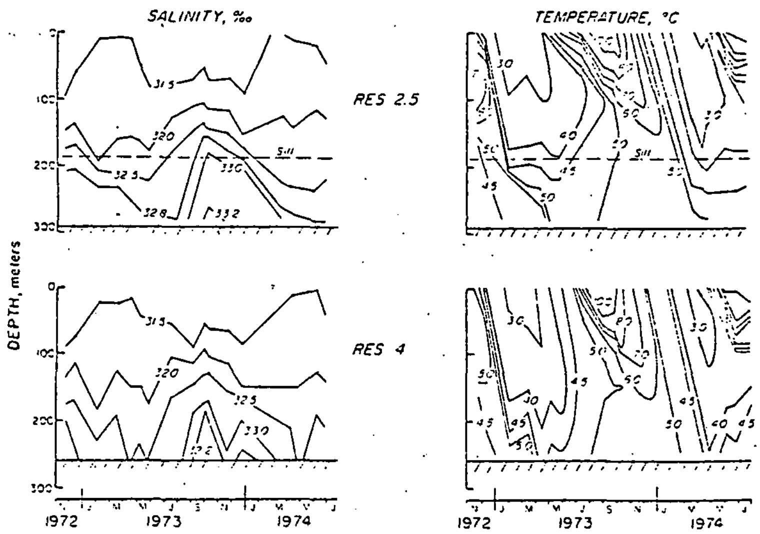

Figure 20. Seasonal variations in temperature and salinity for stations in the inner (Res-2.5) and outer (Res-4) basins, during 1972-1974.

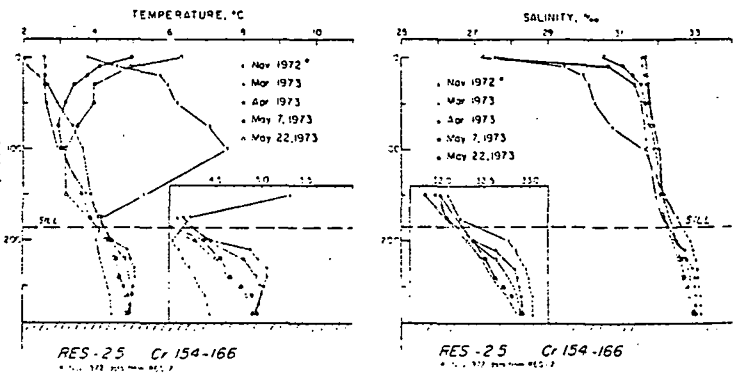

Figure 21. Vertical distributions of temperature and salinity in the inner basin (Res-2.5) during the winter of 1972-1973.

Current measurements were made inside the sill in Resurrection Bay during winter (March-May) and late summer (September-October); these permitted some examination of driving forces responsible for the deep water exchange. During winter strong northerly flows (inward) of 10 to 40 cm s^{-1} were observed at sill depth (185 m) which persisted for one or two days duration (fig. 22), and were not related to the regional semi-diurnal tides. Visual inspection of the current and wind records (fig. 22) suggested some correlation between currents and relative changes in wind speed and direction. Most of the dominant inflows (north currents), except over days 29-31 and 52-54 appeared to be correlated with north winds and/or relaxations of south winds. This apparent coupling was evident on days 0-8, 19-22, 38-40 and 42-46. During these same periods the currents just above the basin floor (286 m) at the same location showed none of these features but were instead dominated by the semi-diurnal tidal signal. The currents at 185 m which result from this apparent coupling, it has been hypothesized (Heggie, 1977) may result from local convergences in the outer reaches of the fjord. These could be a consequence of onshore transports in the Gulf of Alaska (associated with easterly winds) opposed by seaward surface transports within the fjord (driven by north winds).

During late summer currents at 185 m were directed southward while those at 286 m were directed almost continually northward. This can only be explained by an inflow of dense source water across the sill into the bottom of the deep basin. The outflow at 185 m is required by volume continuity as the deep resident water is replaced by inflowing water. These data were supported by successive deep water salinity increases in this basin during the same period (fig. 23). The current and wind records during this period (fig. 24) did not show as distinct relationships as in the winter records. We have computed, however, that approximately two-thirds of the total transport through this basin occurred when winds in the fjord were southerly. Late in September, when they turned northerly, inflow into the basin decreased. North winds in the fjord are generally a reflection of easterly winds in the Gulf which tend to depress isopycnal surfaces at the coastline and in the outer reaches of the fjord and, hence, to lower the horizontal pressure gradient which drives inflow across the sill.

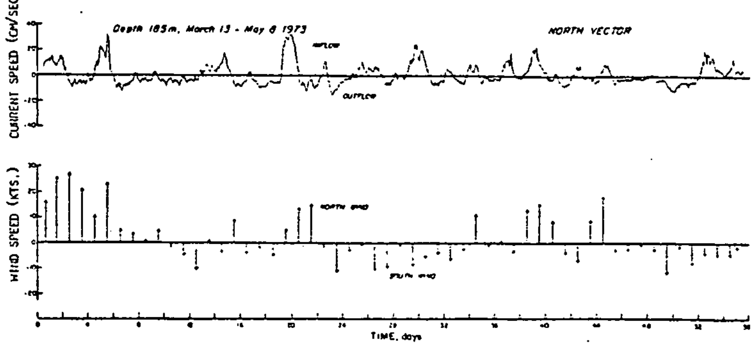

Figure 22. Longitudinal (north vector) current speeds at 185 m and daily mean wind speeds during March-May 1973.

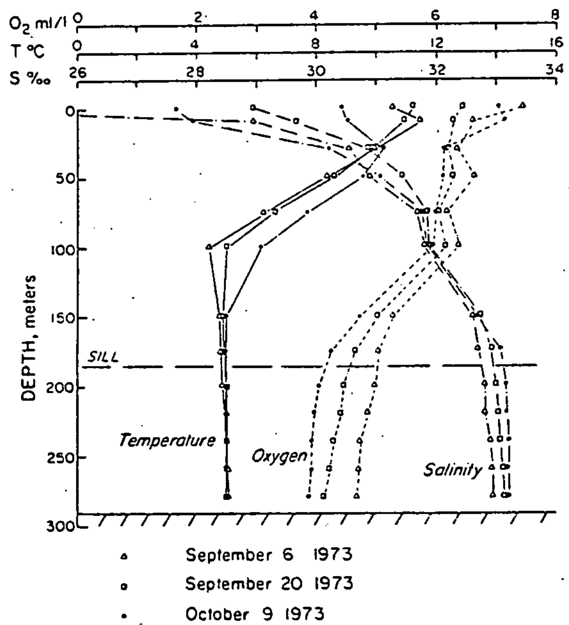

Figure 23. Vertical profiles of salinity, temperature, and oxygen at Res-2.5 during September-October 1973.

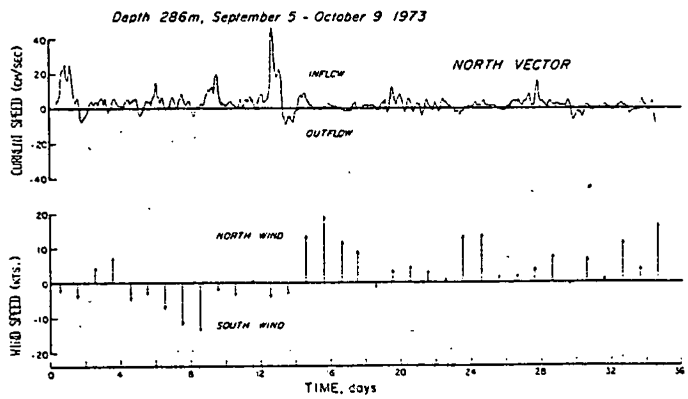

Figure 24. Longitudinal (north vector) current speeds at 286 m and daily mean wind speeds during September-October 1973.

To summarize, both Prince William Sound and Resurrection Bay undergo deep-water renewal during late summer when source water density at the sill is at its maximum. Short-term variations in the characteristics of this source water may be brought about by weather conditions over the Gulf of Alaska, as these affect the slopes of isopycnal surfaces. Winds over the Gulf and in the fjord can also affect the source water inflow rates over the sill. A deep water density decrease during the remainder of the year is due to vertical mixing and is necessary in order for deep-water renewal to be able to occur the following year.

Discussion and Summary

Research in a group of Alaskan fjords has allowed formulation of hypotheses concerning their water circulation inside the sill and below sill depth. Temperature, salinity and derived density data from both inside and outside the sills have made it possible to divide these systems into three classifications based upon sill depth; shallow, intermediate and deep-silled. Shallow-silled fjords are those wherein the sill depth is less than the depth at which minimum annual variation in the Gulf of Alaska source water density occurs. Intermediate-silled fjords have sill depths about equal to the depth of minimum density variation in the source water. Deep-silled systems have sill depths greater than the depth of minimum density variation.

The fjords considered have in common relatively low freshwater inputs even during times of maximum runoff. The inputs fall to virtually zero during mid-winter. Hydrographic data suggest that the gravitational convection mode of flow is negligible. The absence of such a near-surface estuarine flow dictates that motion within the deep waters become highly dependent upon source water density variations, which are necessary for replacement of the deep waters. It is also necessary to have a mechanism to continually decrease deep water density so that displacement type renewal by denser water can occur. Vertical mixing of heat and salt can provide such a mechanism, eddy coefficients being on the order of 1 to 10 $cm^2\ s^{-1}$. An interesting feedback mechanism may act to increase the efficiency of this density decrease. Lack of a near-surface entrainment flow may allow accumulation of low salinity water in the near-surface layers, increasing the vertical salinity gradient. This increased vertical gradient might allow a more rapid upward diffusive flux of salt, thus hastening the density decrease in the deep waters. This was previously suggested for Endicott Arm by Nebert (1972).

There are ample sources of energy to cause vertical mixing deep in these fjords. Regional tide ranges are 6 to 8 m. Even in Russell Fjord the tidal range was effectively undiminished despite the constriction due to the Hubbard Glacier at the sill (personal observation). The deep current measurements in Resurrection Bay have revealed both tidal currents and a mean flow which might contribute energy to turbulent mixing. The nature and variation of mixing parameters deep within these systems remains, however, uncertain. Interleafing of waters must cause a complex vertical variation in both current and density gradients, hence affecting vertical mixing.

The complex mixing processes in these fjords are not easily resolvable from the distributions of temperature and salinity alone. Radon-222, a member of the U-238 decay chain, has been proposed (Broecker, 1965) and used (Broecker and Kaufman, 1970; Broecker *et al.*, 1968; Chung and Craig, 1972) to examine mixing processes in near-bottom waters of different environments. The major marine source of radon-222 is in the bottom sediments, therefore concentrations are high in near-bottom waters and, because of exchange across the air-sea interface and natural decay, low in surface waters. These concentration differences between surface and deep waters may prove useful, particularly in shallow-silled fjords during winter months to examine transient phenomena such as bottom water placement or interleafing of source waters into the bottom waters of the fjords Steady-state radon-222 distributions in deep waters might also cla ify the intensity of mixing processes as a function of distance fr the energy source. Broecker (1974b) has cited examples of how rad profiles reflect different mixing processes in near-bottom waters, and Chung (1973) observed a transient phenomenon (turbidity curren and computed eddy mixing coefficients from radon distributions in the Santa Barbara basin. Radon levels in Alaskan coastal waters remain unknown at this time, but concentrations are controlled by its short half-life (3.85 days) and the sedimentation rate. Concen trations are generally less in nearshore environments than in the deep sea, which unfortunately may preclude its use as a tracer in fjords.

The classification of these fjords according to sill depth has important implications relative to the deep-water circulation (fig. 25). Maximum density source water for shallow-silled fjords is found at sill depth during the winter, and it is then that inflow of source water dense enough to replace the resident deep water can occur. During summer, the source water above sill depth is less dense than water in the basin and, while the source water may continue to enter the fjord, it is of insufficient density to sink and effect replacement of the deep basin water. At the opposite extrem are the deep-silled fjords where the maximum density source water occurs at sill depth during summer. Replacement of the deep water in such systems occurs in summer, rather than during winter as with the shallow-silled systems. Intermediate sill depth systems fall between these two extremes. Since their sills are at a depth where little annual variation in the source water density occurs, inflow of dense enough water to replace deep water can occur consequent to small perturbations in density of the source waters at any time of year. The timing of deep-water replacement, and to some extent the duration of the period of inflow, are therefore controlled in part by the sill depths.

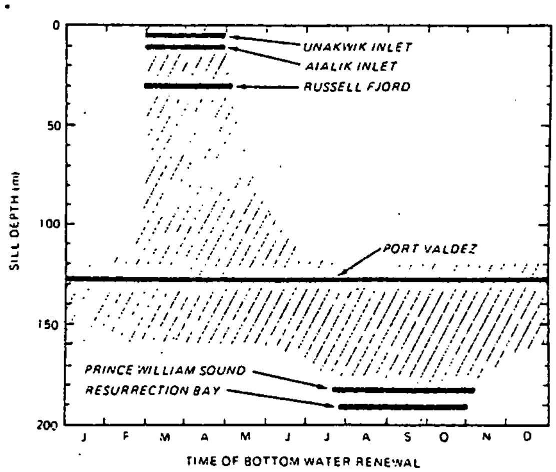

Figure 25. Diagram showing conceptual relation between fjord sill depths and period of renewal of deepest basin water behind the sills.

There are several possible mechanisms for transferring source water over the sill to where it can sink and replace the deep water, given that the requisite density difference exists. The horizontal pressure gradient due to the existence of the density differential itself is an obvious possibility; this pressure gradient can cause an inflow of water over the sill as observed for Resurrection Bay during the summer. The inflow might be aided, especially in shallow-silled fjords, by strong regional tides which can lead to appreciable currents over the sills. Maximum currents through the entrance to Russell Fjord were estimated from moving ice to be approximately 5 m s^{-1}. The source water might be forced inward on the incoming tide and, once over the sill, sink. The ebb tide would then remove near-surface water from within the fjord, leaving the newly formed deep water. Surface winds blowing up- or down-fjord might hinder or aid source water inflow over the sill in a number of ways. A down-fjord wind tends to accelerate the seaward surface flow; volume continuity requires that the inward deep flow increase to keep pace, thus augmenting inward flow of source water. Conversely, an up-fjord wind can cause inward surface flow, leading to a diminution or reversal of inward flow over the sill. Less obvious is the effect of a surface wind on the pycnocline both inside and outside the fjord. Surface winds can alter the depth of the pycnocline and consequently change horizontal pressure gradients due to density difference between water inside and outside the fjord at sill depth and speed and direction of the wind.

Longshore winds over the Gulf of Alaska can have a significant effect on deep-silled fjords which renew their bottom water during summer, inasmuch as these winds drive coastal convergences or divergences which lower or raise, respectively, the isopycnal surfaces. This effect would likely not be significant in the case of shallow-silled fjords which renew their deep waters during winter. By late winter the water column is vertically well mixed through the layers which provide source water, i.e., from the surface down to about 30 to 50 m in Prince William Sound (Muench and Schmidt, 1975) and to the bottom on the Gulf of Alaska shelf (Royer, 1975). Fluctuations in the wind field over the Gulf would therefore have little effect on the vertical density field of the source waters and, consequently, little effect on the density of water available at sill depth. The shallow-silled systems would therefore not be subject to this variability in source water density at sill depth, as the deeper systems appear to be.

It is expected for each of these systems, and documented for Russell Fjord, that inflowing source water would interleaf at shallower and shallower depths as time passed and the sill depth source water density decreased. Renewal of the deepest bottom water in a shallow-silled fjord would occur in March when source water density was at its annual maximum. Subsequent source water would be of lesser density and would assume a final depth atop this bottom water. Thus the entire water column would be renewed, starting from the bottom and working upward, even in the shallowest-silled fjords.

This continual interleafing of inflowing waters, coupled with the fact that some of the inflowing water must mix with ambient water en route, makes estimation of the water volume addition difficult. Reeburgh *et al.* (1976) have estimated, using the conservative variable "NO" as a tracer, that 25% of Russell Fjord water below sill depth was replaced during the period July-September 1973. Heggie and Burrell (1977) have estimated, on the basis of current measurements that inflow of source water was sufficient to replace the deep basin water in Resurrection Bay about five times during a 34-day period. The vastly different estimates of flushing rate reflect accessability of the deep basins to source waters.

In certain cases, vertical heat and salt transfer may occur due to thermohaline convection. This, however, has only been documented on one occasion in Port Valdez during winter 1972. Certainly, the vertically near-uniform conditions which prevail within fjords below sill depth would facilitate such mixing. However, accumulation of low salinity water near the surface, due to lack of an entrainment flow mechanism for removing it, might also impede thermohaline convection. Since ice does not generally form in the systems under consideration, thermal rather than haline convection is the acting mode, and this must overcome a strong vertical salinity gradient. At the low prevailing temperatures, salinity exerts the dominant control over density; hence it might be expected that vertical convection would not be a routine occurrence. In the single documented case, moreover, the salinity increase at depth indicated that some advective addition of water had also occurred along with vertical convection. It is apparently not a simple matter to separate the effects of advective inflow from those of vertical convection. Possibly use of a radioactive tracer such as radon-222, would provide a fruitful approach to solving this problem.

Acknowledgements

Support for this research has been provided by: The National Science Foundation under Grant Nos. GA 35663 and GFS 72-02718-A03; The National Oceanographic and Atmospheric Administration under Grant No. 03-5-022-56; the Alaska Sea Grant Program of the National Oceanographic and Atmospheric Administration under Grant No. 04-3158041; the Energy Resource and Development Administration under Grant No. E(45-1)-2229 #TAI; the Alyeska Pipeline Service Company; and, the Institute of Marine Science, University of Alaska. Invaluable assistance in the form of discussions and manuscript review has been provided by T. C. Royer, W. S. Reeburgh and G. M. Schmidt. Contribution number 312 from the Institute of Marine Science, University of Alasks.

References

Barnes, C. A. and E. E. Collias. 1958. Some considerations of oxygen utilization rates in Puget Sound. *Journal of Marine Research 17:* 68-90.

Broecker, W. S. 1965. An application of natural radon to problems in ocean circulation. In: *Proceedings of Symposium on Diffusion in Oceans and Fresh Waters:* 116-145. T. Ichiye (editor). Lamont-Doherty Geological Observatory (1964).

Broecker, W. S. 1974a. 'NO', a conservative water mass tracer. *Earth and Planetary Science Letters 23:* 100-107.

Broecker, W. S. 1974b. *Chemical Oceanography*. Harcourt Brace Jovanovich, Inc., 214 p.

Broecker, W. S. and A. Kaufman. 1970. Near-surface and near-bottom radon results for the 1969 North Pacific GEOSECS station. *Journal of Geophysical Research 75:* 7679-7681.

Broecker, W. S., J. Cromwell, and Y. H. Li. 1968. Rates of vertical eddy diffusion near the ocean floor based on measurements of the distribution of excess ^{222}Rn. *Earth and Planetary Science Letters 5:* 101-105.

Carlson, R. F., J. Wagner, C. W. Hartman, and R. S. Murphy. 1969. Freshwater studies. In: *Baseline data survey for Valdez pipeline terminal environmental data study:* 7-41. Institute of Marine Science, University of Alaska, Fairbanks, Rept. R69-17.

Chung, Y. 1973. Excess radon in the Santa Barbara Basin. *Earth and Planetary Science Letters 17:* 319-323.

Chung, Y. and H. Craig. 1972. Excess-radon and temperature profiles from the eastern equatorial Pacific. *Earth and Planetary Science Letters 14:* 55-64.

Coote, A. R. 1964. Physical and chemical study of Tofino Inlet, Vancouver, B.C. M.S. Thesis, University of British Columbia, 74 pp.

Craig, H. 1969. Abyssal carbon and radiocarbon in the Pacific. *Journal of Geophysical Research 74:* 5491-5506.

Csanady, G. T. 1974. Barotropic currents over the continental shelf. *Journal of Physical Oceanography 4:* 357-371.

Hansen, D. V. and M. Rattray, Jr. 1966. New dimensions in estuary classification. *Limnology and Oceanography 11:* 319-326.

Heggie, D. T. 1977. Deep-water current measurements in Resurrection Bay, an Alaskan fjord (submitted for publication).

Heggie D. T. and D. C. Burrell. 1977. The exchange of deep water between the gulf of Alaska and Resurrection Bay, a fjord estuary (submitted for publication).

McAlister, W. B., M. Rattray, Jr., and C. A. Barnes. 1959. The dynamics of a fjord estuary: Silver Bay, Alaska. *Technical Report No. 62.* Department of Oceanography, University of Washington, 70 pp.

Muench, R. D. and D. L. Nebert. 1973. Physical Oceanography. In: *Environmental Studies of Port Valdez:* 103-149. D. W. Hood, W. E. Shiels, and E. J. Kelley (editors). Institute of Marine Science Occasional Publication No. 3, University of Alaska, Fairbanks.

Muench, R. D. and G. M. Schmidt. 1975. Variations in the hydrographic structure of Prince William Sound. *Sea Grant Report R75-1.* Institute of Marine Science Report, R75-1, University of Alaska, Fairbanks, 135 pp.

Mungall, J. C. 1973. Current record analysis and tidal computations for Port Valdez, Alaska. *Sea Grant Report R73-6.* Institute of Marine Science, University of Alaska, Fairbanks, 77 pp.

Nebert, D. L. 1972. A proposed circulation model for Endicott Arm, an Alaskan fjord. M.S. Thesis, University of Alaska, 90 pp.

Pickard, G. L. 1967. Some oceanographic characteristics of the larger inlets of Southeast Alaska. *Journal of the Fisheries Research Board of Canada 24:* 1475-1506.

Pickard, G. L. and K. Rodgers. 1959. Current measurements in Knight Inlet, British Columbia. *Journal of the Fisheries Research Board of Canada 16:* 635-678.

Pritchard, D. W. 1967. What is an estuary: physical viewpoint. In: *Estuaries:* 3-5. G. H. Lauff (editor). American Association for the Advancement of Science Publication No. 83.

Rattray, M., Jr. 1967. Some aspects of the dynamics of circulation in fjords. In: *Estuaries:* 52-62. G. H. Lauff (editor). American Association for the Advancement of Science Publication No. 83.

Reesburgh, W. S., R. D. Muench, and R. T. Cooney. 1976. Oceanographic conditions during 1973 in Russell Fjord, Alaska. *Estuarine and Coastal Marine Science 4:* 129-145.

Royer, T. C. 1975. Seasonal variations of waters in the northern Gulf of Alaska. *Deep-Sea Research 22:* 403-416.

Saelen, O. H. 1967. Some features of the hydrography of Norwegian fjords. In: *Estuaries:* 63-70. G. H. Lauff (editor). American Association for the Advancement of Science Publication No. 83.

Searby, W. H. 1969. Coastal weather and marine data summary for Gulf of Alaska, Cape Spencer westward to Kodiak Island. *Environmental Science Services Administration Technical Memorandum 8.* United States Dept. of Commerce, Washington, D. C., 30 pp.

Sholkovitz, E. R. and J. M. Gieskes. 1971. A physical-chemical study of the flushing of the Santa Barbara Basin. *Limnology and Oceanography 16:* 479-489.

Winter, D. R. 1973. A similarity solution for steady-state gravitational circulation in fjords. *Estuarine and Coastal Marine Science 1:* 387-400.

Sediment-Seawater Exchanges of Nitrogen and Transition Metals in an Alaskan Fjord

D. T. Heggie and D. C. Burrell

Preprint of paper presented at
NATO Fjord Oceanographic Workshop,
Victoria, Canada, June 1979.

SEDIMENT-SEAWATER EXCHANGES OF NITROGEN AND TRANSITION METALS IN AN ALASKAN FJORD[1]

David T. Heggie* and David C. Burrell
Institute of Marine Science, University of Alaska
Fairbanks, Alaska 99701

*Present address: Graduate School of Oceanography
University of Rhode Island, Narragansett, R. I. 02882

Resurrection Bay (southcentral Alaska) is a single silled fjord-estuary having a basin depth of 283 m (at Station RES 2.5) and a sill at approximately 185 m. The inner basin is flushed annually over the May-October period, but during the oceanographic winter period the basin waters may be considered to be advectively isolated. The seasonal hydrography and disolved oxygen distributions within this basin have been described by Heggie *et al.* (1977).

Figure 1 shows pore water profiles for NO_3-N and NH_3-N and solid phase and soluble concentrations of the transition metals Fe, Mn, and Cu within the surface sediments of the fjord basin (Station RES 2.5; May 1975). There is no evidence for significant advective transport in these sediments so that the profile inflexions indicate zones of chemical reaction, and transport of species in the pore water is predominantly *via* ionic diffusion down the concentration gradients. Table I gives species concentrations at the base of the water column and for interstitial water extracted from approximately the upper 5.5 cm of the sediment. The computed fluxes across the sediments are for boundary ionic diffusion (coefficients D_a) assuming that the bottom water concentrations listed approximate those at the interface. In view of the large concentration differences involved, (except for NO_3-N) this assumption is not believed to be a major source of error.

[1]Institute of Marine Science, Contribution No. 374.

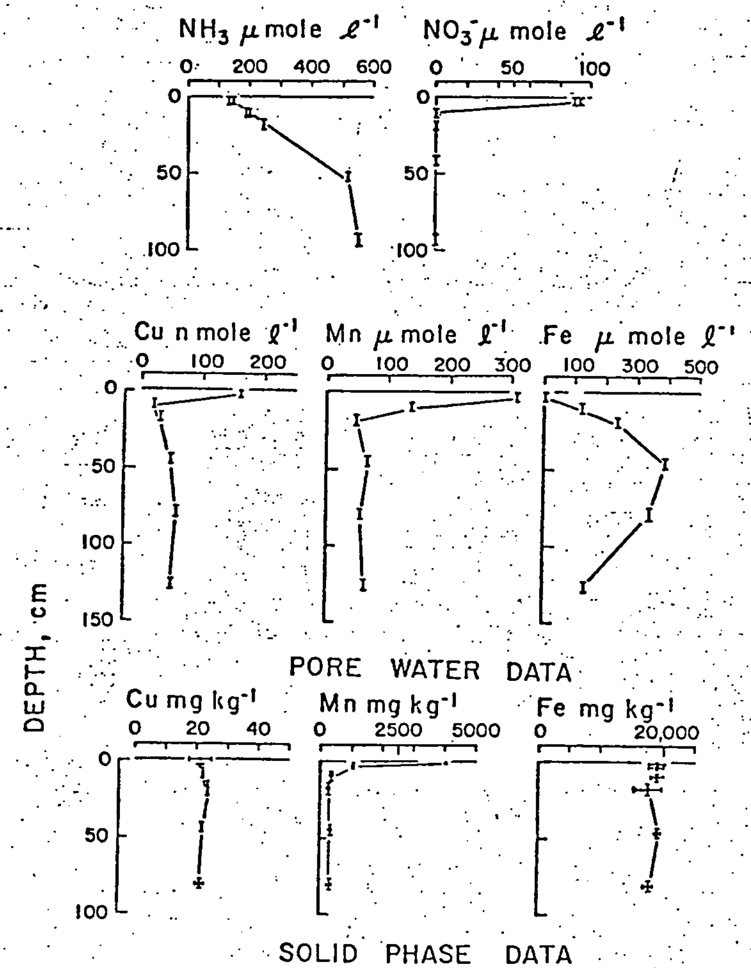

Figure 1. Interstitial water contents of NO_3-N, NH_3-N, Cu, Fe, and Mn and solid phase contents of Cu, Fe, Mn. Resurrection Bay, Station RES 2.5, May 1975.

Dissolved oxygen concentrations in the bottom basin waters over the 1973-75 period decreased from around 160 µ mole ℓ^{-1} immediately after replacement to less than 50 µ mole ℓ^{-1} at the end of the winter isolation period. Minimum consumption rates some 5 m above the sediment have been estimated at 250 µ mole ℓ^{-1} yr $^{-1}$ (Heggie *et al.*, 1977). Although sediment contents have not been measured, the slope of the gradient in the surface layers may be inferred from the depth of nitrate removal. Assuming that interfacial oxygen concentrations approximate those measured at the base of the basin water column, the minimum (molecular) diffusive flux into the sediment is calculated to vary seasonally between 22 and 5 μ mole cm^{-2} yr^{-1}. The volumetric consumtion rate over the top 5 cm of sediment is thus 4000-1000 μ mole ℓ^{-1} yr^{-1}; more than an order of magnitude greater than in the adjacent column. Annual net productivity over this period in Resurrection Bay has been estimated at around 19 mole C m^{-2} yr^{-1} (Heggie *et al.*, 1977). Applying conventional organic matter oxidation stoichiometry, the computed sub-sill basin oxygen consumption could account for approximately 12-7 mole C m^{-2} yr^{-1} — some 66% of the estimated productivity — with less than an additional 1% in the sediment oxic zone.

Maximum nitrate (plus nitrite) concentrations over this period within the oxygenated sediment layer were in excess of 90 μ mole ℓ^{-1} (Fig. 1). In the absence of regeneration, surface sediment contents should approximate those measured at the base of the water column (30-40 μ mole ℓ^{-1}). "Excess" contents will be released by aerobic decomposition of biogenic material, but the computed winter oxygen comsumption should contribute only around 60 μ mole NO_3-N ℓ^{-1} to the surface pore waters.

Since it appears that the measured nitrate contents of the surface interstitial water cannot be accounted for by standard regeneration stoichiometry it is suggested that the "excess" nitrate is due to nitrification at the boundary. Added evidence for such an ammonia oxidation hypothesis is supplied by the indicated gradients and computed benthic flux of this species. The difference in concentration of ammonia is in excess of two order of magnitude across the benthic boundary (Table I) and during the observed 1973-75 period ammonia concentrations at the bottom of the fjord basin at no time exceeded 1 μ mole ℓ^{-1} (although values > 2 μ mole ℓ^{-1} were found 25 m above the boundary in January and April 1975; Heggie *et al.*, 1977). The computed benthic flux of 17.7 μ mole cm^{-2} yr^{-1} is capable of supporting a minimum gradient in ammonia of 1.6×10^{-7} μ mole cm^{-4} (from a mean turbulent diffusion coefficient of 3.5 cm^{-2} sec^{-1} computed for sill height). This would be equivalent to a concentration difference between the sediment interface and the top of the basin at sill height (approximately 100 m) of 1.6 μ mole ℓ^{-1}; far greater than anything found to be sustained in practice.

From Figure 1, it may be seen that interstitial water ammonia increases linearly through the sulfate reduction zone. Diffusive transport along this gradient may be computed at not less than 2.7 μ mole cm^{-2} yr^{-1}; a flux which, at steady state, would be insufficient to maintain the estimated benthic boundary flux discussed above. It is concluded that these several observations require additional production of ammonia at the interface, part of which is oxidized to nitrate.

Maximum pore water concentrations of manganese (305 μ mole kg^{-1}) were found below the surface sediment layer (0 -5.5 cm) decreasing to around 50 μ mole kg^{-1} at the surface (Table I) and at 14-22 cm depth and thereafter remaining relatively constant to the maximum depth sampled (130 cm; Fig. 1). Maximum solid phase concentrations (Table I) occurred in the top 0.5 cm of sediment. These distributions are attributable to diagenetic reduction and mobilization below the redox boundary, with upward diffusion and reprecipitation in the oxic zone.

Pore water contents of iron increase with depth to a maximum of around 390 μ mole kg^{-1} over the 42-47 cm depth zone. From this surface sediment gradient, an ionic diffusion flux of approximately 1.8 μ mole cm^{-2} yr^{-1} may be computed, considerably larger than the estimated flux of 0.08 μ mole cm^{-2} yr^{-1} across the benthic boundary (Fig. 1). It would appear that remobilized reduced iron is efficiently trapped in the surface sediments and that, unlike manganese in this environment, little escape into the water column.

The depth distributions of the redox species O_2, NO_3-N, Mn and Fe are consistent with a model of organic matter degradation in the sediments by oxidants in order of free energies made available to the organism. These oxidants are all consumed in the top 5.5 cm of this fjord basin. Copper does not participate in this redox sequence. The general distribution of this metal in the Resurrection Bay basin sediments is shown in Figure 1 and Heggie and Burrell (1979) have presented a detailed model which incorporates remobilization in the surface sediment with transport up into the water column and down to a removal reaction zone.

A relative measure of the remobility of these transition metals is given by normalizing the computed sediment-seawater flux to the apparent equilibrium solid phase concentration of each metal as shown in Table II. Table III summarizes the computed interface fluxes together with approximate standing stocks in the overlying column. The sub-sill basin water of Resurrection Bay is renewed annually (Heggie *et al.*, 1977). If the time required to double the concentration of a species in the water column *via* input across the benthic boundary were of the same order as the residence time of the water then this transport could be an important component of the estuarine geochemical balance: this appears to be the case only for manganese in this environment. For the other species considered here, riverine influx and regeneration in the water column are quantitatively more important processes.

REFERENCES

Heggie, D. T., D. W. Boisseau and D. C. Burrell. 1977. Hydrography, nutrient chemistry and primary productivity of Resurrection Bay, Alaska 1972-75. Report R77-2. Inst. Mar. Sci., University of Alaska, 111 pp.

Heggie, D. T. and D. C. Burrell. 1979. Depth distributions of copper in the water column and interstitial waters of an Alaskan fjord. *In* K. A. Fanning and F. T. Manhein (eds.) *The dynamic environment of the ocean floor*, D. C. Heath and Co., Lexington, in press.

Table I

Benthic boundary species concentrations and fluxes

Species	C (μ mole ℓ^{-1}) B.W.	C (μ mole ℓ^{-1}) I.W.	$D_a \times 10^{-6}$ ($cm^2\ sec^{-1}$)	F (μ mole $cm^{-2}\ yr^{-1}$)
NO_3-N	25.5	91.7	11.6	2.1
NH_3-N	< 1.0	137.5	11.6	18.3
Mn	0.06	54.6	3.8	6.5
Fe	0.01	1.7	4.2	0.08
Cu	0.03	0.16	4.2	0.006

B.W. = bottom water

I.W. = surface (∿ 0 - 5 cm) interstitial water

Table II

Sediment - seawater flux of Mn, Fe, Cu normalized to apparent equilibrium contents of solid phases

Element	Flux[a] (F) mg $cm^{-3}\ yr^{-1}$	Equil. solid phase conc[b] (C) mg cm^{-3}	C/F yrs
Mn	7×10^{-2}	.66	9.2
Fe	9×10^{-4}	38	4.2×10^{6}
Cu	8×10^{-5}	0.04	500

a = Volumetric flux from surface 5 cm zone

b = Sediment density taken as 2×10^{-3} kg/cm^3

Table III

Benthic flux, standing crop and doubling time. Resurrection Bay 1974-75

Species	Mean water column concs. μ mole ℓ^{-1}	Standing crop (C) μ mole cm^{-2}	Flux (F) μ mole $cm^{-2}\ yr^{-1}$	Doubling time (C/F) yrs
$NO_3 + NH_3$	14.7 - 29.5	420 - 840	21	20 - 40
Mn	0.013	0.37	6.5	0.06
Cu	0.008	0.22	0.006	37

Reaction and Flux of Manganese within the Oxic Sediment and Basin Water of an Alaskan Fjord

T. L. Owens, D. C. Burrell and H. V. Weiss

Preprint in press.

Proceedings of NATO Fjord Oceanographic Workshop,

Victoria, Canada, June 1979.

REACTION AND FLUX OF MANGANESE WITHIN THE OXIC SEDIMENT AND BASIN WATER OF AN ALASKAN FJORD[1]

T. L. Owens and D. C. Burrell
Institute of Marine Science
University of Alaska
Fairbanks, Alaska 99701

H. V. Weiss
Naval Ocean Systems Center
San Diego, California 92152

Manganese occurs in two oxidation states - one insoluble, one mobile - over the redox potential range found in near surface estuarine sediments. This geochemical character leads to partial remobilization of deposited manganese in the sediments below the redox boundary and a flux into the oxic marine environment where oxidation and reprecipitation occur. Such closed sub-cycle behavior is of considerable interest; not least because of potential control on the distribution of many other trace elements.

Using neutron activation analysis, we have determined the distribution of soluble and particulate manganese within the basin and near surface sediments of an Alaskan fjord (Table I, Figs. 1 and 2). Resurrection Bay has a basin (station depth 287 m) separated from the Gulf of Alaska shelf by a sill at approximately 185 m. This basin is flushed annually during the summer-fall but, because of seasonal circulation patterns developed in the Gulf, thereafter remains effectively isolated (Heggie *et al.*, 1977). The data of Table I was collected near the end of the oceanographic winter period (March). At this time, Heggie and Burrell (1979) have shown that the distribution (C) of a non-conservative species within the basin may be closely approximated by a vertical diffusion-reaction model:

$$- \frac{dC}{dt} = \frac{\delta}{\delta z} (K_z \frac{\delta C}{\delta z}) + J \qquad (1)$$

[1]Institute of Marine Science, Contribution No. 375

TABLE I

MANGANESE CONCENTRATIONS IN BASIN WATER COLUMN AND SEDIMENT
Resurrection Bay, Station RES 2.5, March

Depth[a] (m)	Water Column Dissolved μM x 10^{-2}	Water Column Particulate μM x 10^{-2}	Sediment Pore Water Depth[b] (cm)	Sediment Pore Water μM	Sediment Depth[c] (cm)	Sediment mg/g
3	5.04	10.60	2	65.9	0	2.92
8	2.62	9.37	0	288.0	7.5	0.92
18	-	5.66	- 2	922.4	27.5	0.94
28	1.64	3.82	- 4	194.0	52.5	0.86
38	1.57	3.39	- 6	121.6	97.5	0.95
58	1.79	2.29	- 8	107.0		
78	1.20	1.78	-10	82.6		
98	1.04	1.62	-12	96.3		
			-14	63.0		

[a] = Positive upwards from interface
[b] = Positive upwards from reaction zone
[c] = Positive down from interface

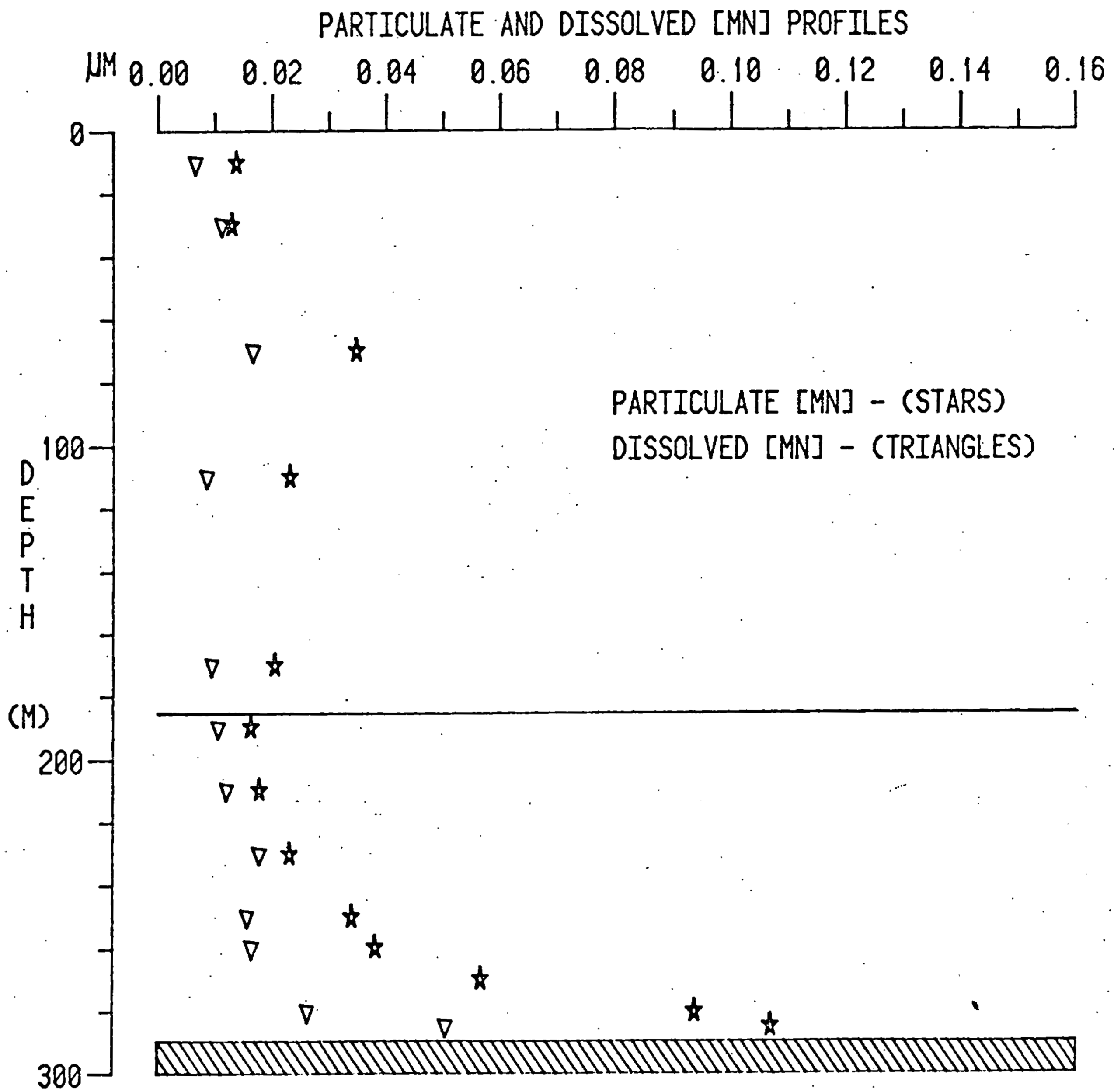

Figure 1. Data point profiles showing exponential increases with depth in both particulate and dissolved manganese in the water column (Resurrection Bay, March).

SEDIMENT AND POREWATER [MN] PROFILES

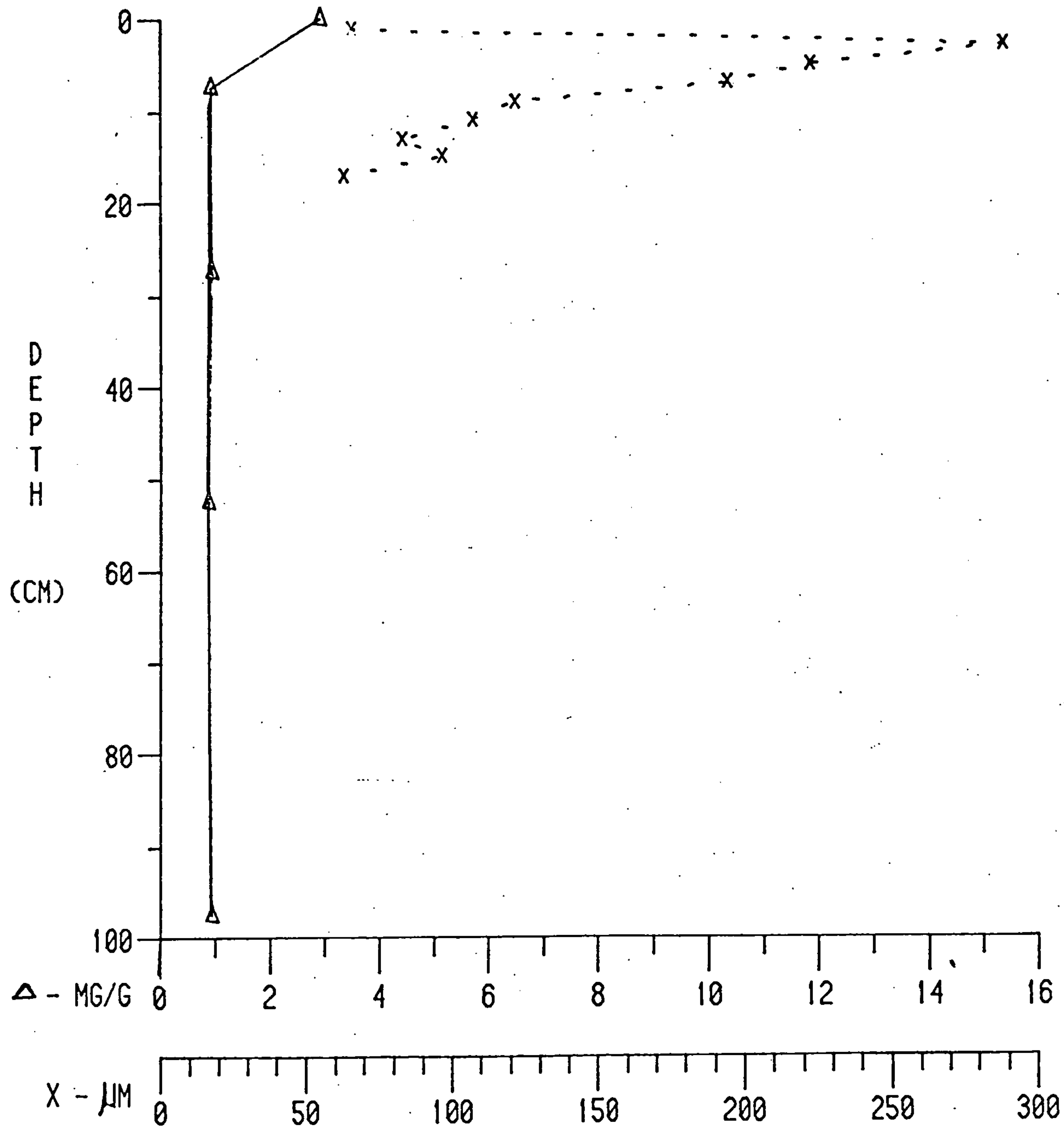

Figure 2. Data point profiles showing surface enrichment of solid phase manganese and negative gradient of interstitial water manganese in the sediment (Resurrection Bay, March).

From profiles of a number of chemical species in the sediment pore waters at this locality, it appears that advective mixing of the surface sediments is undetectable and that equation (1) may generally apply to this environment also.

In the case of dissolved manganese, the major reaction (J) term is oxidation. Following Hemm (1964) and Morgan (1967), we may define an apparent first order oxidation rate constant k:

$$-\frac{d[Mn(II)]}{dt} = k\,[Mn(II)] \qquad (2)$$

We assume that oxidized manganese sorbs onto indigenous particles in the basin column (*via* reactions that are rapid compared with the oxidation kinetics) and that subsequent transport is largely due to gravitational settling (W_s). Then the distribution of particulate manganese (P) shown in Figure 1 is given by:

$$\frac{dP}{dt} = -W_s \frac{\delta P}{\delta Z} + k_w C_w \qquad (3)$$

and the concentrations of dissolved water column and pore water Mn(II) (C_w and C_s; Figs. 1 and 2) may be modeled by:

$$\frac{dC_w}{dt} = \frac{\delta}{\delta Z}\left(K_z \frac{\delta C_w}{\delta Z}\right) - k_w C_w \qquad (4)$$

$$\frac{dC_s}{dt} = \frac{\delta}{\delta Z}\left(\phi D \frac{\delta C_s}{\delta Z}\right) - k_s C_s \qquad (5)$$

The distribution of manganese at the time of year sampled is expected to approximate steady state. Assuming also constant turbulent (K_z) and effective ionic (D; constant porosity ϕ) ionic diffusion coefficients to the interface. The solution to equations (3) - (5) for particulate, dissolved and pore-water manganese respectively are:

$$P - P_\infty = (k_w K_z)^{1/2} \cdot \left(\frac{C_o - C_\infty}{W_s}\right) \exp\left[-\left(\frac{k_w}{K_Z}\right)^{1/2} \cdot Z\right] \qquad (6)$$

$$C_w - C_\infty = (C_o - C_\infty) \exp\left[-\left(\frac{k_w}{K_Z}\right)^{1/2} \cdot Z\right] \qquad (7)$$

$$C_s - C_{s\infty} = (C_{so} - C_{s\infty}) \exp\left[-\left(\frac{k_s}{D}\right)^{1/2} \cdot Z\right] \qquad (8)$$

The interfacial concentration (C_o) of dissolved Mn(II) may be determined *via* a reiterative best fit (r = 0.895) of equation (7) to the data of Table I, setting C_∞ equal to the mean soluble concentration of manganese above sill height (1.04×10^{-2} μM) and using $K_Z = 3.5$ $cm^2 sec^{-1}$ (Heggie *et al.*, 1977). We obtain $C_o = 5.71 \times 10^{-2}$ μM and an oxidation rate constant for the column (k_w) of 1.12×10^{-6} sec^{-1}. Applying the same reiterative fit technique (r = 0.995), and substituting computed values for C_o and k_w, allows solution of equation (6): $P_\infty = 1.60$ μM and $W_s = 1.03 \times 10^{-3}$ cm sec^{-1}. This latter corresponds to particulate manganese settling *via* particles of 20 μM mean diameter.

Similar treatment of the distribution of manganese in the oxic sediment zone using equation (8) is a considerably less satisfactory approach. Table I shows two relevant data points only, each of which is the mean of an approximately 2 cm sediment slice. Assumption of the steady state mode permits a second approach: C_s must equal C_o (5.71×10^{-3} μM) at the interface and the benthic flux of Mn(II) equals the rate of oxidation in the column. The latter relationships may be expressed as:

$$F_w = k_w \int C_w \, dZ \qquad (9)$$

$$F_s = -D \frac{dCs}{dt} = (C_{so} - C_{s\infty})(k_s D)^{1/2} \cdot \exp\left[-\left(\frac{k_s}{D}\right)^{1/2} \cdot Z\right] \qquad (10)$$

Values computed for the constants and relevant boundary conditions using these two approaches are summarized in Table II.

TABLE II

MODELING OF PORE WATER MANGANESE IN THE OXIC SEDIMENT ZONE
(Z positive up from reaction zone; see Table I)

Equation (see text)	$C_{s\infty} \times 10^{-2}$ (μM)	C_s (μM) Z = 0	C_s (μM) z = 2cm	C_s (μM) z = 3cm	$k_s \times 10^{-6}$ (sec^{-1})	$D \times 10^{-6}$ ($cm^2 sec^{-1}$)	$F \times 10^{-7}$ (μ mole cm^{-2} sec^{-1})
8	1.04	288	65.9	31.5*	0.82*	1.5[a]	2.84*
8	1.04	288	65.9	31.5*	1.1 *	2.1[b]	4.33*
8	1.04	288	65.9	31.5*	1.6 *	3.1[b]	5.71*
8	1.04	288	65.9	31.5*	2.1 *	3.8[c]	7.25*
9&10	1.04	288	0.99*	0.057	1.12*	0.14*	1.14

* Values computed from model

a Bender (1971)

b Elderfield *et al.* (unpublished MS)

c Li and Gregory (1974)

Application of the combined fjord basin sediment-water column model has yielded an apparent first order oxidation rate in both sediments and water in the order of 1×10^{-6} sec^{-1}: this gives a mean lifetime of Mn(II) under these conditions of around 10.3 days. The mean settling velocity of the particulate manganese phase is approximately 1×10^{-3} cm sec^{-1}. If the flux of remobilized manganese into the basin is taken as 1.14×10^{-7} μ moles cm^{-2} sec^{-1}, then the standing stock of "excess" manganese (ie., manganese transported from the sediment) may be computed at 0.27 μ moles cm^{-2}. Compared with a "natural" standing stock estimated at 0.76 μ moles cm^{-2}, the recycled fraction constitutes some 25% of the total water column manganese. These are lower limit estimates resulting from use of constant diffusion coefficients to the interface. Applying literature values of D (Table II) to the pore water data of Table I results in 50-90% of the benthic flux being oxidized in the zone between the interface and some 10 cm above. The major need now is for precise, very close interval sampling across the benthic boundary.

References:

Bender, M. L. 1971. Does upward diffusion supply the excess manganese in pelagic sediment? *J. Geophys. Res.* 76:4212.

Heggie, D. T., D. W. Boisseau and D. C. Burrell. 1977. Hydrography, nutrient chemistry and primary productivity of Resurrection Bay, Alaska 1972-75. IMS Report R77-2, Inst. Mar. Sci., Univ. of Alaska. 111 pp.

Heggie, D. T. and D. C. Burrell. 1979. Depth distributions of copper in the water column and interstitial waters of an Alaskan fjord. *In* K. A. Fanning and F. T. Manhein (eds.), *The Dynamic Environment of the Ocean Floor*. D. C. Heath and Co., Lexington. In press.

Hemm, J. D. 1964. Deposition and solution of manganese oxides. Geol. Surv. Water Supply Paper 1667-B.

Li, Y. H. and S. Gregory. 1974. Diffusion of ions in sea-water and in deep-sea sediments. *Geochim. Cosmochim. Acta* 38:703-714.

Morgan, J. J. 1967. Chemical equilibria and kinetic properties of manganese in natural waters. *In: Principles and Applications of Water Chemistry*. Forest and Hunter eds.

Deep Water Renewals in
Resurrection Bay, Alaska

D. T. Heggie and D. C. Burrell

Preprint in press.
NATO Fjord Oceanographic Workshop,
Victoria, Canada, June 1979.

DEEP WATER RENEWALS IN RESURRECTION BAY ALASKA[1]

*David T. Heggie and David C. Burrell

Institute of Marine Science
University of Alaska
Fairbanks, Alaska 99701

Resurrection Bay, a fjord estuary on the south-central Alaskan coastline is approximately 30 km in length and 4.5 km in width. An inner basin (290 m) is separated from the outer fjord and the continental shelf of the Gulf of Alaska by a sill at 185 m. Hydrographic data were obtained from five stations along the length of the fjord at approximately monthly intervals during 1973-75. The precisions of the data are computed to be ± 0.02°C and ± 0.02°/₀₀ in temperature and salinity respectively. During 1973 current meters were installed in the inner basin at depths of 46, 93, 185 and 286 m during March-May, and again during September-October. Two stations were selected to represent oceanographic conditions in the inner fjord (Res-2.5) and adjacent marine source waters (Res-4). Data discussed relate to these two stations.

Seasonal density variations in the fjord are shown in Figure 1. The primary features are:

1) a depth of minimum density variation around 150 m,
2) maximum densities (σ_t > 26.00) in deep (> 150 m) and bottom waters during September-October and,
3) maximum densities (σ_t, 25.00 - 25.50) in surface water (< 150 m) during the winter months (March-April).

This seasonal cycle in density is identical to that found by Royer (1975) on the adjacent continental shelf of the Gulf of Alaska. Here the seasonal variations were governed primarily by the prevailing atmospheric conditions. During winter months the Aleutian low over the Gulf of Alaska and longshore easterly winds resulted in a coastal convergence and deep waters were

*Present address: Graduate School of Oceanography, University of Rhode Island, Narragansett, Rhode Island 02882

[1]Institute of Marine Science, Contribution No. 382

depressed off the continental shelf. Low salinity (32.00-32.50°/₀₀; σ_t 25.00 to 25.50) cold (2.0 to 3.0°C) water persisted there during winter. During summer months, the formation of the North Pacific high and relaxation of the winter downwelling condition permitted more dense (σ_t > 26.00), saline (> 33.00°/₀₀) and warm (∿ 5.0°C) water--which had been depressed off the shelf during winter--to be advected onto the shelf. This dense summer water is able to penetrate the inner reaches of Resurrection Bay. During September-October of 1973 and again in October of 1974 salinities > 33.00°/₀₀ and temperatures ∿ 5.0°C (σ_t > 26.00) were measured in bottom waters of the inner fjord basin. T-S characteristics of bottom waters of the inner basin (Res-2.5) were identical to that of the marine source water (Res-4) from the narrow depth range (175-220 m) which encompassed the sill depth region (185 m).

Current meter data are summarized in Table 1. The daily means of north vector current speeds at 286 and 185 m are shown in Figure 2. The continuous inflow at 286 m and density increases over this period must be due to inflow across the sill to displace less dense basin bottom waters. The outflow required by volume continuity appears to be at sill depth (185 m; Figure 2).

During winter months, T-S diagrams (Figure 3) of marine source waters (Res-4) and inner basin water (Res-2.5) illustrate the more stratified conditions prevailing around the sill depth at the inner basin station (Res-2.5). The outer fjord (Res-4) is subject to downwelling of bottom waters during the winter because of the coastal convergence identified by Royer (1975). The deep and bottom waters of the inner fjord are relatively well isolated from this latter type of flushing by the sill and the secondary pycnocline across the sill depth region. Bottom water oxygen concentrations of the outer fjord are approximately 7.0 ml ℓ^{-1} during March-April, but in contrast, bottom water oxygen concentrations of the inner fjord decrease during winter months to < 1.0 ml ℓ^{-1} by March-April, reflecting the more restricted circulation of the inner fjord.

Density variations are controlled by salinity variations and during the major renewal events of the summers of 1973 and 1974, estimates of the transports, and volumes of water displaced have been calculated from a simplified salt budget. The local rate of salinity change at Res-2.5 below sill depth has been approximated by two terms: a salinity increase because of vertical advection of dense water across the sill and a salinity decrease by vertical mixing:

$$\frac{1}{\Delta t_{2,1}} \sum_{i=s}^{i=b} (S_{2,i}-S_{1,i})\Delta Z_i = W_z(S_I-S_E) - K_z \frac{\Delta S}{\Delta Z}(s)$$

$\Delta t_{2,1}$ is time interval between periods t_2 and t_1
$S_{2,i}$ is salinity at depth i, at time t_2
$S_{1,i}$ is salinity at depth i, at time t_1
ΔZ_i is depth increment
W_z is vertical advection velocity
S_I is salinity of influx water
S_E is salinity of efflux water
K_z is vertical exchange coefficient
$\frac{\Delta S}{\Delta Z}(s)$ is mean vertical salinity gradient across the sill

Intra-basin contributions to the salinity at Res-2.5 have not been accounted for (homogeneous conditions were observed during 1973); W_z and K_z have been assumed constant with depth during renewals and the salinity flux across the sediment-seawater interface has been neglected. The product of W_z (obtained from solution to the above equation) and the cross-sectional area of the sill depth contour yields the transport during renewals; (Table 2). During a 35 day period in September-October of 1973 the topographic basin volume was replaced 2-3 times over. An estimate of the transport during this same period from current meter data (Table 1) yields a transport of $4.1 \times 10^8\ m^3\ day^{-1}$: sufficient to replace the topographic basin volume 2.8 times over. During the renewal events of 1974, however, the basin volume was replaced approximately 1.5 times over in a four month period (Table 2).

References

Royer, T. C. 1975. Seasonal variations of waters in the northern Gulf of Alaska. *Deep-Sea Research*, 22:403-416.

Table 1

Current Meter Data 1973

Depth (m)	March 13 - May 8 Average speed cm sec^{-1}	March 13 - May 8 Direction degrees	September 5 - October 9 Average speed cm sec^{-1}	September 5 - October 9 Direction degrees
12	-	-	3.69	8 (I)
93	0.79	11 (I)	0.88	119 (O)
185	1.13	35 (I)	1.13	179 (O)
286	0.25	147 (O)	3.11	28 (I)

I = inflow
O = outflow

Table 2

Transport Estimates and Volumes Exchanged During Major Renewal Events of 1973 and 1974

Date	Transport $m^3\ day^{-1}$	Percent Volume of Inner basin below sill depth
September 6, 1973		
	5.0×10^8	133
September 20, 1973		
	2.5×10^8	108
October 10, 1973		
July 25, 1974		
	7.9×10^7	140
October 18, 1974		

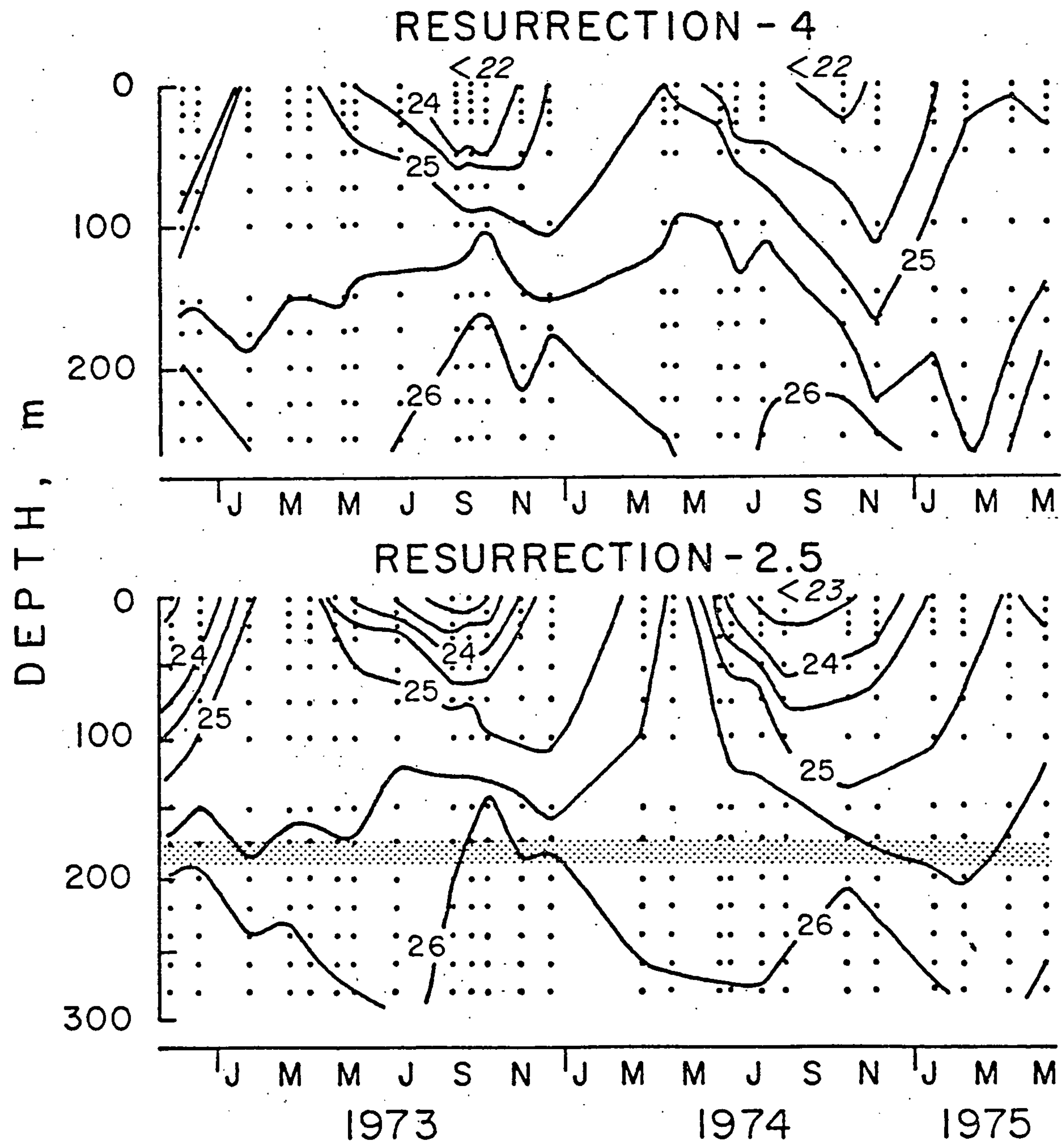

Figure 1. Seasonal density variations Resurrection Bay stations Res-4 and Res-2.5, 1973-1975.

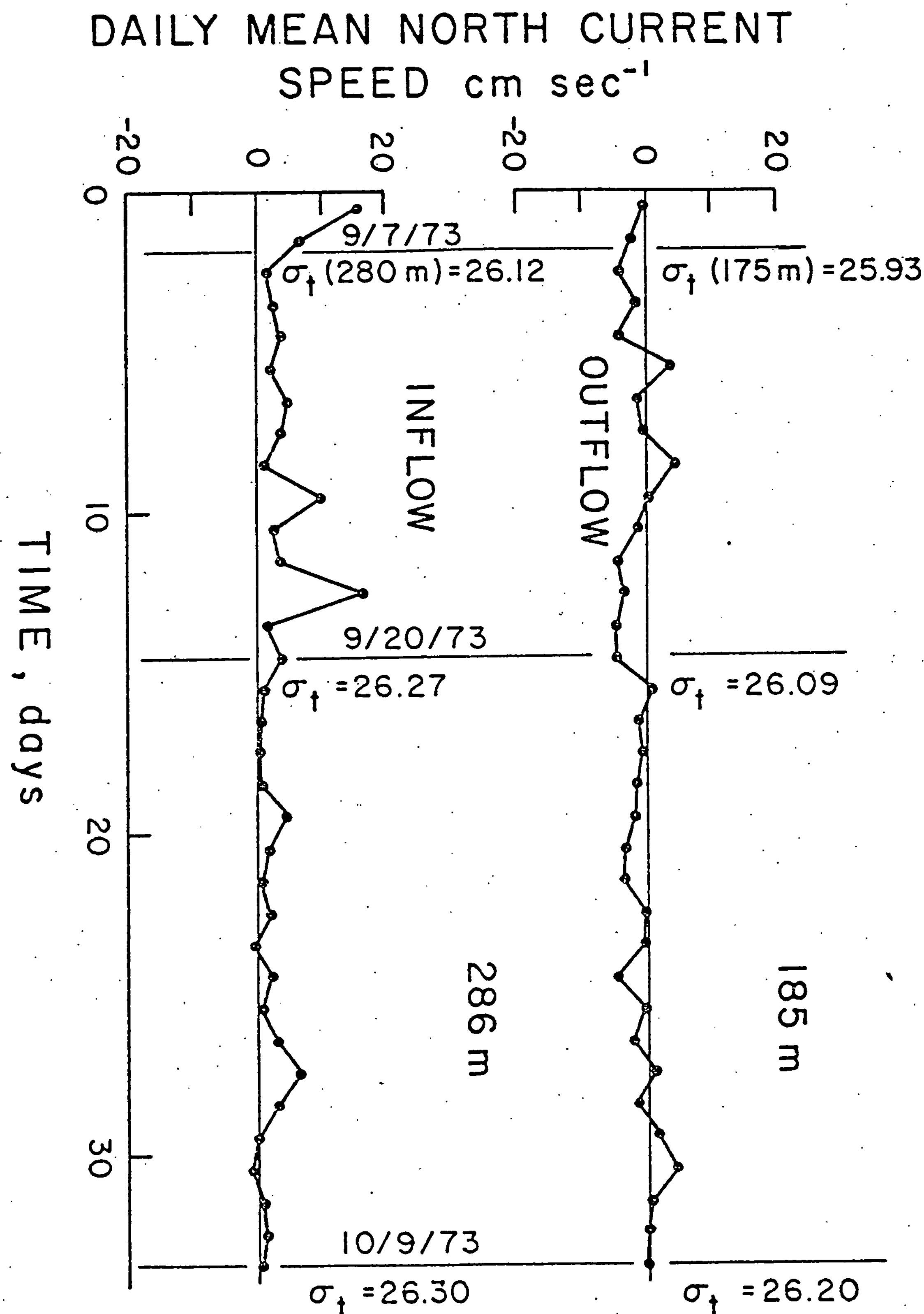

Figure 2. Daily mean north vector current speeds 286 m and 185 m Res-2.5 during September-October 1973.

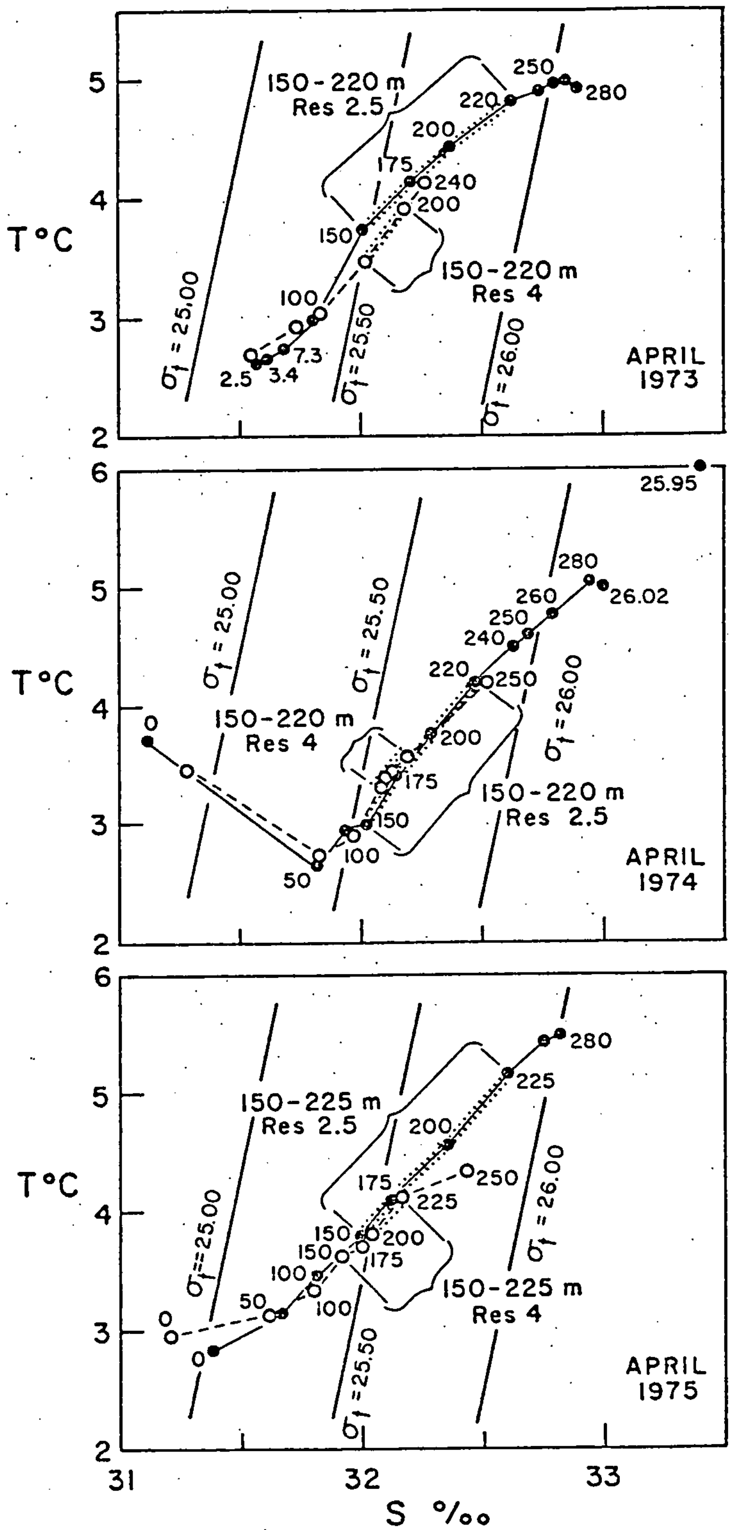

Figure 3. T-S diagrams Res-2.5 and Res-4 during April of 1973, 74 and 75.

THE BEHAVIOR OF IRON, MANGANESE AND ZINC IN A HEAVILY POLLUTED RIVER - ESTUARY SYSTEM

(Abstract Only)

David C. Burrell

Unpublished Manuscript

ABSTRACT

The physical-chemical behavior of iron, manganese and zinc has been observed in the freshwater and estuarine zone of a river system — the Da-tuo Chi, draining the region surrounding the third largest population center (Taichung) of Taiwan — which is being heavily contaminated with industrial and urban effluents. This preliminary survey relates to one time of year only: immediately before the rainy season when river discharge was at a minimum. At this time iron was present in the river upstream from the zone of urbanization largely in particulate form. Downstream from Taichung high concentrations of iron, manganese and zinc are present in an organically complexed form and in true solution. Within the estuarine mixing zone, particulate speciation again predominates. Here total water column levels are much reduced whereas labile (acid extractable) sediment contents are relatively high. It appears that estuarine scavenging is an efficient removal process even where the freshwater input contains high concentrations of heavy metals as soluble organic complexes.

SECTION III

CRUISE REPORTS 1978-79

University of Alaska, Fairbanks

Fairbanks, Alaska 99701

M E M O R A N D U M

TO: J. M. Colonell, E. R. Dieter, J. J. Goering, R. S. Hadley, H. J. Niebauer, K. R. Turner, M. J. Roberts, D. C. Burrell, T. C. Royer

FROM: D. L. Nebert

DATE: May 15, 1978

SUBJECT: Cruise report for Acona Cruise 260.

I. Project Title: Circulation and Water Masses in the Gulf of Alaska/NOAA-OCSEAP Grant #03-5-022-56, task order 19 (Royer) and task order 12 (Burrell).

II. Chief Scientist: D. L. Nebert

III. Cruise Dates and Ports: Cruise AC 260 was divided into 3 legs:

Leg 1: Commenced on 21 April 1978 in PWS. Included PWS and Resurrection Bay; Task order 19. Terminated on 23 April 1978 in Seward.

Leg 2: Commenced on 23 April 1978 in Seward. Included work in Resurrection Bay only; Task order 12. Terminated on 24 April 1978 in Seward.

Leg 3: Commenced on 25 April 1978 in Seward. Returned to Seward same day due to impassable weather. Remained in port during 26 April through midday 27 April. Includes work in PWS, Gulf of Alaska, and Resurrection Bay; Task order 19. Terminated on 8 May 1978 in Seward.

IV. General Scientific Purpose:

Task Order 12: To determine heavy metals pathways in esturine systems.

Task Order 19: To conduct an STD survey from which density and hence currents can be derived.
To recover and deploy current meters.
Together these measurements will allow description of the physical environment and prediction of possible pollutant pathways.

V. Summary of Scientific Work:

Accomplishments:

a. 88 STD casts
b. 3 current meter mooring deployments
c. 2 current meter mooring recoveries
d. 5 Nansen casts
e. 5 special chemistry cast
f. 7 horizontal plankton tows
g. 3 vertical plankton tow
h. 3 otter trawls
i. 6 benthos cores.

Items d. through i. were completed on leg 2, b. and c. on leg 3 and item a. on all legs.

Considering the restrictions placed on the cruise by foul weather, the above accomplishments constitute a successful cruise.

Problems:

a. The weatter was the biggest problem during the cruise - making it impossible to complete all objectives. Only 54 of the planned 110 "outside" stations were occupied while all Prince William Sound work was completed even though it had the lowest priority.

b. We experienced several current meter failures including one on which the bottom of the pressure case "fell off". It's time to reevaluate maintenance and handling procedures.

c. One meter was lost during recovery (S.N. 624) when the line became entangled in the ships propeller. The line was cut and the meter fell to the bottom.

d. Two (expensive) POE floats used for primary subsurface floation flooded and lost some of their bouyancy. The cause is unclear - the current meter records will indicate whether or not they dived deeper than the recommended 75 m.

e. The STD tape deck (Kennedy 1600) failed during the third leg of the cruise. At present it is not clear how much of the data is bad. (The tape transport appeared to fail intermittantly.)

f. With anchors, floatation, and meters for three moorings on board, it appears we are pushing the limits of the Acona. If more gear and/or weight is to be carried, the cruise should be broken into legs inbetween which the Acona can return to Seward for additional gear. The limits of safety are being pushed when the deck is full of gear allowing little room for deployment/recovery activities.

VI. Personnel:

Leg 1:	Leg 2:	Leg 3:
W. Kopplin	Dr. D. Burrell	D. Nebert
Dr. J. Colonell	H. Weiss	W. Kopplin
G. Schmidt	T. Owens	T. Weingartner
B. Chiodo	D. Wiehs	J. Jehle
	S. Hale	B. Vail
	W. Kopplin	

All personnel are IMS employees.

VII. Station Listing

STATION NAME	POSITION LAT (N)	LONG(W)	APPROX DEPTH (M)	TYPE OF STATION
PWS 728	60°36.0'	147°14.0'	192	STD
PWS 727	60°35.6'	147°04.8'	256	STD
PWS 724	60°35.0'	146°55.0'	431	STD
PWS 723	60°33.7'	146°46.6'	393	STD
PWS 722	60°32.5'	146°36.0'	113	STD
PWS 721	60°27.0'	146°54.0'	380	STD
PWS 729	60°27.0'	147°11.0'	219	STD
PWS 730	60°25.0'	147°33.0'	120	STD
PWS 734	60°16.2'	147°38.6'	142	STD

Station Listing (continued)

STATION NAME	POSITION LAT (°N)	LONG(°W)	APPROX DEPTH (M)	TYPE OF STATION
PWS 733	60°16.3'	147°36.0'	285	STD
PWS 732	60°15.5'	147°33.0'	80	STD
PWS 731	60°11.5'	147°26.0'	106	STD
PWS 735	60°07.8'	147°47.0'	243	STD
PWS 736	60°05.6'	147°48.8'	248	STD
PWS 740	59°57.8'	147°50.5'		Interogate CM Mooring
PWS 738	59°58.8'	147°50.5'	230	STD
PWS 737	59°40.0'	148°30.0'	175	STD
RES 005	59°50.7'	149°28.0'	267	NAN,STD
RES 004	59°54.7'	149°24.5'	263	NAN,STD
RES 3.5	59°57.9'	149°20.7'	195	STD
RES 003	59°59.0'	149°20.5'	292	NAN,STD
RES 2.5A	60°01.2'	149°23.0'	285	STD
RES 2.5B	60°01.2'	149°20.6'	285	STD
RES 002	60°03.5'	149°23.4'	193	NAN,STD Hori
RES 02.5	60°01.2'	149°21.5'	288	NISK/V.T.s/M.Trace/NAN/Plan
RES 001	60°06.5'	149°23.0'	263	Horiz Tows, Plankton
RES 02.5	60°01.2'	149°21.5'	289	Benthos Cores
RES 02.5	60°01.2'	149°21.5'	289	Horiz. Tows, Plankton
GAK 001	59°50.7'	149°24.6'	263	STD
PWS 037	59°58.8'	147°50.5'	241	STD
MSA	59°58.3'	147°51.2'		Picking up Current Meter
MSB	59°58.42'	147°48.8'		Deploy Current Meter
PWS 740	59°58.42'	147°48.8'	240	STD
GAK 716	60°11.2'	146°37.7'	206	STD
GAK 715	60°13.9'	146°58.7'	243	STD
PWS 718	60°18.5'	146°51.9'	353	STD
PWS 719	60°19.0'	146°49.0'	285	STD
PWS 720	60°19.7'	146°45.7'	250	STD
PWS 721	60°27.0'	146°54.0'	380	STD
PWS 724	60°35.0'	146°55.0'	435	STD
PWS 725	60°42.0'	147°00.0'	446	STD
PWS 726	60°46.1'	147°01.6'	444	STD
GAK 715	60°13.9'	146°58.7'	243	STD
GAK 714	60°11.1'	147°01.8'	270	STD
GAK 713	60°08.3'	147°04.8'	220	STD
GAK 712	60°03.5'	147°05.0'	265	STD
GAG WA	59°51.4'	147°08.6'	221	Deploy Current Meter
GAG WA	59°51.4'	147°08.6'	221	STD
GAK 711	59°48.3'	147°06.4'	194	STD
GAK 710	59°38.3'	147°06.0'	194	STD
GAK 709	59°28.0'	147°05.8'	210	STD
GAK 708	59°18.6'	147°09.3'	190	STD
GAK 707	59°09.3'	147°12.8'	960-1050	STD
GAK 706	58°59.9'	147°16.3'	1370	STD
GAK 705	58°50.5'	147°19.9'	2384	STD
GAK 704	58°41.1'	147°23.4'	2543	STD
GAK 703	58°31.8'	147°26.9'	2469	STD
GAK 702	58°22.4'	147°30.4'	2220	STD
GAK 701	58°14.1'	147°39.0'	1920	STD
GAK 700	58°05.8'	147°47.6'	1850	STD
GAK 699	58°14.5'	147°56.2'	1800	STD
GAK 011	58°23.2'	148°04.8'	1397	STD
GAK 010	58°32.3'	148°13.2'	1390	STD

Station Listing (continued)

STATION NAME	POSITION LAT (°N)	LONG(°W)	APPROX DEPTH (M)	TYPE OF STATION
GAK 009	58°41.1'	148°21.6'	278	STD
GAK 008	58°49.7'	148°30.1'	280	STD
GAK 007	58°58.7'	148°38.7'	238	STD
GAK 006	59°07.2'	148°47.5'	142	STD
GAK 005	59°16.0'	148°56.0'	177	STD
GAK 004	59°24.5'	149°04.9'	201	STD
GAK 003	59°33.0'	149°13.2'	217	STD
GAK 002	59°41.5'	149°22.0'	198	STD
GAK 001	59°50.7'	149°28.0'	265	STD
GAG 072	59°46.0'	148°54.0'	192	STD
GAG 073	59°38.5'	148°44.0'	172	STD
GAG 074	59°28.5'	148°36.5'	98	STD
GAG 075	59°19.0'	148°28.5'	95	STD
GAG 076	59°11.0'	148°18.0'	117	STD
GAG 077	59°00.0'	148°00.0'	183	STD
GAG 078	58°53.5'	147°54.0'	980	STD
GAG 079	58°44.0'	147°45.0'	2048	STD
GAG 080	58°37.5'	147°37.5'	1960	STD
GAG 008	59°12.0'	144°50.5'	3600	STD
GAG 007	59°21.0'	144°51.0'	1775	STD
GAG 006	59°30.0'	144°52.5'	281	STD
GAG 005	59°39.5'	144°53.5'	139	STD
GAG 004	59°48.6'	144°55.0'	175	STD
GAG 003	59°55.0'	144°49.0'	214	STD
GAG 002	60°02.5'	144°41.0'	194	STD
GAG 001	60°08.5'	144°42.5'	29	STD
GAG 009	60°10.5'	145°02.5'	20	STD
GAG 010	60°04.0'	145°10.0'	106	STD
GAG 011	59°51.5'	145°15.0'	110	STD
GAG 012	59°39.5'	145°14.5'	113	STD
GAG 013	59°29.0'	145°16.5'	208	STD
GAG 014	59°20.0'	145°17.0'	2103	STD
GAG 022	59°15.0'	145°37.0'	2545	STD
PE 001	60°20.6'	146°32.8'	22	STD
RES 004	59°54.7'	149°54.7'	260	STD
RES 2.5	60°01.2'	149°21.2'	289	STD
HEB	60°18.1'	146°50.7'		Deploy Current Meters
HEA	60°21.3'	146°51.8'		Recover Current Meters

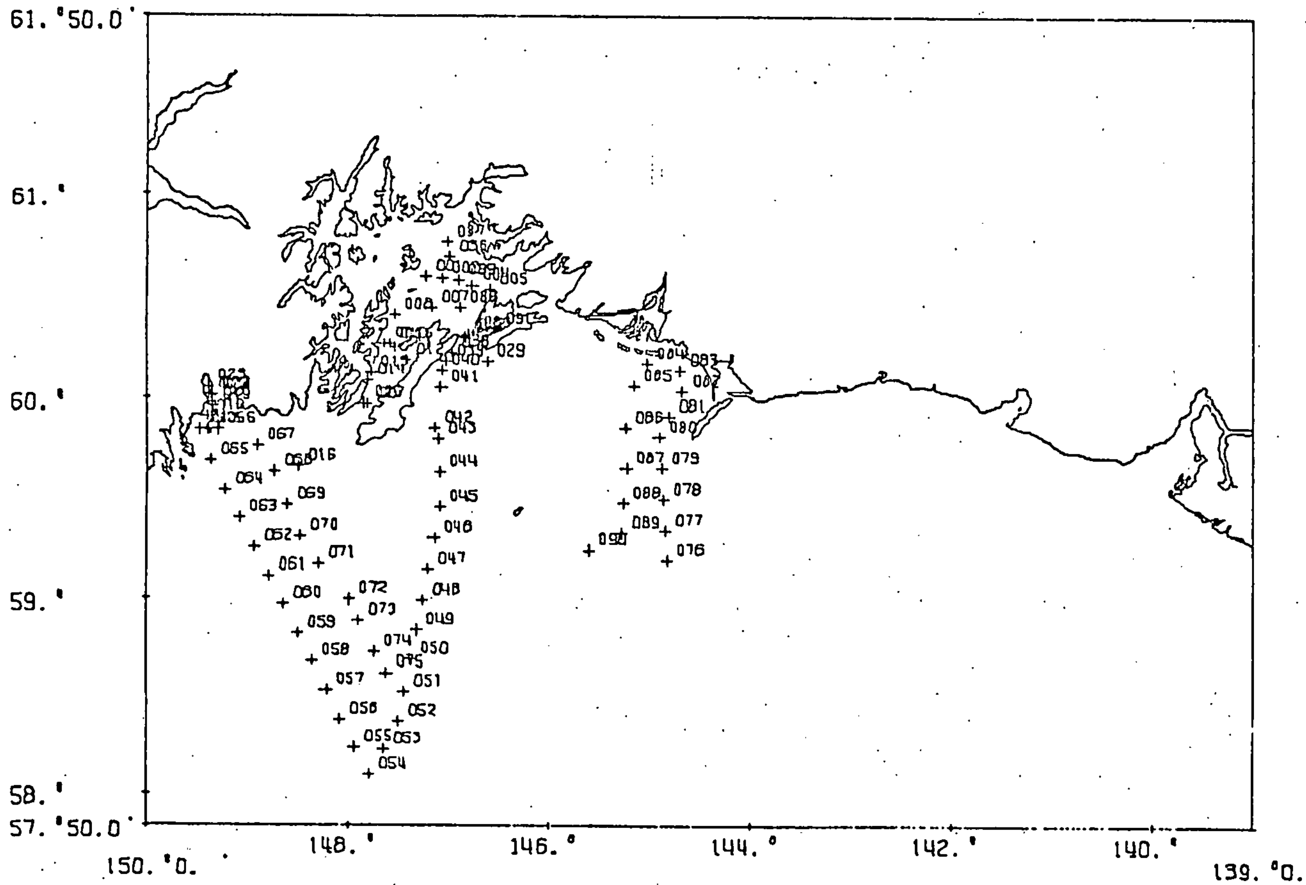

CRUISE AC 260

APR-MAY 1978

CRUISE REPORT

Acona Cruise 262 10-11 July, 1978

Kinetic Studies of Methane Consumption in Marine Sediments
OCE 76-08891

Distribution and Dynamics of Heavy Metals in
Alaskan Shelf Environments Subject to Oil Development
NOAA/OCS 03-5-022-56 Task order 12

W. S. Reeburgh - Chief Scientist

Scientific Objectives

1. Obtain cures from Resurrection Bay for methane analysis and methane oxidation rate measurements.

2. Particle size and concentration measurements in Resurrection Bay waters.

3. Obtain samples for dissolved and particulate cadmium at Res 2.5.

Summary of Scientific Work

This cruise consisted of two day cruises with sample work-up at dockside and in the shore laboratory.

During the first day Res 2.5 was sampled extensively using non-metallic gear. Samples for cadmium analysis were taken and preserved. Samples were taken for analysis with the laser particle size analyzer. Gravity cores were taken and analyzed for methane at the shore lab. These cores were very fluid and were collected with great difficulty. No methane was detected.

The Resurrection Bay station line was run the second day. Hydrographic samples, nutrient samples and samples for particle size analysis were taken. Gravity cores were taken for methane analysis. No methane was detected. Isotopic measurements of sulfate reduction rates and methane oxidation rates were initiated.

Personnel

W. S. Reeburgh	Chief Scientist	U of A
Tom Owens	Graduate Student	U of A
Malcolm Robb	Graduate Student	U of A
Donna Weihs	Technician	U of A
Barbara Hood	Technician	U of A
Scott Reeburgh	Observer	Fairbanks, Ak.

Acona Cruise 262

Hydrographic Station Listing 10-11 July, 1978

Sta #	Name	Latitude	Longitude	
002	Res 2.0	60°03.5'	149°23.4'	223 m
004	Res 5	59°50.7'	149°27.9'	264 m
005	Res 4	59°54.7'	149°24.0'	257 m
006	Res 3	59°59.0'	149°20.5'	289 m
007	Res 2.5	60°01.2'	149°21.5'	287 m

CRUISE REPORT

R/V *ACONA* CRUISE 272
RESURRECTION BAY

William S. Reeburgh
Chief Scientist

March 1979

CRUISE REPORT
R/V *ACONA* CRUISE 272

Dates: 6, 7 March 1979

Scientific Objectives:

a. Measure sulfate reduction rates in Resurrection Bay sediments
b. Studies of interstitial water chemistry
c. Calibrate XBT system
d. Deploy sediment trap and ancillary corrosion experiment at Res 2.5
e. Studies of suspended material; concentration and size distributions
f. Collect pink shrimp larvae
g. Conduct trawl reconaissance of Resurrection Bay benthic fauna

Summary of Scientific Work:

Electronic problems forced us to abandon objective c before the cruise commenced. No larval shrimp were collected in numerous hauls, so our success with objective f was limited. All other objectives were met without incident: the mooring deployment (d) went very smoothly coring (a, b) revealed changes in sediment consistency since July, 1978.

Observers from the Seward Marine Station were a welcome addition to the scientific party. We appreciate the flexivility and cooperation of the relief captain, Wolfgang Mikat, and the crew of the *Acona*.

Scientific Personnel:

6 March	7 March
W. S. Reeburgh	W. Reeburgh
T. Owens	J. Colonell
M. Robb	D. Harris
S. Sugai	G. Mueller
A. Ippolito	T. Owens
R. Erickson	M. Robb
P. Shoemaker	S. Sugai
N. Foster	C. Cremo
J. Trettner	A. Ippolito
C. Cremo	P. Shoemaker
	N. Foster

Station Locations:

1)	Res 2.5	60°01.2'N	149°21.5'W	287 m
2)	Res 4	59°54.7'N	149°24.0'W	257 m

Institute of Marine Science

CRUISE REPORT

Vessel: R/V *Acona*

Cruise No.: 275

Sponsoring Agencies: U.S. Borax Corp.
U.S. Dept. of Energy

Project Titles: (1) Marine Environmental Studies in Boca de Quadra
(2) Transport and reaction of heavy metals in Alaskan fjord estuaries

Dates: April 18 - April 29, 1979

Personnel: D. C. Burrell, Chief Scientist
M. Robb
S. Sugai
T. Paluszkiewicz
W. Kopplin
P. Shoemaker

Itinerary: Vessel departed Seward 0000 hours April 18 for testing of 3 and 4 channel STD systems. Returned Seward to disembark ET. Departed Seward 0710 for Yakutat Bay. Arrived Yakutat Bay 1800 April 19. Depart Yakutat Bay 0655 April 20. Arrive Ketchikan 0920 April 22. Arrive Boca de Quadra area 1334 April 22. Arrive Ketchikan 0600 April 26.

Scientific Objectives:

Leg I. To obtain full spring hydrographic coverage in Yakutat Bay.

Leg II. To continue detailed seasonal environmental survey in Boca de Quadra, Wilson and Bakewall Arms and Smeaton Bay. Including retrieving and setting current meters, benthic trawling to obtain biota samples for heavy metal analysis, and sampling of Keta River for chemical parameters.

Operations: Resurrection Bay

4-18	0049	001	RES-2.5	287 m	STD, neph, T, S, O_2, nuts
	0830	002	RES-4	262 m	STD

Yakutat Bay (see accompanying location listing)

4-19	1800	003	YAK-12	236 m	STD
	1930	004	YAK-10	75 m	STD
	2010	005	YAK-9B	148 m	STD
	2045	006	YAK-9BA	137 m	STD
	2108	007	YAK-8	90 m	STD
	2124	008	YAK-7B	155 m	STD
	2150	009	YAK-7	174 m	STD
	2225	010	YAK-8A	60 m	STD
	2247	011	YAK-9A	97 m	STD
	2315	012	YAK-6B	60 m	STD
	2340	013	YAK-7A	104 m	STD
	2359	014	YAK-6	95 m	STD
4-20	0016	015	YAK-5	172 m	STD
	0042	016	YAK-5A	164 m	STD
	0117	017	YAK-4	142 m	STD
	0347	018	YAK-3	247 m	STD
	0427	019	YAK-3A	245 m	STD
	0645	020	YAK-9	155 m	STD

Boca de Quadra area

4-22	1334	021	BQ-15	373 m	STD, T, S, O_2, nuts
	1615	022/3	BQ-14	84-92 m	STD deploy current meters (E-1)
	1702	024	BQ-11B	252 m	STD
	1755	025	BQ-11	364 m	STD, T, S, O_2, nuts
	1910	026	BQ-11A	238 m	STD
	2010	027	MB-2	102 m	STD
	2035	028	MB-1	121 m	STD
	2123	029	MA-2	183 m	STD
	2200	030	MA-1	174 m	STD
	2220	031	BQ-9	384 m	STD, T, S, O_2, nuts

4-23	0002	032	BQ-7	289 m	STD
	0055	033	BQ-5	280 m	STD
	0158	034	BQ-4	111 m	STD, T, S, O_2, nuts
	0342	035	BQ-3B	135 m	STD, PL
	0445	036	BQ-3	150 m	STD, T, S, O_2, nuts
	0635	037	BQ-3A	159 m	STD
	0740	038/41	BQ-3	110-54 m	PL Recover current meters Deploy current meters (S-2)
	1629	042	BQ-5	278 m	STD, T, S, O_2, nuts, POC, DOC, POP, PON, Nitex, pH, vertical plank. tow
	2208	043	BQ-3	155 m	vertical plank. tow
	2335	044	BQ-3A	135 m	PL
4-24	0037	045/6	BQ-3	153 m	POC, DOC, POP, PON, Nitex, pH, benthos cores
	0735	047/8	BQ-4		Recover current meters, STD, PL
	0915				Keta River sampling
	1320	049			Otter Trawl No. 1
	1450	050	BQ-3		Van Veen
	1540	051	BQ-3	150 m	STD, neph
	1612	052	BQ-3B	135 m	STD, neph
	1629	053	BQ-4	108 m	STD, neph
	1711	054	BQ-5	277 m	STD, neph
	1812	055	BQ-3	154 m	Benthos core, grab
	1903	056		152 m	grab
	1910	057	BQ-3A	157 m	grab
	1920	058		108 m	grab
	1930	059		91 m	grab Otter trawl #2
	2040	060	BQ-3		Otter trawl #3
	2145	061		155 m	grab

	2157	062		161 m	grab
	2222	063	BQ-3B	137 m	grab
	2352	064	BQ-7	288 m	STD, neph
4-25	0175	065	BQ-9	356 m	STD, neph
	0225	066	BQ-11A	245 m	STD, neph
	0258	067	BQ-11	362 m	STD, neph
	0349	068	BQ-11B	252 m	STD, neph
	0416	069	BQ-14	109 m	STD, neph
	0445	070	BQ-15	373 m	STD, neph
	0635	071	BC-10	452 m	STD, neph, T, S, O_2, nuts
	0830	072	SB-5	448 m	STD, neph
	0945	073	SB-4	154 m	STD, neph
	1040	074	SB-3	254 m	STD, neph, T, S, O_2, nuts
	1243	075	SB-2	166 m	STD, neph
	1326	076	SB-1	248 m	STD, neph, T, S, O_2, nuts
	1444	077	SB-0	241 m	STD, neph
	1509	078	WA-1	151 m	STD, neph
	1640	080	BA-1	150 m	STD, neph, T, S, O_2, nuts
	2100	082	BA-1	155 m	STD
	2117	083	SB-0	238 m	STD
	2139	084	SB-1	247 m	STD
	2200	085	SB-2	188 m	STD
	2218	086	SB-3	238 m	STD
	2240	087	SB-4	155 m	STD
	2315	088	SB-5	452 m	STD
4-26	0147	089	BC-10	600 m	STD

Problems:

Third current meter string could not be deployed because of non-arrival of acoustic release.

Cruise 275: Shipek grab stations

a	55	19.4	130	29.2	91 m
b	55	19.2	130	29.5	108 m
c ≡ 3A	55	19.0	130	29.8	157 m

d	55	18.6	130	30.7	152 m
e ≡ 3	55	18.3	130	30.9	154 m
f	55	18.1	130	31.1	155 m
g	55	17.7	130	31.5	161 m
h ≡ 3B	55	17.1	130	31.8	137 m

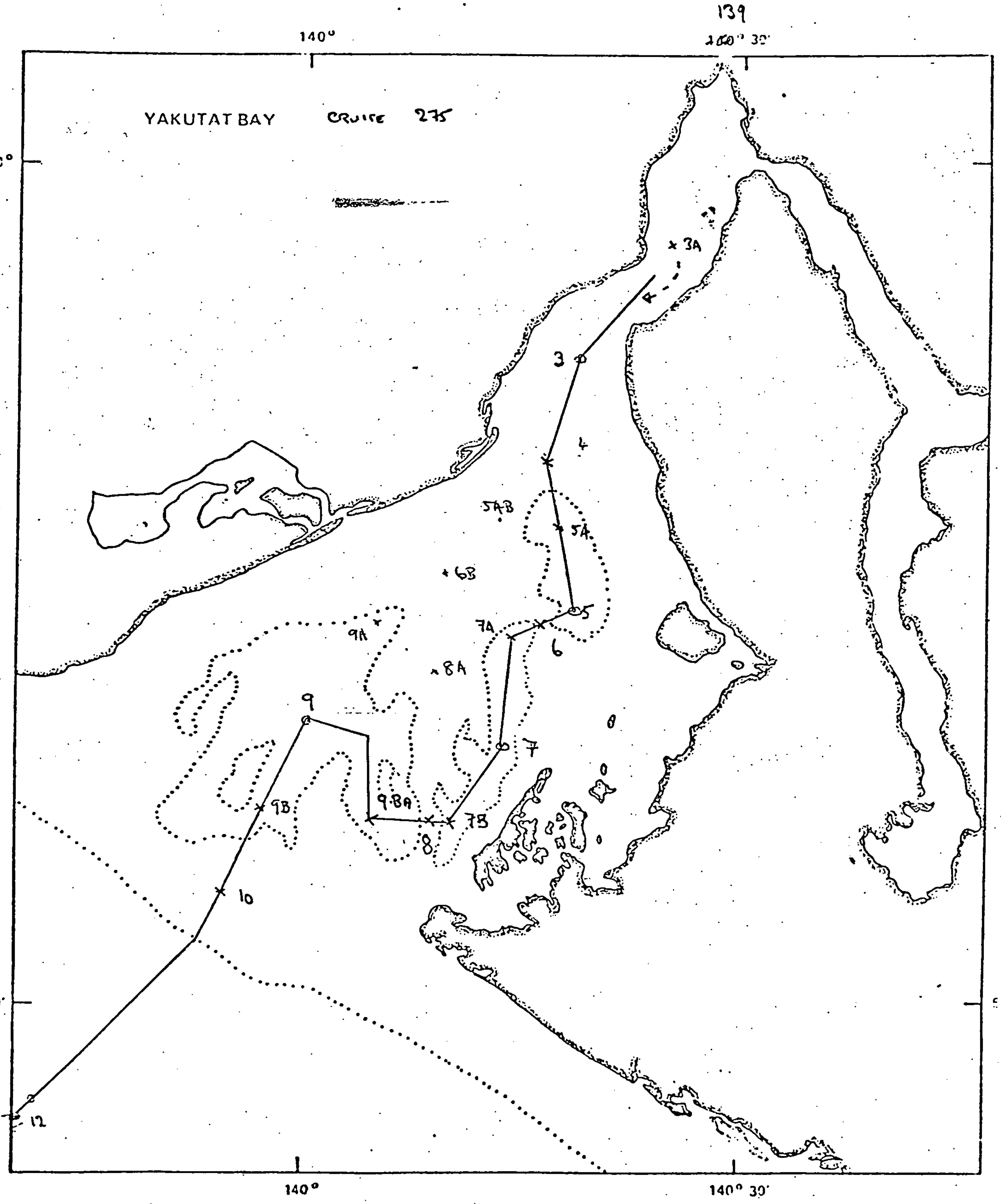
139
140°
140° 30'
YAKUTAT BAY
CRUISE 275
60°
60
59° 30'
59°
3A
3
4
5AB
5A
6B
5
7A
6
9A
8A
9
7
9B
9.8A
7B
8
10
12
140°
140° 30'

Yakutat Bay - Cruise #275 - April 1979 - STD Stations

3A	59°	55.1	139°	38.8
3	59°	52.5	139°	40.5
4	59°	48.0	139°	42.2
5A	59°	46.7	139°	41.7
5	59°	44.0	139°	40.5
6	59°	43.5	139°	43.2
7A	59°	43.0	139°	45.5
7	59°	39.5	139°	46.0
7B	59°	37.4	139°	48.8
8	59°	37.1	139°	51.5
9BA	59°	37.2	139°	55.6
9	59°	40.0	139°	59.5
9B	59°	36.5	140°	03.2
10	59°	34.5	140°	05.6
12	59°	27.5	140°	23.0
8A	59°	42.0	139°	50.4
9A	59°	43.4	139°	54.5
6B	59°	45.2	139°	49.1
5AB				

STANDARD STATIONS

Boca de Quadra

BQ	3A	55° 19.0	130° 29.8
BQ	3	55° 18.3	130° 30.9
BQ	3B	55° 17.1	130° 31.8
BQ	4	55° 16.8	130° 32.2
BQ	5	55° 12.0	130° 37.0
BQ	7	55° 08.3	130° 41.9
MA-1		55° 07.0	130° 41.9
MA	2	55° 08.0	130° 35.8
BQ	9	55° 06.8	130° 43.5
MB-1		55 05.5	130° 43.3
MB	2	55° 03.3	130° 42.2
BQ	11A	55° 07.3	130° 48.8
BQ	11	55° 06.2	130° 53.0
BQ	11B	55° 04.7	130° 58.8
BQ	14	55° 04.6	131° 02.6
BQ	15	55° 03.0	131° 07.0
CST	0	55° 51.5	131° 42.0

Smeaton Bay System

BC	10	55° 14.8	131° 03.0
SB	5	55° 18.9	130° 55.0
SB	4	55° 17.8	130° 49.8
SB	3	55° 18.1	130° 47.4
SB	2	55° 18.5	130° 45.6
SB	1	55° 18.1	130° 43.5
SB	0	55° 18.9	130° 41.6
WA	1	55° 20.1	130° 41.3
BA	1	55° 18.2	130° 39.5

BOCA DE QUADRA PROJECT

Standard Operations

Station	Environment	Depth	Operations
BQ-3A	Basin	145	STD, neph, hydro, nuts, chem. susp. sed.
BQ-3	Basin	155	STD, neph, hydro, nuts, chem. susp. sed.
BQ-3B	Basin	136	STD, neph
BQ-4	Sill	110	STD, neph
BQ-5	Basin	275	STD, neph, hydro, nuts, chem. susp. sed.
BQ-7	Basin	286	STD, neph
MA-1	Arm	164	STD, neph
MA-2	Arm	183	STD
BQ-9	Basin	357	STD, neph, hydro, nuts
MB-1	Arm	93	STD, neph
MB-2	Arm	102	STD
BQ-11A	Basin	232	STD, neph
BQ-11	Basin	355	STD, neph, hydro, nuts
BQ-11B	Basin	252	STD, neph
BQ-14	Sill	90	STD, neph
BQ-15	Exterior	360	STD, neph, hydro, nuts
CST-0	Exterior	450	STD
BC-10	Exterior	600	STD
SB-5	Basin	448	STD, neph, hydro, nuts
SB-4	Sill	154	STD, neph
SB-3	Basin	254	STD, neph, hydro, nuts
SB-2	Sill	166	STD, neph
SB-1	Basin	248	STD, neph, hydro, nuts
SB-0	Basin	240	STD, neph
WA-1	Arm	150	STD, neph
BA-1	Arm	155	STD, neph, hydro, nuts

CRUISE REPORT

R/V ACONA CRUISE 276

RESURRECTION BAY

J. Colonell

Chief Scientist

May 1979

CRUISE REPORT

R/V ACONA CRUISE 276

Date: 10 May 1979

Scientific Objectives:

(a) Retrieve current meter and sediment trap mooring from Station Res 2.5

(b) Redeploy above mooring

(c) Studies of suspended material; concentration and size distributions

(d) Studies of interstitial water chemistry

Summary of Scientific Work:

Due to the necessity to modify sediment trap design, objective (b) was not completed; all other objectives were completed on schedule. Processing of chemistry samples was completed at the Marine Station.

We thank the relief captain, Phil Smith, and the crew of the _Acona_ for their cooperation, and George Mueller for making the facilities of the marine station available.

Scientific Personnel:

J. Colonell	M. Robb
D. Burrell	N. Muransky
D. Harris	
W. Kopplin	
P. Shoemaker	
J. Trettner	
S. Sugai	

SECTION IV

REPORTS AND PUBLICATIONS 1975-79

Institute of Marine Science
University of Alaska
Fairbanks, Alaska 99701

TRANSPORT AND REACTION OF HEAVY METALS IN ALASKAN FJORD-ESTUARIES

U.S. Department of Energy
Contract No. EY-76-C-06-229 T.A. #1

Reports and Publications 1975-79

Burrell, D. C. 1974. Atomic spectrometric analysis of heavy metal pollutants in water. Ann Arbor Sci. Publ. Inc., Ann Arbor, Michigan. 331 pp. Reprinted 1978

Burrell, D. C. 1977. A review of the chemical speciation of copper in seawater. Unpublished report, 35 pp.

Burrell, D. C. and Meng-Lein Lee. 1975. Critical Review of analytical techniques for the determination of soluble pollutant heavy metals in seawater. 58-70 pp. *In* Water Quality Parameters, Monograph No. STP 573, ASTM, Philadelphia.

Burrell, D. C. and M. L. Lee. 1976. Determination of some soluble heavy metals in marine waters by carbon filament atomic spectroscopy. 5th international Confer. Atomic Spectros., Melbourne, Sept. 1975.

Burrell, D. C. and M. L. Lee. 1977. Inorganic speciation of copper in estuarine environments. 461-465 pp. *In* Methods and Standards for Environmental Measurement, W. H. Kirchoff, ed., Special Publication No. 464, National Bureau of Standards, Washington, D. C.

Heggie, D. T. 1977. Copper in the sea: A physical-chemical study of reservoirs, fluxes and pathways in an Alaskan fjord. Ph.D. dissertation, University of Alaska. 222 pp.

Heggie, D. T. and D. C. Burrell. 1976. Differential pulsed anodic stripping voltametry: Application to measurement of copper in seawater. 27th Alaska Science Conference.

Heggie, D. T. and D. C. Burrell. 1977. Hydrography, nutrient chemistry and primary productivity of Resurrection Bay, Alaska. Inst. Mar. Sci. Report R77-2, University of Alaska, Fairbanks. 111 p.

Heggie, D. T. and D. C. Burrell. Depth distributions of copper in the water column and interstitial waters of an Alaskan fjord. *In* K. A. Fanning and F. T. Manheim, eds., *The Organic Environment of the Ocean Floor*. In press.

Heggie, D. T. and D. C. Burrell. Deep water renewals in Resurrection Bay, Alaska. Fjord Oceanographic Workshop. In press.

Heggie, D. T. and D. C. Burrell. Sediment-seawater exchanges of nutrients and transition metals in an Alaskan fjord. Fjord Oceanographic Workshop. In press.

Hoskin, C. M., D. C. Burrell and G. R. Freitag. 1976. Suspended sediment dynamics in Queen Inlet, Glacier Bay, Alaska. *Mar. Sci. Commun.*, 2(2):95-108.

Hoskin, C. M., D. C. Burrell and G. A. Freitag. 1978. Suspended sediment dynamics. Blue Fjord, western Prince William Sound, Alaska. *Est. Coast. Mar. Sci.* 7:1-16.

Muench, R. D. and D. T. Heggie. 1977. Deep water exchange in Alaskan subarctic fjords. Proceedings of Symposium on Transport Processes on Estuarine Environments. 7th Belle W. Baruch Institute for Marine Biology and Coastal Research Symposium.

Owens, T. L., D. C. Burrell and H. V. Weiss. Reaction and flux of manganese within the oxic sediment and basin water of an Alaskan fjord. Fjord Oceanographic Workshop. In press.